785
-24-79

DR. 2496

VPI-SU-5648-4

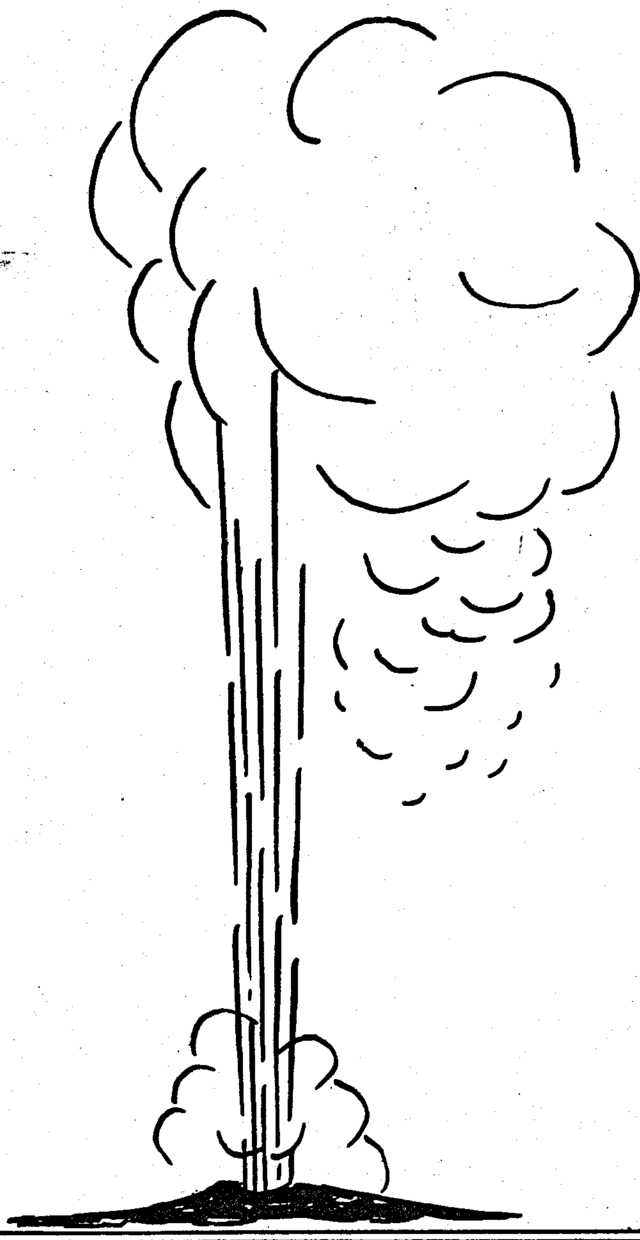

EVALUATION AND TARGETING OF GEOTHERMAL ENERGY RESOURCES IN THE SOUTHEASTERN UNITED STATES

Progress Report for July 1—September 30, 1978

By
John K. Costain
Lynn Glover III
A. Krishna Sinha

MASTER

Work Performed Under Contract No. ET-78-C-05-5648

Virginia Polytechnic Institute and State University
Department of Geological Sciences
Blacksburg, Virginia

U. S. DEPARTMENT OF ENERGY

Geothermal Energy

Available from the National Technical Information Service, U. S. Department of Commerce, Springfield, Virginia 22161.

Price: Paper Copy $8.00
Microfiche $3.00

DISCLAIMER

VPI-SU-5648-4
Distribution Category UC-66a

EVALUATION AND TARGETING OF GEOTHERMAL ENERGY RESOURCES IN THE SOUTHEASTERN UNITED STATES

Progress Report

John K. Costain, Lynn Glover III, and A. Krishna Sinha
Principal Investigators
Department of Geological Sciences
Virginia Polytechnic Institute and State University
Blacksburg, VA 24061

July 1, 1978 - September 30, 1978

PREPARED FOR THE U. S. DEPARTMENT OF ENERGY UNDER
CONTRACT NO. ET-78-C-05-5648

TABLE OF CONTENTS

ABSTRACT AND OVERVIEW

In this report, the first results for the Atlantic Coastal Plain drilling program are reported by the Geophysics group for 17 holes drilled in New Jersey, Delaware, Maryland, and Virginia. Average geothermal gradients range from about 25 °C/Km to a high of 45 °C/Km. Three sites, Salisbury, MD, Crisfield, MD, and Wallops Island, VA, have sufficiently high thermal gradients to warrant further study to outline the thermal anomaly and to discover if they are associated with a potential field anomaly. Hole 25 drilled at the center of a well-defined negative gravity anomaly near Portsmouth, VA has a gradient of 35 °C/Km which is significantly greater than the 25°C/km gradient of hole 26 drilled nearby. This supports the radiogenic model and suggests that such gravity lows are associated with granitic rocks which act as greater than normal heat sources buried by the insulating cover of the coastal plain.

Dashevsky describes his work on the approach to thermal equilibrium of the coastal plain holes. The original temperature gradient is disturbed by the drilling and, more importantly, by the heat of crystallization of the cement used to seal the holes. The holes approach their equilibrium gradient exponentially and are within 5% of their equilibrium value at approximately 450 hours after cementing.

Costain, Perry, Dashevsky, and Sans report a new heat flow value for the Siloam 1 drill hole in the Siloam Pluton, GA of 1.53 x 10^{-6} cal/cm^2-sec (1.53 HFU). This is the highest value reported in the southeastern USA. The authors conclude that a similar pluton, buried under the insulating cover of the Atlantic Coastal Plain, could easily account for the high geothermal gradients now being found there. Using the empirical linear relation between heat flow and heat generation, the Siloam pluton was originally chosen to be drilled because the high heat production of the surface samples would predict a high heat flow. Costain and Perry, in their section on the linear relationship between heat flow (Q) and heat production (A), discuss the importance of the Siloam in confirming this relationship given by

$$Q \text{ (HFU)} = 0.65 + 8.0A \text{ (HGU)}$$

for values of A greater than 6 HGU (1 HGU = 10^{-13} cal/cm^3-sec) for the smaller, post- and pre-metamorphic plutons of the southeastern USA. The failure of the larger, syntectonic plutonic complexes such as the Petersburg and Rolesville to conform to this linear relationship remains unexplained. It must be noted, however, that this linear relation still provides a minimum estimate of heat flow in these cases.

Regular readers of these reports are aware of the lively interest in the reason or reasons why the heat productions of near-surface rocks, subject to varied histories, should give a good indication of heat flow from the earth s crust lying beneath them. Explanations eventually reguire knowledge of the geologic behavior of the radiogenic elements, particularly uranium and thorium, which would form the basis or test of any explanation. Speer, for the Liberty Hill, and Becker, for the Winnsboro, report for these granites on the location of uranium by fission track techniques. They find the majority of the U in accessory minerals: uranothorianite, thorite, allanite, xenotime, zircon, apatite, and epidote. Previously identified Th sites are thorite, uranothorianite, allanite, and xenotime. The remaining U is associated with alteration features of the rocks and microcracks as a result of absorption or reduction of mobile U^{+6} to immoble U^{+4} by oxidation of iron oxides and silicates. These studies demonstrate the theoretical possibility that the more mafic rocks are able to buffer the oxygen fugacity and prevent uranium loss by preventing U^{+4} oxidation to hte more soluble U^{+6} complexes. The question remains on how efficient this process is and how much uranium has migrated out of the system.

Sans, in his discussion of the Woodstock granite in Maryland, shows the feasibility of the Th being largely present in the allanite.

The basis for models, hypotheses, and assumptions concerning the behavior of radiogenic elements and what lies beneath the Atlantic Coastal Plain requires geologic knowledge. These studies continue in several areas of the southeast. Bobyarchick reports on the setting of the exposed Petersburg granite of Virginia. This is a large, 4000 km^2, syntectonic granite with a large extension beneath the coastal plain. It is one of the plutons which does not follow the linear relationship between heat flow and heat generation. Bobyarchick finds the granite is bounded by a much larger number of ductile deformation zones and superimposed brittle faults than previously supposed.

Speer and Becker describe the Palmetto pluton, Georgia, one of the post-metamorphic plutons which has been drilled for heat flow determination. They find this westernmost pluton has crystallized under a higher water pressure than those to the east. The heat production of the Palmetto granite is significantly higher than the enclosing granitic country rock.

Becker reports on the petrography and chemistry of the Cuffytown Creek drill hole, SC. She finds the rocks similar to the surface rocks which were reported previously (Becker, VPI&SU-5648-3). This hole will be interesting in terms of its heat flow in view of its high average heat production of 12.5 HGU.

Hall, in his effort to characterize the major element chemistries of the granites, discusses the results from the Palmetto, Pageland, and Siloam granites. He finds the granites to have alkaline to calc-alkaline affinities.

In a continuing and intensive study of the small Woodstock granite in Maryland, Sans reports on the chemistry and differentiation of the granite and their concentric nature. This is discussed in light of his previously reported concentric distribution of Th (VPI&SU-5648-3). Uranium is uncorrelated with any chemical parameter which is attributed to the arbitrary effects of weathering.

RESEARCH OBJECTIVES

The objective of this research is to develop and apply targeting procedures for the evaluation of low-temperature radiogenically-derived geothermal resources in the eastern United States utilizing geological, geochemical, and geophysical data.

The optimum sites for geothermal development in the tectonically-stable Eastern United States will probably be associated with areas of relatively high heat flow derived from crustal igneous rocks containing relatively high concentrations of radiogenic heat-producing elements. The storage of commercially-exploitable geothermal heat at accessible depths (1-3 km) will also require favorable reservoir conditions in rocks overlying a radiogenic heat source. In order to systematically locate these sites, a methodology employing geological, geochemical, and geophysical prospecting techniques is being developed and applied. The distribution of radiogenic sources within the igneous rocks of various ages and magma types will be determined by a correlation between radioelement composition and the bulk chemistry of the rock. Surface sampling and measurement of the radiogenic heat-producing elements are known to be unreliable as they are preferentially removed by ground-water circulation and weathering. The correlation between the bulk chemistry of the rock (which can be measured reliably from surface samples) and radiogenic heat generation is being calibrated by detailed studies at a number of locations in the eastern United States.

Initial studies are developing a methodology for the location of radiogenic heat sources buried beneath the insulating sedimentary rocks of the Atlantic Coastal Plain. Choice of a drill site in the Atlantic Coastal Plain with a high geothermal resource potential depends on favorable:

(1) concentration of radiogenic elements in granitic rocks beneath a sedimentary insulator;

(2) thermal conductivity of the sedimentary insulator;

(3) thickness of the sedimentary insulator; and

(4) reservoir conditions in the permeable sedimentary rocks overlying the radiogenic heat source.

Because it is not economically feasible to select drilling sites on the Atlantic Coastal Plain without geophysical and geological models, it is advisable to base the development of these models on a substantial and accurate data base which can be partially derived from the exposed rocks of the Piedmont and enhanced by basement studies beneath the Atlantic Coastal Plain.

PERSONNEL OF PROGRAM

July 1, 1978 - September 30, 1978

GEOLOGY AND PETROLOGY, Lynn Glover III, Principal Investigator

J. A. Speer, Research Associate
S. S. Farrar, Research Associate
S. W. Becker, Research Associate
R. J. Gleason, Research Associate
A. Bobyarchick, Research Associate

GEOCHEMISTRY, A. Krishna Sinha, Principal Investigator

J. R. Sans, Research Associate
S. T. Hall, Research Associate
B. Hanan, Graduate Research Associate
S. Dickerson, Laboratory Aide
S. P. Higgins, Laboratory Aide
C. R. Miner, Laboratory Aide
C. M. Sadick, Data Entry Operator

GEOPHYSICS, John K. Costain, Principal Investigator

A. H. Cogbill, Research Associate
L. D. Perry, Research Associate
J. J. Lambiase, Research Associate
S. Dashevsky, Research Specialist
B. U. Sans, Research Specialist
M. Svetlichny, Research Specialist
T. H. Arnold, part-time Laboratory Aide
R. W. Meier, Co-op Student

ADMINISTRATIVE ASSISTANT
Margaret Paterson

SECRETARIES
Margie Strickler
Tish Glosh
Nhury Schurig

DRAFTSMAN-PHOTOGRAPHER
David Brown

DRILLERS
W. G. Coulson, Core Driller
David Thomas, Driller Helper

TALKS GIVEN TO DATE

1. Low-temperature resources of the eastern United States, Second NATO-CCMS Meeting on Dry Hot Rock Geothermal Energy, Los Alamos Scientific Laboratory, Los Alamos, New Mexico, June 28, 1977 (Speaker: J. K. Costain).

2. Low-temperature geothermal resources of the eastern United States, Geological Society of Washington, Washington, D. C., October 12, 1977 (Speaker: J. K. Costain).

3. Low-temperature geothermal resources in the eastern United States, 1977 Annual Meeting of the Geological Society of America, November 8, 1977 (Speaker: J. K. Costain).

4. Evaluation of the geothermal potential of hot springs in Northwestern Virginia, American Nuclear Society, Denver, Colorado, April 13, 1977 (Speaker: P. A. Geiser, University of Connecticut).

5. Low-temperature geothermal resources in the eastern United States, Potomac Geophysical Society, November 17, 1977 (Speaker: J. K. Costain).

6. Structural controls of thermal springs in the Warm Springs anticline, by P. A. Geiser and J. K. Costain, Southeastern Geological Society of America meeting, Winston-Salem, North Carolina, 1977 (Speaker: P. A. Geiser).

7. Geothermal resource potential of the eastern United States, Geothermal Resource Council Special Short Course No. 7, "Geothermal Energy: A National Opportunity" (The Federal Impact), May 17-18, 1978, Washington, DC (Speaker: J. K. Costain).

8. Geothermal resource potential of the eastern United States, Nordic Symposium on Geothermal Energy, Gothenburg, Sweden, May 29-31, 1978 (Speaker: J. K. Costain).

ABSTRACTS PUBLISHED TO DATE

1. Evaluation of the geothermal potential of the hot springs of northwestern Virginia, by P. A. Geiser and J. K. Costain, Abstracts of ANS Topical Meeting on Energy and Mineral Resource Recovery, Golden, Colorado, April 12-14, 1977, p. 33.

2. Structural controls of thermal springs in the Warm Springs anticline, Virginia, by P. A. Geiser and J. K. Costain, Abstracts, Geol. Soc. America SE Section, Winston-Salem, North Carolina, 1977.

3. Low-temperature geothermal resources in the eastern United States, by J. K. Costain, L. Glover III, and A. K. Sinha, Program with Abstracts, Annual Meeting of Geological Society of America, Seattle, Washington, 1977.

4. Relationship between heat flow and heat generation in the southeastern United States, by J. K. Costain and A. K. Sinha, Program with Abstracts, Geological Society of America, SE Section Meeting, April, 1978.

5. A new model for the linear relationship between heat flow and heat generation, J. K. Costain, Transactions, American Geophysical Union, 59, 1978, p. 392.

PAPERS SUBMITTED FOR PUBLICATION

1. Molybdenum mineralization in the Liberty Hill and Winnsboro Plutons, South Carolina, by J. Alexander Speer, Economic Geology, 1978 (in press).

2. Low-temperature geothermal resource potential of the eastern United States, by J. K. Costain, L. Glover, III, and A. K. Sinha, submitted for publication in EOS, Transactions, American Geophysical Union.

PROGRESS

A. GEOLOGY AND PETROLOGY

Lynn Glover III, Principal Investigator

J. A. Speer, Research Associate

S. S. Farrar, Research Associate

S. W. Becker, Research Associate

R. J. Gleason, Research Associate

A. Bobyarchick, Research Associate

RECONNAISSANCE GEOLOGIC SETTING OF THE PETERSBURG GRANITE AND REGIONAL GEOLOGIC FRAMEWORK FOR THE PIEDMONT IN SOUTHEASTERN VIRGINIA

Andy R. Bobyarchick

Preface

This article is a revision, with addition of new data collected during August and September, 1978, of a previous article, "The Petersburg Batholith" (Bobyarchick, 1977, Progress Report VPI&SU-5103-4, p. A-26-41).

Abstract

The Petersburg granite comprises three elongate bodies in the Piedmont of southeastern Virginia which together underlie a minimum of 4000 km**2 of area west of the fall line. The Petersburg, which occurs in porphyritic, massive and foliated phases, has at least one foliation, inferred to be a syntectonic igneous foliation, and was emplaced in the waning stages of regional prograde metamorphism. Xenoliths of the granitic and partially migmatitic country rocks which the granite intruded were strongly foliated before the time of emplacement. Metavolcanic rocks correlated with the eastern Carolina slate belt are, except for possible high

grade equivalents west of the Petersburg granite, allochthonous and bound by mylonite zones or brittle faults. Structurally lower amphibolite facies gneisses have an uncertain relationship to the slate belt rocks. They could be as old as 1.0 b.y. or as young as Cambrian.

After emplacement of the Petersburg about 300 m.y. ago, a system of late Paleozoic mylonite zones, including the Hylas zone, formed in a 10-15 km wide corridor between the westernmost and easternmost bodies of granite. The Triassic Richmond basin and approximately contemporaneous high grade brittle faulting were superimposed on this corridor, primarily localizing along mylonite zones. Thus, the regional framework for the southeastern Virginia crystalline Piedmont is one characterized by post-metamorphic ductile deformation zones and superposed brittle faults.

Introduction

> "Here the water has washed the granite bare, and this locality is especially noteworthy. One encounters all of the principal constituents of granite, but not always equally and exactly mixed. Here are clumps of pure granular quartz, there, erratic chunks of beautiful and partly crystallized feldspar, at another place crude masses of finely flaked mica, mainly black--here are mica and quartz, mica and feldspar, feldspar and quartz, now by themselves, now all three mixed together. One sees a hardened dough whose constituents, when it was still soft and fluid, were not properly kneaded together."
>
> --Johann David Schopf (1787)
> (written of granite along the James River in Richmond)

Watson (1906) described three phases of granitic rocks from the Richmond, Petersburg and Fredericksburg areas in Virginia: (1) light gray, medium to coarse grained granite with phenocrysts from 1 mm to 5 mm long (the Richmond-Petersburg light gray granite); (2) a finer grained dark blue granite of approximately the same composition (the Richmond-Fredericksburg dark blue gray granite); and (3) in the vicinity of Midlothian, Virginia, a porphyritic granite with euhedral potassium feldspar phenocrysts as much as 5 cm long. Watson (1906, p. 534) assumed the dark blue granite to be younger than the light gray phase because apparent xenoliths of light gray granite in the dark blue phase were exposed locally in quarries in the Richmond area. However, Bloomer (1939, p. 143) concluded that the blue granite was essentially contemporaneous with the gray granite because of gradational contacts between the two phases, the finer grained phase representing partially assimilated xenoliths of gneiss or schist from the country rocks. Bloomer s interpretation is supported by the present study.

Granitic rocks apparently of igneous origin south of Richmond to the North Carolina state line in the eastern Piedmont were shown as "Petersburg granite" on the 1928 geologic map of Virginia (Stose, 1928). Shortly thereafter, Jonas (1932, p. 243) referred to undeformed late Paleozoic granite in Virginia southwest of Richmond as "Petersburg granite." Bloomer (1939, p. 141) specified "Petersburg granite" as that granite exposed in Hanover County, Virginia, southward into North Carolina.

The purpose of the present study is to describe the regional geologic framework into which Petersburg granite was emplaced and to outline modifications of that framework by post-intrusion deformations. Because field investigation for this study was primarily reconnaissance in nature, a comprehensive detailed analysis is not provided. The broad framework that is presented may form a basis for future detailed studies.

Regional Geology

Precambrian(?) and Paleozoic(?) Rocks

Few published detailed studies of the eastern Piedmont of Virginia south of the James River are available. Goodwin (1970), Weems (1974), Poland (1976), and Bobyarchick and Glover (in press) have investigated metamorphic rocks near the James River. The 1963 geologic map of Virginia (Virginia Division of Mineral Resources) shows metamorphic rocks enclosing the Petersburg granite in three broadly defined units: (1) mica gneiss; (2) phyllite; and (3) hornblende gabbro and gneiss. Narrow belts of metamorphosed volcanic and sedimentary rocks are indicated near

Lawrenceville, Virginia, and along the Brunswick County-Greensville County boundary of the North Carolina state line. Parker (1968) published a reconnaissance structure map of the central eastern North Carolina Piedmont.

Country rocks associated with Petersburg granite comprise either fault-bounded, greenschist facies metavolcanic rocks or migmatitic layered gneiss (Figure A1). Non-migmatitic, strongly layered biotite gneiss, intercalated with amphibolite, biotite schist and granitic gneiss is dominant along the James River and northward. Coarse grained, weakly foliated metadiorite crops out near the Nottoway River, southwest of Petersburg and appears to be bound by mylonite zones.

<u>Granitic gneiss</u> (<u>grgn</u>). Fine to medium grained, strongly foliated, variably layered granitic gneiss forms a migmatite terrane between the eastern and western bodies of Petersburg granite; the smaller central body of granite is surrounded by this lithology. Selvages of biotite gneiss and amphibolite are numerous within the granitic gneiss and occur as discontinuous, irregular masses varying in size between a few cm and several m. Where uninterrupted by later dike intrusion, the gneissic selvages generally lie concordantly to the foliation in enclosing granitic gneiss.

Lineated, medium to coarse grained (0.5 mm to 0.8 mm) biotite-muscovite granitic orthogneiss (compositionally granodioritic with less than 10 percent mafics) with

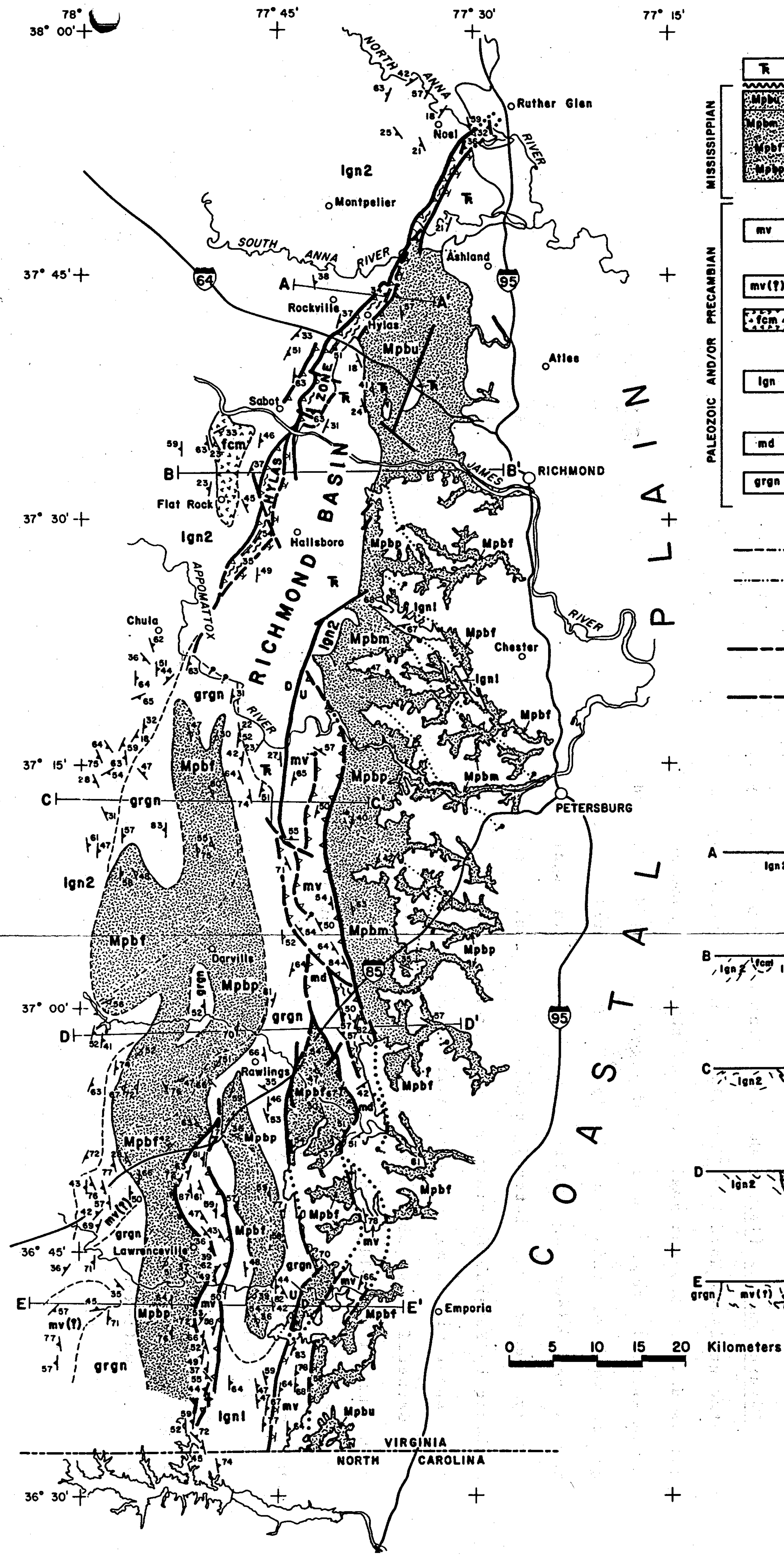

EXPLANATION

MISSISSIPPIAN

PALEOZOIC AND/OR PRECAMBIAN

Ʀ Triassic sedimentary rocks.

Mpbu / Mpbm / Mpbf / Mpbp Petersburg granite. Mpbu--undifferentiated granite; Mpbm--medium to coarse grained, weakly or nonfoliated massive granite; mpbf--moderately to strongly foliated, medium grained gray granite; Mpbp--coarse grained, moderately to strongly foliated porphyritic granite.

mv Metamorphosed sedimentary and volcanic rocks. Includes: red and green variegated argillite or slate; greenish gray phyllite; gray to white fine grained crystal tuff; rhyodacitic epidote-actinolite(?)-plagioclase gneiss; graphitic andalusite phyllite and schist; muscovite schist; biotite-muscovite schist; chlorite schist and chlorite-amphibole-talc. Equivalent to eastern Carolina slate belt.

mv(?) Biotite-muscovite schist and gneiss with local pods of chlorite schist. Probably equivalent to mv.

fcm Fine Creek Mills Granite (Poland, 1976).

lgn Layered gneiss. lgn1--layered intermediate to mafic gneiss east of easternmost Petersburg granite and metamorphic screens within the granite. Dominantly medium grained biotite gneiss with minor amphibolite. lgn2--garnetiferous muscovite-biotite schist and gneiss interlayered with coarse amphibole gneiss and amphibolite. Includes Sabot Amphibolite and Maidens Gneiss (Poland, 1976).

md Coarse grained metadiorite.

grgn Fine to medium grained, strongly foliated, variably layered migmatitic granitic gneiss. Includes lineated, medium to coarse grained muscovite-biotite granitic orthogneiss at Rawlings, Virginia.

Contacts

Geologic contact; dashed where inferred, dotted where covered, queried where doubtful.

Phase boundary in Petersburg granite; dotted where covered, queried where doubtful.

Faults

Shear or shear zone boundary; teeth indicate dip of mylonitic foliation, dashed where inferred, dotted where covered, queried where doubtful. Wavy dashes indicate shear zones. Tick on tooth edge indicates brittle fault present.

Brittle fault; dashed where inferred, dotted where covered, queried where doubtful. U--upthrown side; D--downthrown side.

Structure Symbols

30 77 80 30 45

S_b S_1 S_2 S_g S_e

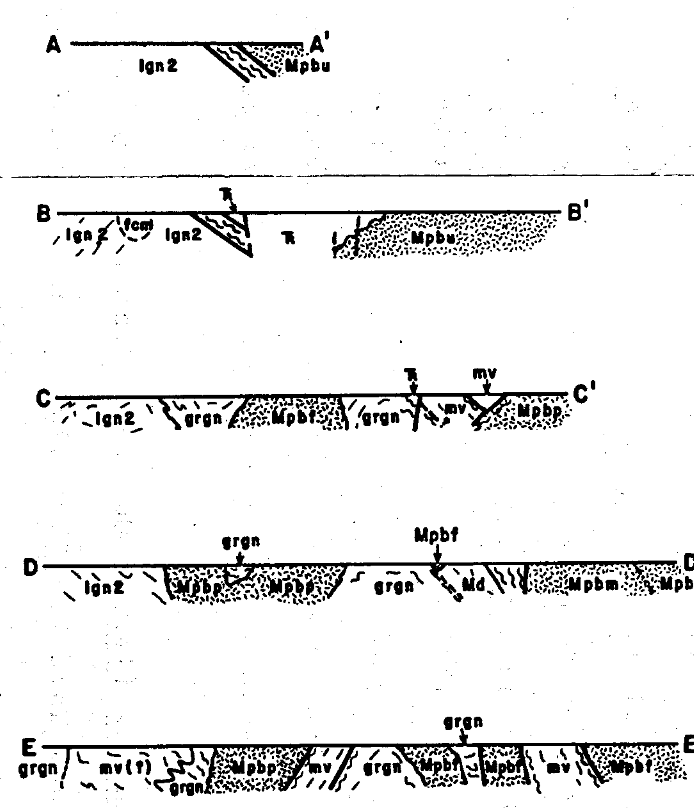

numerous thin mafic schlieren occurs at Rawlings, Virginia. The orthogneiss, although possessing a weak compositional layering of quartzofeldspathic and micaceous bands, is texturally and compositionally homogeneous when observed in larger outcrops. The regional extent of orthogneiss is uncertain because of its similarity in saprolitized exposures to fine grained migmatitic granitic gneiss. Therefore, the Rawlings orthogneiss is not mapped separately on Figure A1.

Layered gneiss (lgn). Complexly interlayered, strongly foliated gneisses have been broadly grouped into two layered gneiss units. Layered gneiss east of the Hylas zone and its southwestward projection is designated lgn1 while layered gneiss west of this zone is lgn2. In general, biotite gneiss and minor amphibolite are dominant in lgn1 and locally occur as interdigitating metamorphic screens enclosed by Petersburg granite. Smaller bodies of this unit also appear within migmatitic granitic gneiss.

Garnetiferous muscovite-biotite schist interlayered with thin (generally less than a few m) amphibolite or amphibole gneiss is characteristic of lgn2 south of the Appomattox River. Here, the layered gneiss is locally intensely intruded by coarse grained, slightly discordant felsic pegmatite swarms. Rotation of angular gneiss fragments by invading pegmatites was observed. It is likely that the well-known Amelia pegmatites (Pegau, 1932) were contemporaneous with these dike swarms. North of the Appomattox River, lgn2 includes biotite gneiss and granitic gneiss, mapped by Poland (1976) as, respectively, Maidens Gneiss and State Farm Gneiss. These rocks are not characterized by abundant discordant pegmatites.

Metavolcanic rocks (mv). Stratified rocks primarily of volcanic origin occur in three narrow, sinuous belts that are bound by mylonite zones or brittle faults (Figure A1). Although the belts are structurally distinct and regional metamorphism varies from belt to belt, it is apparent that the dominant lithology is very fine grained, locally red and green variegated slate or argillite at low metamorphic grade. Preserved original layering, which is generally discordant to the oldest metamorphic foliation, locally shows weak grading. Easternmost belts of mv rocks contain slates and phyllites, derived from the same or similar protolith, interlayered with fine grained crystal tuffs, rhyodacites with euhedral quartz and zoned plagioclase phenocrysts, greenstones, chlorite schist and chlorite-amphibole-talc schist.

The belt of mv rocks east of Lawrenceville is dominated in its central region by graphitic chiastolite phyllite and graphite-bearing biotite-andalusite-muscovite schist. However, fine-grained felsic tuffs also occur in this belt interlayered with more abundant muscovite schist. Coarse pyroclastic deposits, such as those described by Glover and

Sinha (1973) and Wright (1975) from the western Carolina slate belt, and those noted by S. S. Farrar (personal communication) in the northeastern North Carolina Piedmont were not observed in the mv unit in the present study.

Metaigneous rocks. Two igneous bodies occur in the study area outside the Petersburg granite. The Fine Creek Mills Granite (fcm, Figure A1) crops out in the core of a regional antiformal structure. Poland (1976, p. 30-36) described the petrography and structure of this rock, which is a two feldspar biotite granite. It is apparently a synmetamorphic intrusion into lgn2 gneisses.

Coarse grained (as much as 0.7 mm), weakly foliated metamophosed (original mineralogy) allanite-biotite-(hornblende?)-clinopyroxene-plagioclase (An_{34} to An_{40}) diorite (md) crops out west of DeWitt and extends southward to apparently disappear beneath the Coastal Plain near the southeastern boundary of the study area (Figure A1). The present mineralogy of this rock is pyrite-titanite-quartz-epidote-chlorite-biotite-hornblende-clinopyroxene-plagioclase with minor accessory apatite. Crystal forms of plagioclase appear to have been little affected by regional metamorphism. Pyroxene now occurs as turbid, skeletal relicts in hornblende grains, which locally retain pyroxene shapes. However, many pyroxene grains appear relatively unaltered where they are surrounded by plagioclase and/or quartz. Grain boundaries of the original igneous rock are very straight whereas those apparently produced during metamorphism, especially in hornblende, are irregular.

Mesozoic and Cenozoic Rocks

Terrestrial clastic sedimentary rocks and coal of Upper Triassic age (Roberts, 1928, p. 137-139) occur in fault or nonconformable contact with country rocks or the Petersburg granite (Figure A1). These rocks, which form the Richmond Basin and Taylorsville Basin, are generally quartz arkose, subarkose and hematitic mudstone with lesser amounts of coal, and fanglomerate as marginal facies. The feather edge of the Coastal Plain overlap in this study area is characterized by a thin veneer of generally unconsolidated hematitic clay and arenite, and locally in upland areas by quartz cobble alluvial deposits. Quaternary alluvial sediments occur extensively in lowland creeks and along major rivers; these have been omitted from Figure A1.

The Petersburg Granite

General

Petersburg granite crops out in three elongate, northerly-trending bodies in the study area (Figure A1).

Together, granite underlies a minimum of 4000 km^2 of area in the Virginia Piedmont west of the fall line. Three mappable phases recognized in the eastern Petersburg pluton are shown on Figure A1. Generally, all phases are modally granites so that the phase designations are based on grain size and texture. Except for coarse grained porphyritic microcline granite, which contains euhedral microcline phenocrysts, all rocks are hypidiomorphic granular to allotriomorphic granular and massive. Some foliate phases show incipient compositional layering and shape oriented fabrics defined by quartz and some feldspars. The primary mineralogy comprises quartz, plagioclase, microcline and less than about five percent green-brown biotite with minor amounts of muscovite, allanite and titanite. Foliated and porphyritic phases are predominant in the granite. Massive, weakly or nonfoliated granite and aplite dikes are relatively minor constituents.

Igneous Phases

<u>Massive phase</u> (<u>Mpbm</u>). The massive phase of the Petersburg granite is a medium to coarse grained, weakly- or nonfoliated, massive pink biotite with grain sizes of 5 mm to 1 cm. Potassium feldspar is microcline or microperthitic microcline. This phase contains schlieren a few cm long formed by biotite aggregates, especially in marginal zones close to country rocks.

Porphyritic phase (Mpbp). Coarse to very coarse grained, locally strongly lineated, moderately foliated porphyritic microcline granite crops out in a northwest to southeast trending belt along the medial part of the eastern Petersburg body and in north or northeast trending belts in the central and western bodies. This phase contains euhedral microcline phenocrysts as much as 3 cm long. Most exposures of porphyritic granite have a strongly lineatd fabric defined by orientation of long axes of tabular microcline phenocrysts.

Foliated Phase (Mpbf). Fine to medium grained biotite granite (CI = 5-15 percent) is the least distinct and most variable phase of the Petersburg granite; some varieties may be granodiorite. Weak compositional layering, defined mainly by segregation of mafic and felsic minerals, is best expressed at the marginal zones of the granite where this phase is present. The foliated phase of the Petersburg granite is distinguished by always having a moderately to strongly developed foliation in fine to medium grained, roughly equigranular granite.

The relationship of the three dominant phases of Petersburg granite in this paper to those of Watson (1906) and Bloomer (1939) is uncertain because these earlier workers concentrated on quarry localities, several of which were not examined for this study. However, it is probable that the foliated phase (Pgf) is equivalent to "dark blue granite" because of a relatively greater mafic content and fine to medium grain size. "Light gray granite" probably refers to the massive phase (Pgm), which is usually pink upon weathering. Porphyritic phases appear identical. Trends of the phase boundaries are generally discordant to the elongate shape of Petersburg granite bodies except for the smaller central body. Because of poor exposure and locally widely-spaced observation stations, these boundaries must be considered approximate, but within the eastern body they consistently form northwest-trending zones. A similar consistency is maintained by northeast-trending boundaries in the western body. The porphyritic and foliated phases generally lie in parallel belts and do not clearly show relative intrusive relationships. They are considered approximately contemporaneous. Aplites clearly intrude porphyritic and foliated phases as planar, nonfoliated dikes. The massive, weakly or nonfoliated phase of Petersburg granite is of uncertain relationship to the other phases.

Metamorphism

Only one regional prograde metamorphism has been interpreted to affect rocks in the lgn2 unit along the James River (Bobyarchick and Glover, in press), although recent Rb/Sr isotope studies of the State Farm Gneiss (Glover and others, 1978) may indicate at least some of the rocks were metamorphosed previously. Retrograde metamorphism was contemporaneous with ductile shearing throughout mylonite zones in the study area and post-dated regional prograde metamorphism. In addition, during Triassic time fracturing and faulting at depth facilitated zeolite facies metamorphism.

Regional Metamorphism (M_1)

All country rocks older than the Petersburg granite have been subjected to regional metamorphism ranging from lower greenschist facies to at least lower amphibolite facies. Descriptive mineralogy of gneisses along the James River is given by Poland (1976) and Bobyarchick (1976). In general, metamorphic grade increases from east to west along the James River; kyanite occurs in pelitic schists just west of the Richmond Basin while rocks of similar bulk composition near Thorncliff, Virginia, contain sillimanite (Poland, 1976). Unfortunately, most lithologies in the grgn and lngl units in the Petersburg border zones are not of appropriate composition for formation of metamorphic index minerals.

Because metavolcanic rocks in the mv unit are allochthouous in post-metamorphic belts, it is difficult to relate their present mineralogy to M_1 There does appear to be an east to west increase from belt to belt, however, ranging from weakly metamorphosed slate in the eastern belt to graphitic andalusite-muscovite schist in the westernmost belt. It is not clear whether andalusite in these schists is regionally significant or whether it is related to pre-faulting contact metamorphism. A progression within the western belt from phyllites to schists, and eventually to biotite-muscovite schist with thin (less than 5 cm) concordant felsic segregations of metamorphic origin is indicative of prograde metamorphism within the belt. Quartzites interlayered with biotite-muscovite schist in mv(?) rocks west of the Petersburg granite contain kyanite. Here, much of the kyanite is fibrous in hand specimen and the mineral may have replaced sillimanite.

Retrograde Metamorphism (M_2)

Syntectonic recrystallization localized in ductile or semiductile shear zones occurred as a result of mylonitization post-dating regional metamorphism (Bobyarchick and Glover, in press). Recrystallization, where it has been observed in amphibolite facies rocks, produced characteristic greenschist facies minerals including chlorite, white mica, epidote, and sodic plagioclase. Therefore, the metamorphism was retrogressive in relation to regional metamorphism in the lgn units and the grgn unit. However, mylonite zones other than the Hylas zone (Bobyarchick and Glover, in press), especially those bounding low grade mv rocks, have not been examined in detail petrographically. Whether recrystallization occurred in these rocks is at present uncertain.

Zeolite Metamorphism (M_3)

Zeolites are widespread throughout the Piedmont (Privett, 1974). In all quarry sites in the Petersburg granite investigated for this report zeolites were found in fracture zones and as fracture surface coatings. In more intensely deformed areas, zeolites have been observed in the groundmass of country rocks and locally replace plagioclase. Laumontite, confirmed optically and by x-ray diffractometry, is the only zeolite identified so far in fracture zones in the Hylas zone and is usually accompanied by calcite, quartz and pyrite.

Brittle fractures that created the zeolite environment are concentrated around the margins of the Richmond Basin and extend north and south from the basin generally as superposed deformation on older mylonite zones.

Structure

A discussion of the detailed structure of the eastern Piedmont of Virginia is beyond the scope of this paper. Bobyarchick and Glover (in press) and Poland (1976) present this data for rocks along the James River in the northern part of the present study area. However, the general structural framework developed by Bobyarchick and Glover (in press) can be applied tentatively to the terrane south of the James River because continuity of structural elements has been established by reconnaissance mapping. This framework is reviewed below.

Review of Regional Ductile Deformations

Two periods of ductile deformation, D_1 and D_2, were approximately coeval with regional metamorphism in rocks which reached greenschist or amphibolite facies. D_1, the principal deformational event, resulted in a pervasive schistosity in the lgn units and grgn unit and phyllitic lamination or slaty cleavage in the mv unit (S_1). In outcrops where original sedimentary or igneous layering, S_b, was preserved, S_1 generally transects S_b at a moderate angle. Although regional bulk compositional layering appears parallel to S_1, most mesoscopic compositional layering in gneissic rocks, S_0, is probably of metamorphic origin, because there appears to have a progressive segregation of mafic and felsic minerals parallel to S_1 during metamorphism.

S_2, a non-pervasive cleavage formed during D_2, is of slightly different character in the mv unit than in higher grade rocks. Microstructures indicate that in amphibolite facies rocks, D_2 was accompanied by a subtle recrystallization and reorientation of biotite folia (S_2) axial planar to F_2 folds. Brittle deformation, such as bending or kinking, is absent in the micas. Well equilibrated grain boundaries and lack of ubiquitous strain suggest the thermal episode maintained a fairly consistent temperature throughout D_2 However, S_2 occurs as either a simple rock cleavage (in slates and some phyllites) or a locally strong crenulation of S_1, with incipient chlorite recrystallization along the crenulations, in the mv unit.

Granite Foliation

Foliations in the Petersburg granite are complex in origin. The foliation, S_g, is defined by planar orientation of tabular microcline phenocrysts, biotite folia and shape orientation of quartz. Recrystallization and deformation effects are best demonstrated by quartz. Most grains have undulatory extinction and show early stages of subgrain development varying from very diffuse, shadowy boundaries to sharply defined but irregular boundaries. Some quartz aggregates have straight or smoothly curved grain boundaries, although individual grains show some subgrain development. Here, the lower energy (smoothly curved) boundaries might be of igneous origin. Deformation of quartz appears most intense in porphyritic granite phases. However, microscopically and mesoscopically in some coarser phases of Petersburg granite mica grains show a poorly developed parallel orientation and probably more closely resemble an igneous texture.

Post-metamorphic Deformations

Paleozoic post-metamorphic ductile deformation was most intense in mylonite zones such as the Hylas zone (Bobyarchick and Glover, in press). Several shear zones south of the James River are considered contemporaneous with the Hylas zone because of their relation with the regional structure.

This period of localized shearing is D_3 Mylonites and ultramylonites formed in the shear zones by semiductile deformation and contemporaneous retrograde metamorphism. Microcline, garnet, and plagioclase reacted to stress by brittle fracture and dislocation. However, quartz and most mafic minerals (hornblende, biotite, allanite) were altered and recrystallized to a fine matrix of chlorite, epidote, magnetite, titanite, and quartz. The foliation thus formed is S_c (Bobyarchick and Glover, in press).

D_3 was apparently the last compressional deformation in the study area. Approximately 220 m.y. ago fracturing and high angle faulting were superimposed on the crystalline rocks (D_4) (Bobyarchick, 1976, p. 68). Faulting occurred in areas of prior weakness: 1) along postmetamorphic shear zones, and 2) locally along margins of the Petersburg pluton. Silicified breccia or microbreccia define these late faults. It was also at this time that differential subsidence initiated terrestrial sedimentation to form the Richmond-Taylorsville basin, which contains late Triassic sedimentary rocks.

Emplacement of the Petersburg Granite

Mapping in the contact zones and border facies of the Petersburg granite revealed that intrusion of the granite, which achieved batholithic proportions, post-dated D_1 Xenoliths, ranging in size from rafts several m long to mafic selvages a few cm long, generally exhibit pre-inclusion metamorphic foliations. Larger tabular xenoliths, particularly where enclosed by strongly foliated porphyritic granite, now lie concordant to the granite foliation and were locally fragmented into plates separated by granite. These xenoliths may be surrounded by fine grained felsic alteration rinds a few mm wide. In migmatitic rocks around the granite, S_1 was plastically deformed by flow folding and high temperature shears. Apophyses of granite occupy core zones of folds contemporaneous with intrusion that are defined by deformation of S_0 and S_1 Where amphibolite facies gneiss or schist was intruded by granite, the country rock was thoroughly recrystallized as evidenced by common optical orientaton of some mineral aggregates, such as hornblende, and straight grain boundaries not common to similar rocks away from the contact.

Final emplacement of the Petersburg granite and formation of S_g were approximately contemporaneous with D_2 and probably occurred during the waning stages of M_1 The granite intruded a gneiss terrane that had already developed at least one well defined metamorphic foliation. The elongate shape of Petersburg granite bodies in conformity to the general trend of foliations in the migmatite terrane, where 2, has probably been reoriented during intrusion, and the tectonic-igneous nature of S_g support a syntectonic emplacement of the granite. Conversely, pre-existing orientation of S_1 may have partially influenced the shape and orientation of Petersburg granite.

The relationship between Petersburg granite and rocks in the mv unit is obscured by fault zones. Blue-green amphibole and andalusite that occur locally in mv rocks have no strongly preferred linear orientations but their long crystallographic axes lie within foliation planes. Unlike hornfels produced by post-metamorphic granite intrusion into

Carolina slate belt rocks, mv rocks possess moderate to strong foliations.

Regional Framework

Stratigraphy in the mv unit is similar to sequences in the eastern Carolina slate belt (Cohee, 1962) as described by Parker (1963, 1968) and Wilson and Carpenter (1975) but differing in the relative proportions of rock types present. Fine grained ash and interlayered tufts probably represent distal facies in a primarily volcanic terrane. Although Sundelius (1970) indicated the Carolina slate belt ends near Petersburg , Virginia, the present paper extends slate belt lithologies as far north as central Chesterfield County. Glover and Sinha (1973, p. 243) showed that the age of volcanic rocks in the western Carolina slate belt near Roxboro, North Carolina, probably ranges from about 740 m.y. to about 575 m.y.; this range agrees with plutonism in the area (Fullagar, 1971). Glover (1974) suggested that the slate belt volcanics as young as 520 m.y. in central North Carolina are unconformable on the older sequence near Roxboro. McConnell (1974) confirmed the younger limit of volcanicity at about 520 m.y. ago. Correlation of volcanic rocks in the study area to dated rocks in North Carolina is difficult because of the lack of mapping in intervening areas.

Amphibolite facies rocks in the lgn and grgn units, which are considered part of the Raleigh belt (see Glover and Sinha, 1973) in Virginia, can not be clearly correlated with slate belt rocks. Biotite-muscovite schist and gneiss in the mv (?) unit west of Lawrenceville (Figure A1) are similar in bulk composition to lower grade rocks in the mv unit east of Lawrenceville. These rocks occur as irregular, but apparently conformable, masses within locally migmatitic granitic gneiss. A similar relationship was found by S. S. Farrar (personal communication) in the southern continuation of this terrane in northern North Carolina. Farrar (1977, progress report to D.O.E., V.P.I.&S.U.-5648-1, p. A-29) found that the Raleigh belt-eastern Carolina slate belt transition around the southern end of the Rolesville batholith is a metamorphic grade change. Tobisch and Glover (1969) reported that the western Carolina slate belt - Charlotte belt boundary is also a metamorphic isograd.

Layered gneisses in the lgn 2 unit, which includes in this report all gneisses northwest of the Hylas zone, are of uncertain relationship to gneisses around the Petersburg granite. At the southwest corner of the Richmond basin, a magnetic lineament is coincident with the boundary between lgn 2 gneisses and migmatitic granitic gneiss. At Deep River in the Wellville quadrangle, coarse grained, strongly foliated amphibole gneiss and amphibolite lie along the lineament. The lineament is considerably subdued where it intersects 78° longitude but southwestward projection of it across a gneiss terrane of relatively low magnetic relief indicates a possible intersection with the eastern edge of the western Carolina slate belt. Casadevall (1977), based on an aeromagnetic lineament, has extended the Nutbush Creek fault on the eastern edge of the western slate belt to the Falls, Virginia, near the northern terminus of the western Carolina slate belt (Virginia Division of Mineral Resources, 1963). Mapping for the present study did not reveal mylonites along the magnetic lineament between the Hylas zone and the Nutbush Creek fault. Instead, this lineament is presently interpreted to result from the compositional difference between lgn 2 gneisses and migmatitic granitic gneiss. If migmatization forming the grgn rocks and penetration of lgn 2 rocks by felsic pegmatites are part of the same process initiated by emplacement of Petersburg granite or even an earlier high grade event, the linear magnetic anomaly produced at the grgn-lgn 2 boundary may then be considered metamorphic in origin.

Glover and others (1978) reported a 1 b.y. Rb/Sr age for an igneous phase of the State Farm Gneiss, which occurs across the James River from the Fine Creek Mills Granite in an antiformal structure in lgn 2 rocks (Figure A1). (State Farm Gneiss is not shown on Figure A1). They suggested that amphibolite and metagraywacke conformably overlie State Farm Gneiss in this region; that granitic gneisses, especially those with migmatite textures, south of the Richmond basin may be correlative to State Farm Gneiss; and that Carolina slate belt rocks (mv unit in this paper) unconformably overlie these gneisses. Clearly, this correlation is acceptable should the Nutbush Creek fault, or the geophysical lineament that is known to define a mylonite zone on the eastern margin of the western slate belt, project not northeastward into the Hylas zone but more northerly to coincide with a remarkably linear eastern boundary on a large granite gneiss complex as shown on the geologic map of Virginia (Virginia Division of Mineral Resources, 1963). The relationship, then, between mv (?) rocks and structurally lower granitic gneiss west of Lawrenceville becomes problematic, for no obvious unconformable contact is present.

Intrusion of the Petersburg granite about 330 m.y. ago (Wright and others, ;1975) was probably part of a large magmatic episode in what is now southeastern Virginia and northeastern North Carolina. The Rolesville batholith (Parker, 1968, 1977; Wilson and Carpenter, 1975; Becker and Farrar, 1977, progress report to E.R.D.A., V.P.I.&S.U.-5103-3, p. A-53-77) shares similar textural variations, composition, and relationships to country rocks with Petersburg granite. Although the age of the main part of the Rolesville is uncertain, the Castalia pluton on the northeast side of the batholith is about 320 m.y. old

(Julian, 1972). Because there is a possible correlation between part of the State Farm Gneiss and granitic gneiss around the Petersburg, it cannot be discounted that an earlier high grade, migmatitic terrane was intruded by granite, thereby, producing polymetamorphosed gneisses. However, the early prograde metamorphism must have occurred prior to deposition of slate belt rocks because these volcanic rocks have only endured one regional prograde metamorphism.

Nonfoliated aplite dikes and felsic pegmatites discordantly intruding both Petersburg granite and country rocks are thought to represent terminal igneous activity associated with emplacement of the Petersburg granite. Bobyarchick and Glover (in press) tentatively concluded from detailed mapping along the James River (Bobyarchick, 1976; Poland, 1976; Bourland, 1976) and isotope data of Fullagar (1971) on the Columbia granite that regional metamorphism in the eastern Virginia Piedmont took place about 340 m.y. ago. Geochronology and structural data, therefore, indicate that the Petersburg granite was emplaced within the latter phases of M1. Relative quiescence reigned until the vicious onslaught of mylonitization in late Paleozoic time.

Mylonites and Brittle Faults

A complex system of mylonite zones has resulted in locally profound modification of geologic relationships in the study area, particularly within a 10-15 Km wide corrider south of the Richmond basin along the margin of the eastern body of Petersburg granite (Figure A1). These shear zones may be regarded as part of the Eastern Piedmont fault system (Hatcher and others, 1977), which extends along the eastern edge of the Piedmont from Virginia to Alabama. All mylonites in the study area are interpreted to have been formed in late Paleozoic time, principally post-dating M1. Detailed studies of the Hylas zone (Bobyarchick, 1976; Bobyarchick and Glover, in press) indicate that ductile deformation in D_3 was contemporaneous with retrograde metamorphism within amphibolite facies rocks. Because Petersburg granite was mylonitized by some shear zones, deformation must have occurred after about 330 m.y. ago. Brittle faulting locally superimposed on mylonites was probably initiated about 220 m.y. ago (Bobyarchick and Glover, in press). Therefore, D_3 occurred in the 330 - 220 m.y. range. Some mylonite zones in the Eastern Piedmont fault system are older than this range. The Gold Hill fault in South Carolina is intruded by the Catawba granite, dated at about 330 m.y. old (Butler and Fullagar, 1977).

Motion along mylonite systems in southeastern Virginia is uncertain. Low to moderate dips of mylonite foliations are present in the Hylas zone. Motion along mylonite systems in southeastern Virginia is uncertain. (Bobyarchick, 1976), suggesting possible thrust movement. However, cataclastic thrust faults and folding of S_c in latter phases of D_3 have been documented in the Hylas zone (Bobyarchick and Glover, in press) and folding of mylonite zones south of Richmond is possible from their map patterns (Figure A1). Dip symbols on mylonite zone boundaries, therefore, reflect only the present mylonite foliation dips and do not necessarily indicate relative plate motion.

Although metavolcanic rocks in the mv unit are shear bound and allochthonous to structurally lower, higher grade gneisses, any postulated framework must explain apparently conformable relationships between the two terranes south of the Rolesville batholith, and possible similar relationships between mv (?) rocks and grgn rocks west of Lawrenceville. Principal thrust movement, with presumed westward vergence, may not be associated with large magnitude displacement because bodies of Petersburg granite occur on either side of the shear zone corridor. An alternate proposal for displacement is oblique or transverse motion of small magnitude. If shearing were accompanied by folding within nonmylonitic parts of mv belts, steeply dipping S_1 and S_c foliations could be explained without invoking intense post-mylonitization folding necessary to produce Sc patterns in the mv belt.

Regardless of displacement directions along the shear zones, the present study area lies approximately along the axis of the Virginia promontory (Williams, 1978), a southeastward convexity in the Appalachian orogen. This axis is approximately coincident with the junction zone between the central and southern Appalachians and is characterized in the Appalachian foreland by northerly structural trends north of the junction, on the dextral arm of the promontory, and more northeasterly structural trends on the sinistral arm of the promontory (Virginia Division of Mineral Resources, 1963; Williams, 1978). This geometry is partially mirrored in structural trends in the eastern Piedmont of Virginia and North Carolina (Virginia Division of Mineral Resources, 1963; Stuckey, 1958). Stubbs (1977) concluded from analyses of late discfolds in the Millboro Formation that the arcuate geometry of the junction zone resulted not from distortion of an early structural trend by superposed flexure of the orogen but from concurrent movement of material out of the junction. Thus, strain systems of probable late Paleozoic age affected the Appalachians from the eastern Piedmont to at least the eastern edge of the foreland. The position of the present study area, close to the axis of the Virginia promontory and within the zone of intense deformation, may have been responsible for the complex post-metamorphic shear systems imposed upon it.

Brittle deformation, essentially high angle faulting and fracturing, has been intermittently active in the Piedmont from the Early Triassic to at least the Paleocene. Bobyarchick and Glover (in press) determined that late Paleozoic mylonites in the Hylas zone were loci for Mesozoic deformation, initiated about 220 m.y. ago. A similar relationship applies to several mylonite zones in the study area.

Summary

The Petersburg granite was syntectonically emplaced into a gneissic terrane as young as Cambrian and possibly as old as 1 b.y. It is inferred to have been emplaced in the waning stages of regional metamorphism. The relationship between rocks of the eastern Carolina slate belt and structurally lower gneisses is obscured by mylonite zones and brittle faults ranging from the late Paleozoic to at least early Mesozoic. Thus, the original intrusive contacts of the Petersburg granite are preserved only along the western margin of the western body, around the smaller central body, and partially around metamorphic screens near the James River.

The fundamental structural framework of the Piedmont in southeastern Virginia is strongly influenced by the presence of numerous mylonite zones, whose magnitude and vergence are uncertain.

REFERENCES

Bloomer, R. O., 1939, Notes on the Petersburg granite: Virginia Geol. Survey Bull. 51-F, p. 137-145.

Bobyarchick, A. R., 1976, Tectogenesis of the Hylas zone and eastern Piedmont near Richmond, Virginia: unpublished MS thesis, Dept. of Geological Sciences, Virginia Polytechnic Institute and State University, Blacksburg, VA, 168 p.

Bobyarchick, A. R., and Glover, L., III, in press, Deformation and metamorphism in the Hylas zone and adjacent parts of the eastern Piedmont in Virginia: Geological Society of America Bulletin.

Bourland, W. C., 1976, Tectogenesis and metamorphism of the eastern Piedmont from Columbia to Westview, Virginia, along the James River: unpublished MS thesis, Dept. of Geological Sciences, Virginia Polytechnic Institute and State University, Blacksburg, VA, 113 p.

Butler, J. R., and Fullagar, P. D., 1977, The Gold Hill fault zone in the Carolinas: age of movement and southwesternmost extension: Geological Society of America Abstracts with Programs v.9, no.2, p. 125.

Casadevall, T., 1977, The Nutbush Creek dislocation, Vance County, North Carolina, and Mecklenburg County, Virginia -- a probable fault of regional significance: Geological Society of America Abstracts with Programs 9, p. 127-128.

Cohee, G. V. (ch.), 1962, Tectonic map of the United States: U. S. Geol. Survey and Am. Assoc. Petroleum Geologists.

Fullagar, P. D., 1971, Age and origin of plutonic intrusions in the Piedmont of the southeastern Appalachians: Geol. Soc. m Am. Bull., v. 82, no. 10, p. 2845-2862.

Glover, L., III, 1974, Speculations on the relation between eastern and western Piedmont volcanism (Abstract): Geol. Soc. America Abs. with Programs, v. 6, no. 7, p. 757.

Glover, L., III, and Sinha, A. K., 1973, The Virgilina deformation, a Late Precambrian to Early Cambrian (?) orogenic event in the central Piedmont of Virginia and North Carolina: Am. Jour. Sci., Cooper v. 273-A, p.234-251.

Glover, L., III, Mose, D. G., Poland, F. B., Bobyarchick, A. R., and Bourland, W. C., 1978, Grenville basement in the eastern Piedmont of Virginia: implications for orogenic models: Geological Society of America Abstracts with Programs, v. 10, no. 4, p. 169.

Goodwin, B. K., 1970, Geology of the Hylas and Midlothian quadrangles, Virginia: Virginia Division of Mineral Resources Rept. of Inves. 23, 51 p.

Hatcher, R. D., Jr., Howell, D. E., and Talwani, P., 1977, Eastern Piedmont fault system: speculations on its extent: Geology, v. 5, p. 636-640.

Jonas, A. I., 1932, Structure of the metamorphic belt of the southern Appalachians: Am. Journ. Sci., 5th ser., v. 24, p. 228-243.

Julian, E. L., 1972, The Castalia adamellite in Franklin and Nash counties, North Carolina, and the petrogenesis of some associated aplites and pegmatites (m.s.): Raleigh, North Carolina State University, 61 p.

McConnell, K. I., 1974, Geology of the Late Precambrian Flat River Complex and associated volcanic rocks near Durham, North Carolina: unpublished MS thesis, Dept. of Geological Sciences, Virginia Polytechnic Institute and State University, 64 p.

Parker, J. M., III, 1963, Geologic setting of the Hamme tungsten district, North Carolina and Virginia: U. S. Geol. Survey Bull. H22-G, 69 p.

__________, 1968, Structure of easternmost North Carolina Piedmont: Southeastern Geology, v. 9, no. 3, p. 117-131.

__________, 1977, Structure of Raleigh belt of eastern Piedmont in Wake County, North Carolina (Abstract): Geol. Soc. America Abs. With Programs, v. 9, no. 2, p. 173.

Pegau, A. A., 1932, Pegmatite deposits of Virginia: Virginia Geological Survey Bulletin 33, 123 p.

Poland, F. B., 1976, Geology of the rocks along the James River between Sabot and Cedar Point, Virginia (M.S.):

Blacksburg, Virginia Polytechnic Institute and State University, 99 p.

Privett, D. R., 1974, Widespread laumontization in the Central Piedmont of North Carolina and southern Virginia (Abstract): Geol. Soc. America Abs. with Programs, v. 6, no. 4, p. 389-390.

Roberts, J. K., 1928, Geology of the Virginia Triassic: Virginia Geol. Survey Bull. 29, 205 p.

Schopf, J. D., 1787, Beytrage zur Mineralogischen Kenntniss des Ostlichen Theils von Nord-Amerika und seiner Geburge (Contributions to the mineralogical knowledge of the eastern part of North America and its mountains), in, Spieker, E. M., translator, 1972, Contributions to the History of Geology, Volume 8: New York, Hafner Publishing Co., translation 171 p.

Stose, G. W., editor, 1928, Geologic map of Virginia: Virginia Geol. Survey.

Stubbs, J. L., Jr., 1977, Kinematic analyses of discfolds in Devonian Millboro Formation in the central-southern Appalachian junction zone (M.S.): Blacksburg, Virginia Polytechnic Institute and State University, 131 p.

Stuckey, J. L., 1958, Geologic map of North Carolina: North Carolina Division of Mineral Resources, 1 sheet, 1:500,000.

Sundelius, H. W., 1970, The Carolina slate belt, in Studies of Appalachian Geology: Central and Southern, Fisher,

G. W., Pettijohn, F. J., Reed, J. C., Jr., and Weaver, K. N. (eds.): New York, Interscience Publishers, p. 351-368.

Tobisch, O. T., and Glover, L., III, 1969, Metamorphic changes across part of the Carolina slate belt-Charlotte belt boundary, North Carolina and Virginia: U. S. Geol. Survey Prof. Paper 650-C, p. C1-C7.

Virginia Division of Mineral Resources, 1963, Geologic map of Virginia: 1 sheet, 1:500,000.

Watson, T. L., 1906, Lithological characters of the Virginia granites: Geol. Soc. Am. Bull., v. 17, p. 523-540.

Weems, R. E., 1974, Geology of the Hanover Academy and Ashland quadrangles, Virginia: unpublished MS thesis, Dept. of Geological Sciences, Virginia Polytechnic Institute and State University, Blacksburg, 100 p.

Williams, H., 1978, Tectonic lithofacies map of the Appalachian orogen: Memorial University of Newfoundland, 2 sheets, 1:1,000,000.

Wilson, W. F., and Carpenter, P. A., III, 1975, Region J. Geology: A guide for North Carolina mineral and resource development and land use planning: Region Geology Series 1, North Carolina Dept. Natural and Economic Resources, 76 p.

Wright, J. E., Sinha, A. K., and Glover, L., III, 1975, Age of zircons from the Petersburg Granite, Virginia; with comments on belts of plutons in the Piedmont: Am. Jour. Sci., v. 275, p. 848-856.

DESCRIPTION OF THE PALMETTO PLUTON, GEORGIA

J. Alexander Speer and Susan W. Becker

The Palmetto pluton, located in Fulton, Coweta and Fayette Counties, Georgia, is probably the westernmost of the coarse-grained, Late Paleozoic plutons in the southeast U.S.A. It is one of several post-metamorphic plutons in the vicinity of Atlanta (Figure A-2).

During this study, the Palmetto and Tyrone plutons were found to be parts of the same pluton. The other nearby granitic bodies are the Ben Hill, Stone Mountain, and Panola plutons.

Previous Work

Rocks from the Palmetto pluton were first described by Watson (1902), who gave petrographic descriptions, field occurrences, and chemical analyses from several localities. Watson pointed out the similarity between the "porphyritic granite of Campbell (now Fulton), Coweta, and Fayette counties" (i.e., the Palmetto) and what are now called the Lilesville and Mt. Mourne plutons, N. C. Chemical analyses given by Watson for the Palmetto granite are listed with sample localities in Table A-1.

Mapping of the entire pluton was completed for the Geologic Map of Georgia (1976). Previously, only the

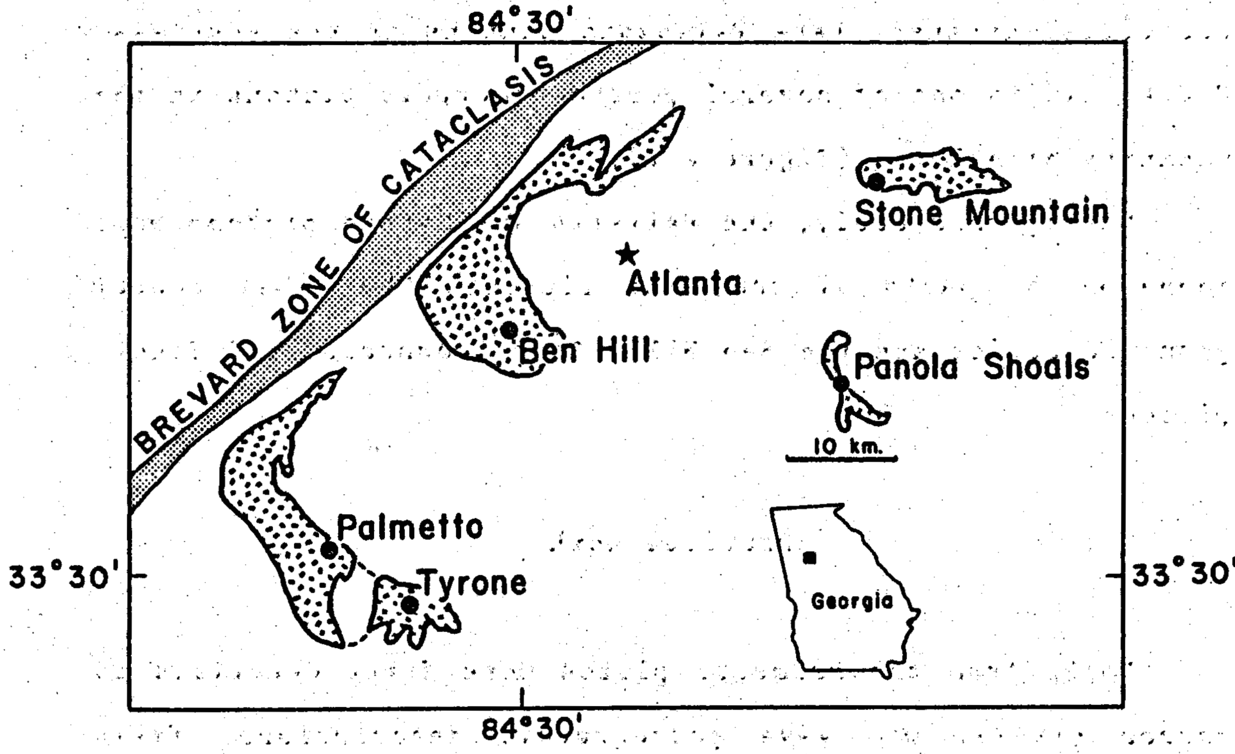

Figure A-2. Location map of the post-metamorphic granite plutons in the vicinity of Atlanta, Georgia from the Georgia State Geologic Map (1976).

Table A-1

Analyses for the Palmetto granite, Georgia, from the literature.

	1	2	3	4
SiO_2	63.65	64.40	70.88	70.39
TiO_2				0.37
Al_2O_3	20.46	18.97	15.86	14.95
Fe_2O_3	2.20	0.37	1.77	
FeO				2.33
MnO				0.08
CaO	3.38	0.59	1.79	1.46
MgO	1.50	tr	0.93	0.91
Na_2O	4.75	3.60	3.94	3.81
K_2O	4.58	11.40	4.64	4.83
P_2O_5				0.18
ignition	0.42	0.19	0.49	
total	100.94	99.52	100.30	99.31

1--Fresh granite, McCollum quarry (loation B7-428), Coweta Station, Coweta Co. (Watson, 1902).
2--K feldspar megacryst from the same locaity (Watson, 1902).
3--Fresh granite, McElwaney place, Fayette Co. (1 mile north of AS8-314 on east side of Line Creek) (Watson, 1902).
4--CB7-5, Tyrone quarry.

northern margin had been mapped by Higgins (1966, 1968) in his study of the Brevard fault zone. Higgins descriptions of the "Palmetto granite" are actually of the Ben Hill pluton. A K-Ar biotite date for the granite in the Tyrone quarry has been reported by Kulp and Eckelmann (1961) and recalculated by Tilton (1965) as 286 m.y. The coarse-grained porphyritic biotite granites of Georgia have been previously grouped as the Palmetto-type granite by Crickmay (1951) and the Ben Hill-type by Cofer (1958).

Palmetto Granite

General Relations

The Palmetto granite has a crescentic outcrop, elongated northwest-southeast, of 140 km^2 area. Only one rock type was encountered and with slight variation is a porphyritic, coarse-grained biotite granite. The country rock which the Palmetto intrudes is largely granitic gneisses with abundant amphibolite on the southern border. The Palmetto granite intrudes the Brevard zone and is involved in some deformation as discussed later. The map distribution of the granite and the locations of the samples collected for chemistry and heat production are illustrated in Figure A-3 .

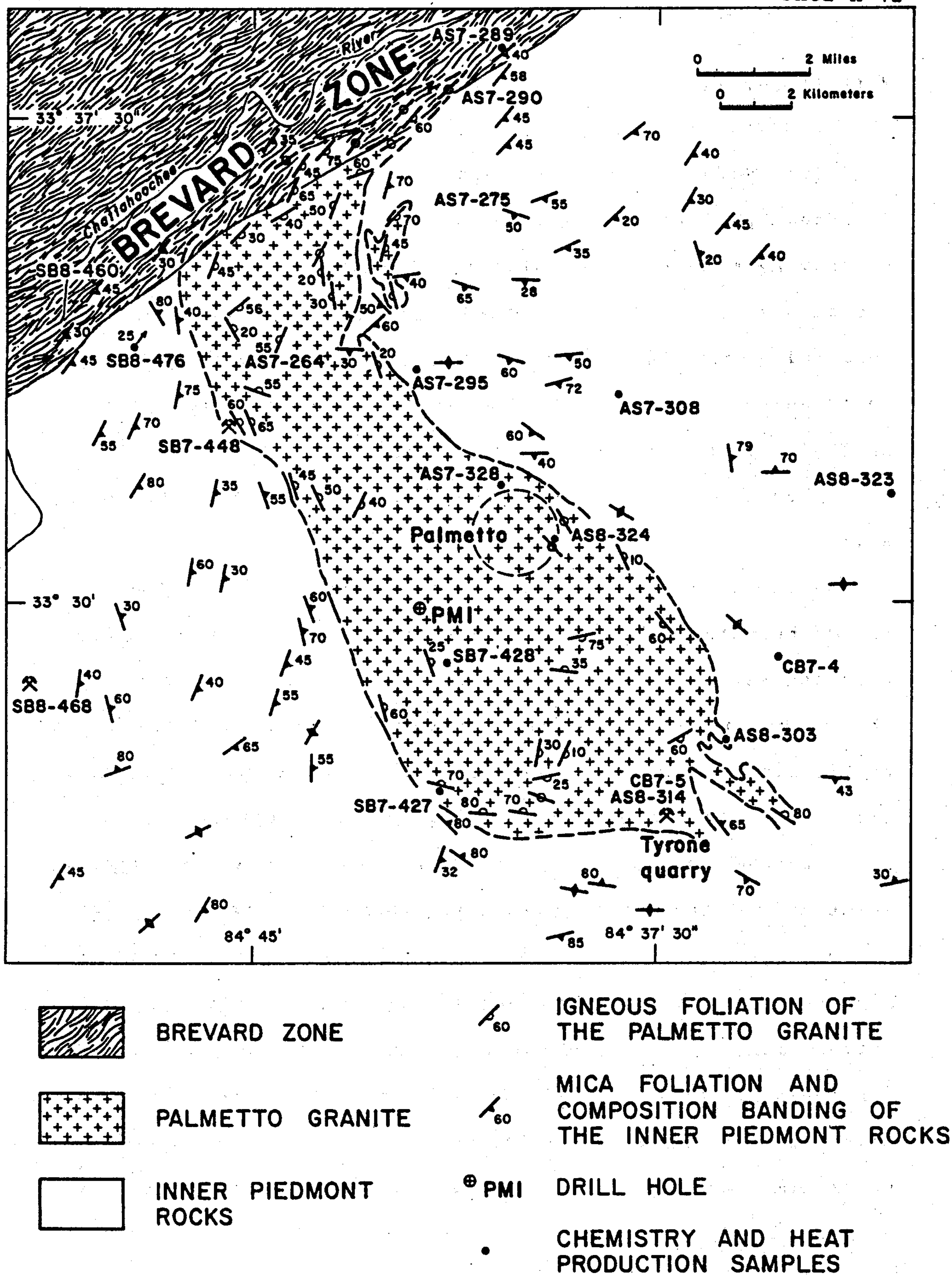

Figure A-3. Geologic map of the Palmetto pluton, Fulton, Coweta, and Fayette counties, Georgia.

Petrography.

The Palmetto pluton consists of a coarse-grained, hypidiomorphic-inequigranular, biotite-feldspar-quartz rock containing megacrysts of alkali feldspar, 2-8 cm long. The percentage of feldspar megacrysts varies, but remains generally over 20%. The rock has a very coarse-grained appearance, but the average grain size of the matrix minerals is 4 mm or less.

Modal analyses on slabs of Palmetto granite (Figure A-4a)

show the rock is a monzogranite to granodiorite according to the IUGS plutonic rock nomenclature (Streckeisen, 1976). This is the most plagioclase rich of the coarse-grained granites of the southeast U.S.A. The color index varies between 2 and 13 (Figure A-4b) and reflects the varied color index evident in outcrop.

Tabular, subhedral to euhedral, pink to white alkali feldspar is the most conspicuous mineral because of its large size (1-8 cm). The alkali feldspar is microcline micro- and macroperthite exhibiting both primary growth twins, largely Carlsbad twins, and albite and pericline inversion twins. The alkali feldspar is poikilitic with oriented inclusions of plagioclase, quartz and biotite, which are commonly confined to zones. A textural zoning is also defined by differing amounts of perthite. Watson

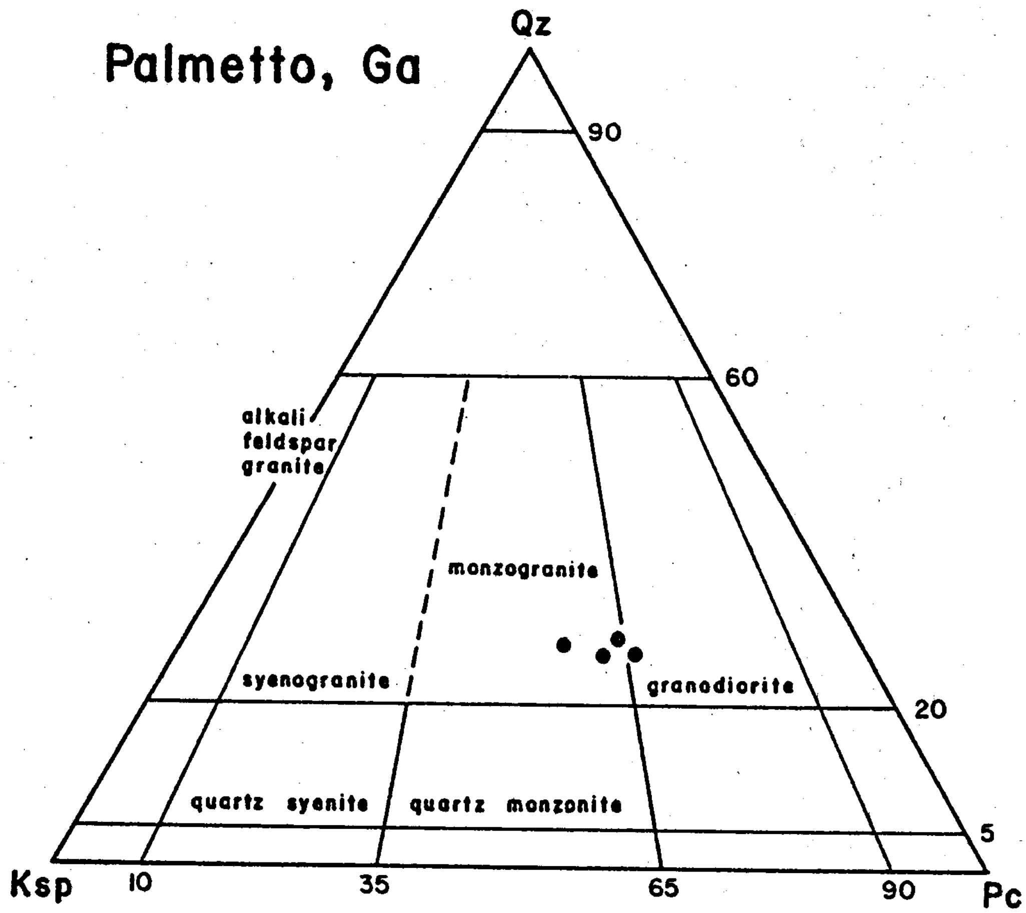

Figure A-4a. Triangular diagram of model volume percent of alkali feldspar (Ksp), plagioclase (Pc), and quartz (Qz) for samples from the Palmetto granite. The fields are from Streckeisen (1976).

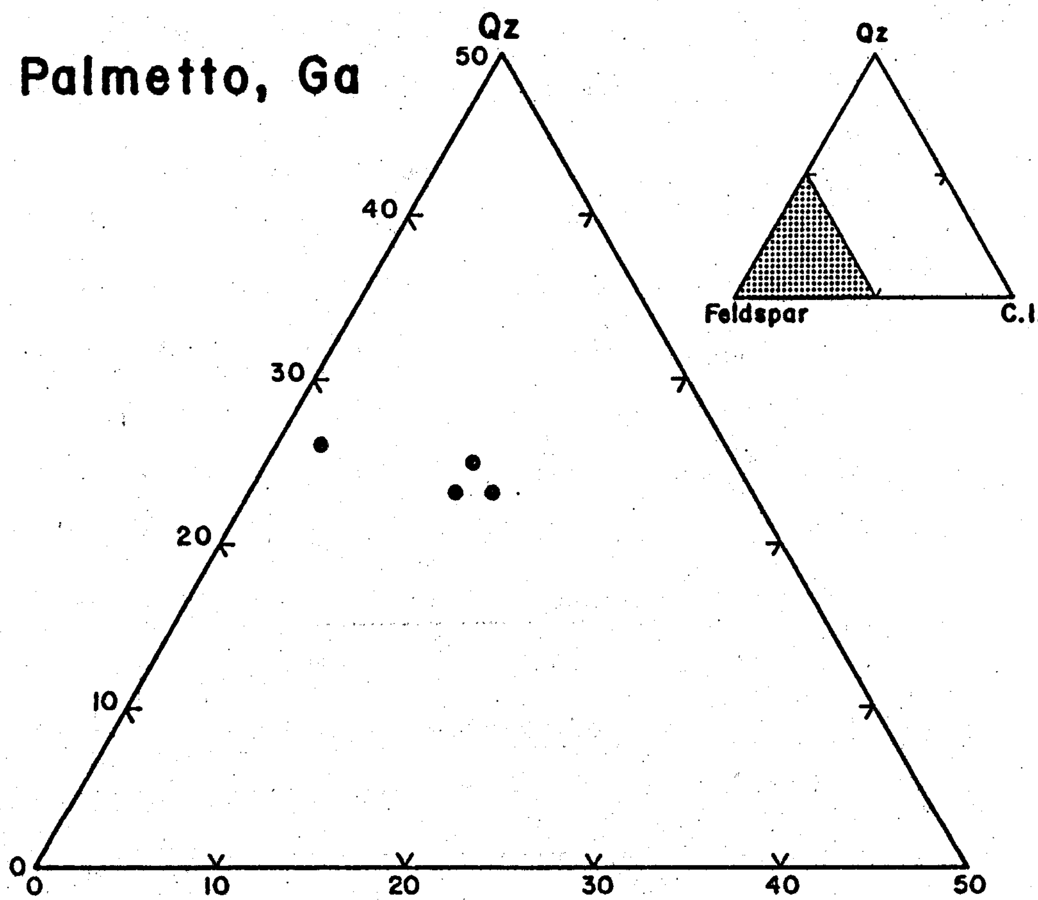

Figure A-4b. Triangular diagram of model volume percent of total feldspar, lor index (C.I.), and quartz (Qz) for samples from the Palmetto granite.

(1902) has found the bulk composition of an alkali feldspar megacryst to be $Or_{67}An_{32}An_{1}$ (Table A-1). The subhedral to anhedral plagioclase grains are smaller than the alkali feldspar, less than 1 cm, and are white. Optical compositional determinations by the a- normal method (Smith, 1974) show the plagioclase is oligoclase having broad, normal oscillatory zoning of An_{29} to An_{20} Most have sharp, discontinuous rims of albite, usually associated with myremekite. Biotite is the major ferro-magnesian mafic mineral. It is pleochroic dark browwn to tan and occurs as anhedral, shredded flakes.

Primary accessory minerals include allanite, titanite, apatite, zircon, a rhombohedral oxide now exsolved to ilmenite + hematite, and chalcopyrite. The titanite and the large, zoned allanites with wide epidote rims are the characteristic accessories similar to those in other late Paleozoic plutons in the southeast. Late-stage magmatic minerals include fairly common muscovite, albite, epidote, and titanite. Deuteric stage minerals are hematite, muscovite, chlorite, zoisite, and calcite.

A well-developed igneous flow foliation, defined by the alignment of the tabular alkali feldspar megacrysts and xenoliths, parallels the crescentic outline of the Palmetto pluton (Figure A-3). The attitudes of the foliation suggest the pluton dips to the northeast.

Contact Metamorphic Effects

The Palmetto granite intrudes regionally metamorphosed rocks which are above a sillimanite isograd in a kyanite-sillimanite metamorphism (Smith et al., 1968). In a study of $^{40}Ar/^{39}Ar$ incremental-release ages, Dallmeyer (1978) concluded that the regional metamorphism occurred about 365 m.y. ago and that the country rocks had cooled below argon retention temperatures of 300-345°C prior to the emplacement of the Late Paleozoic plutons. The regional metamorphic mineral assemblages of the country rocks encountered in this study for the granitic gneisses are:

biotite + muscovite + epidote + garnet
+ K feldspar + oligoclase + quartz

for the metabasites:

green hornblende + plagioclase + epidote + biotite + quartz

garnet + green hornblende + epidote + biotite
+ plagioclase + quartz

The metabasite xenoliths have quite a number of differing mineral assemblages, reflecting differences in rock composition and contact metamorphic conditions. The assemblages are:

cpx + opx + brn hbl + bt + pc + qz

cpx + brn hbl + pc + qz

gar + cpx + grn hbl + ep + pc

cumm + brn hbl + An_{70} + bt + qz

cumm + grn hbl + An_{60} + bt + qz

gar + cumm + bt + pc +qz

The coexisting cummingtonite and brown hornblende have intermediate Fe-Mg compositions (Table A-2). These assemblages are characteristic of the hornblende- and pyroxene-hornfels facies and differ markedly from those observed and reported for the regional metamorphism.

The metamorphic mineral assemblages of the pelitic xenoliths are:

gar + sil + bt + ms + Ksp + An_{30} + qz (1)

gar + bt + ms + An_{10} + qz (2)

staur + gar + sil + bt + An_{6} + qz (3)

The garnet and biotite of assemblage 1 (B7407B and PM1-509) are more magnesian than those of assemblage 2 (AS7-267) (Table A-3 and A-4).

These two assemblages lie either on the continuous reaction

ms + gar + bt + sil + qz (1)

or

bt + sil + qz + gar + Ksp (2)

depending on whether the decomposition of muscovite + quartz to sillimanite + K feldspar has occurred or not. In the

Table A-2

Amphibole analyses from Palmetto hornfelses.

	AS8-314D, green	AS8-314D, colorless
SiO_2	44.04	53.80
Al_2O_3	15.36	2.75
FeO	17.15	23.30
TiO_2	0.70	0.15
MnO	0.11	0.28
CaO	9.80	0.91
MgO	9.61	16.55
Na_2O	1.33	0.16
K_2O	0.36	0.03
H_2O	2.05	2.06
sum	100.54	100.01
	Number of cations based on 24(O,OH)	
Si	6.448	7.820
Al^{IV}	1.552	0.180
	8.000	8.000
Al^{VII}	1.097	0.291
Ti	0.078	0.016
Fe	2.100	2.832
Mg	2.098	3.586
Mn	0.014	0.035
	5.387	6.760
Na	0.379	0.046
Ca	1.538	0.142
K	0.068	0.006
	1.985	0.194

Table A-3
Biotite analyses from Palmetto hornfelses.

	AS7-267	AS8-314A	AS8-314D	B7407B	PM1-509
SiO_2	35.72	37.90	38.36	36.44	35.90
Al_2O_3	19.86	18.85	17.72	20.24	19.58
FeO	23.10	14.73	16.63	17.99	18.16
TiO_2	2.75	1.81	2.30	2.86	2.48
MnO	0.05	0.11	0.06	0.13	0.03
CaO	0.05	0.06	0.10	0.04	0.07
MgO	6.47	13.38	12.99	9.51	10.75
Na_2O	0.10	0.45	0.28	0.12	0.30
K_2O	9.17	8.33	8.45	9.50	9.23
H_2O	3.97	4.09	4.10	4.04	4.02
sum	101.27	99.71	101.00	100.87	100.52
Number of cations based on 24(O,OH)					
Si	5.392	5.558	5.603	5.398	5.350
Al^{IV}	2.608	2.442	2.397	2.602	2.650
	8.000	8.000	8.000	8.000	8.000
Al^{VI}	0.925	0.815	0.653	0.931	0.788
Ti	0.313	0.200	0.253	0.318	0.278
Fe	2.917	1.806	2.032	2.228	2.263
Mn	0.007	0.014	0.007	0.017	0.004
Mg	1.457	2.925	2.828	2.100	2.388
	5.619	5.759	5.774	5.594	5.720
Ca	0.009	0.009	0.016	0.006	0.011
Na	0.031	0.128	0.081	0.034	0.087
K	1.766	1.558	1.1574	1.796	1.754
	1.805	1.695	1.671	1.836	1.851

Table A-4

Garnet analyses from Palmetto hornfelses.

	AS7-267	AS7-314A	B7407B	PM1-509
SiO_2	36.85	38.14	38.16	36.98
Al_2O_3	21.84	21.54	21.12	21.79
FeO	37.60	28.58	31.40	34.70
TiO_2	0.14	0.09	0.22	0.18
MnO	0.94	5.13	5.11	1.86
CaO	1.01	0.27	1.12	1.45
MgO	2.67	5.51	3.39	3.67
Na_2O	0.02	0.00	0.02	0.01
K_2O	0.01	0.01	0.01	0.04
sum	101.07	99.31	100.45	100.68
	Number of cations based on 12 oxygens			
Si	2.951	3.025	3.031	2.950
Ti	0.009	0.005	0.013	0.011
Al	0.040	0.000	0.000	0.039
	3.000	3.031	3.045	3.000
Al	2.020	2.014	1.982	2.010
Fe	2.518	1.896	2.092	2.315
Mg	0.319	0.652	0.402	0.436
Mn	0.064	0.345	0.345	0.126
Ca	0.086	0.023	0.096	0.124
Na	0.003	0.001	0.003	0.002
K	0.001	0.002	0.001	0.004
	2.990	2.918	2.938	3.007
Al	84.3	65.0	71.3	77.1
Py	10.7	22.4	13.7	14.5
Sp	2.1	11.8	11.7	4.2
Gr	2.9	0.8	3.3	4.1

third pelitic assemblage (AS7-314A), garnet appears from textural evidence to be growing at the expense of staurolite. This assemblage indicates conditions at the discontinuous reaction:

$$ms + staur \pm gar + sil + bt \quad (3)$$

or below it on the continuous reaction:

$$staur + qz \pm gar + sil + H2O.$$

The mineral assemblages of the metapelite xenoliths do not differ from what would be anticipated in inner Piedmont rocks which are above the sillimanite isograd. In order to use them to deduce P-T conditions of the Palmetto granite, the assumption would have to be made that they reequilibrated while they were xenoliths. This is probably a good assmption considering their small size. Richardson (1968) found reaction 2 to occur above 3.5 kb over a small temperature range near 680°C for the iron end-members buffered by quartz-fayalite-magnetite. The temperature and pressure would increase at higher oxygen fugacities and with substitution of magnesium for iron. In contrast, other components such as calcium and manganese would expand the garnet field. The occurrence of muscovite, which has not decomposed to form an aluminum silicate, in xenoliths of a granitic melt similarly indicates a minimum pressure of 3.5 kb. The occurrence of almandine-rich garnet rather than cordierite in the sillimanite-bearing assemblages of the xenoliths suggests a minimum pressure of 4 kb (Lee and Holdaway, 1977). The only upper pressure estimate presently available is the 7-9 kb regional metamorphic pressure estimate of Dallmeyer (1978).

As in the case of the Siloam pluton (Speer, VPI&SU-5648-1), the higher pressure garnet + sillimanite assemblage rather than the lower-pressure cordierite assemblages indicates a greater total or water pressure of crystallization of the Palmetto than the Winnsboro, Liberty Hill, Pageland and Lilesville plutons.

Palmetto Granite in the Brevard zone

At the nothern contact of the Palmetto pluton, the granite crosscuts the phyllonites, blastomylonites, and mylonite gneisses of the Brevard zone at small angles. In this area, the Palmetto granite exhibits a wide variety of textures, from rocks showing only incipient deformation through mylonite gneiss to blastomylonite. An outstanding feature of the Palmetto granite is the crystalloblastic texture seen in thin section. The mineralogy of the deformed rocks is identical to that of the undeformed granite. The similarity in mineralogy and the recrystallized texture suggest that the granite was deformed and recrystallized while the rocks were at elevated temperature and that no subsequent movement involving the

Palmetto granite occurred along the Brevard zone. The intensity of deformation of the Palmetto granite does not vary systematically with distance from the Brevard zone, but the intensity of deformation can change within a small area, suggesting that zones of most intense deformation are fairly narrow and occur throughout a broad region.

Heat Generation

The Palmetto granite is emplaced in granite and granodiorite gneisses, migmatites, and amphibolites. Because of their predominantly granitic composition, the country rocks may have heat productions approaching those of the post-metamorphic granites. This feature could make the thermal anomaly associated with the granite pluton larger than the granite outcrop itself. For this reason, a number of country rock granite gneisses were collected for heat production. Their locations are indicated in Figure A-3 and their heat productions are listed with those from the Palmetto granite in Table A-5. The results show a sharp break between the Palmetto granite with heat productions between 6.8 and 13.7 HGVU and the country rock with less than 2.9 HGVU.

TABLE A-5

U, Th, K contents and heat production for the Palmetto pluton, GA and adjacent country rock.

	U PPM	TH PPM	K WT %	HGVU
CB7-5	9.6	41.2	3.8	13.7
SB7-427	2.7	32.9	3.8	7.9
SB7-428	3.2	32.9	3.7	8.1
SB7-448	3.3	30.8	3.8	7.9
AS7-264	6.7	27.3	3.6	9.3
AS7-326	UNAVAILABLE			
AS7-328	UNAVAILABLE			
AS8-303	5.0	42.4	3.5	10.7
AS8-314	6.8	38.9	3.7	11.3
AS8-324	3.0	29.0	3.7	7.4
ADJACENT GRANITIC COUNTRY ROCKS				
CB7-4A	2.2	4.1	3.1	2.7
CB7-4B	2.1	6.7	1.9	2.9
AS7-275				
AS7-289				
AS7-290	UNAVAILABLE			
AS7-295				
AS7-308				
AS8-323	1.0	8.0	2.0	2.4
SB8-460	0.5	2.9	0.8	0.9
SB8-468	0.7	4.2	1.7	1.4
SB8-476	3.9	8.0	4.6	4.7
PALMETTO DRILL HOLE, PM1				
PM1-28(92)	3.2	27.0	3.3	7.1
PM1-39(128)	3.0	25.1	3.5	6.8
PM1-50(164)	2.8	26.6	3.4	6.9
PM1-61(201)	2.9	28.4	3.6	7.3
PM1-77(253)*	7.0	55.3	2.6	13.9
PM1-86(282)	3.2	24.4	2.8	6.7
PM1-93(305)	3.0	34.9	3.3	8.5
PM1-141(463)	3.7	26.2	3.1	7.4
PM1-165(541)	3.3	25.1	3.5	7.0
PM1-175(574)	2.9	26.3	3.2	6.9
PM1-187(613)	3.1	31.9	3.4	7.8
PM1-196(643)	3.1	30.2	3.8	7.8

*GRANITE AND XENOLITH

Palmetto Drill Hole

A hole 211 m (692 ft) was drilled in the southcentral portion of Palmetto granite (PM1, Figure A-5).

Core recovered from this hole consists mainly of moderately foliated, coarse-grained granite with C.I._ 10. The rock is hypidiomorphic with large, euhedral crystals of alkali feldspar (to 4 cm) and smaller grains of quartz and plagioclase (to 1 cm) enclosed in a medium- to fine-grained matrix of feldspar, quartz, biotite, titanite, and opaque minerals. The granite remains uniform in texture and mineralogy throughout the core.

Numerous mafic xenoliths, varying in length from a few centimeters to 9 meters, were encountered in the hole. These rocks are composed of biotite with lesser amounts of quartz and feldspar. The assemblabe gar + sil + bt + ms + An_{30} + qz was found in the xenolith at 154-163 m. Pegmatite veins, varying in width from 1-30 cm, contain quartz, alkali feldspar, plagioclase, biotite and muscovite. They are located throughout the core, and are commonly associated with the mafic xenoliths.

The gamma log of PM1 accurately reflects the rock types encountered in the core. Zones of relatively low counts correspond to the locations of xenoliths, and anomalously high peaks correlate with pegmatite veins. The granite

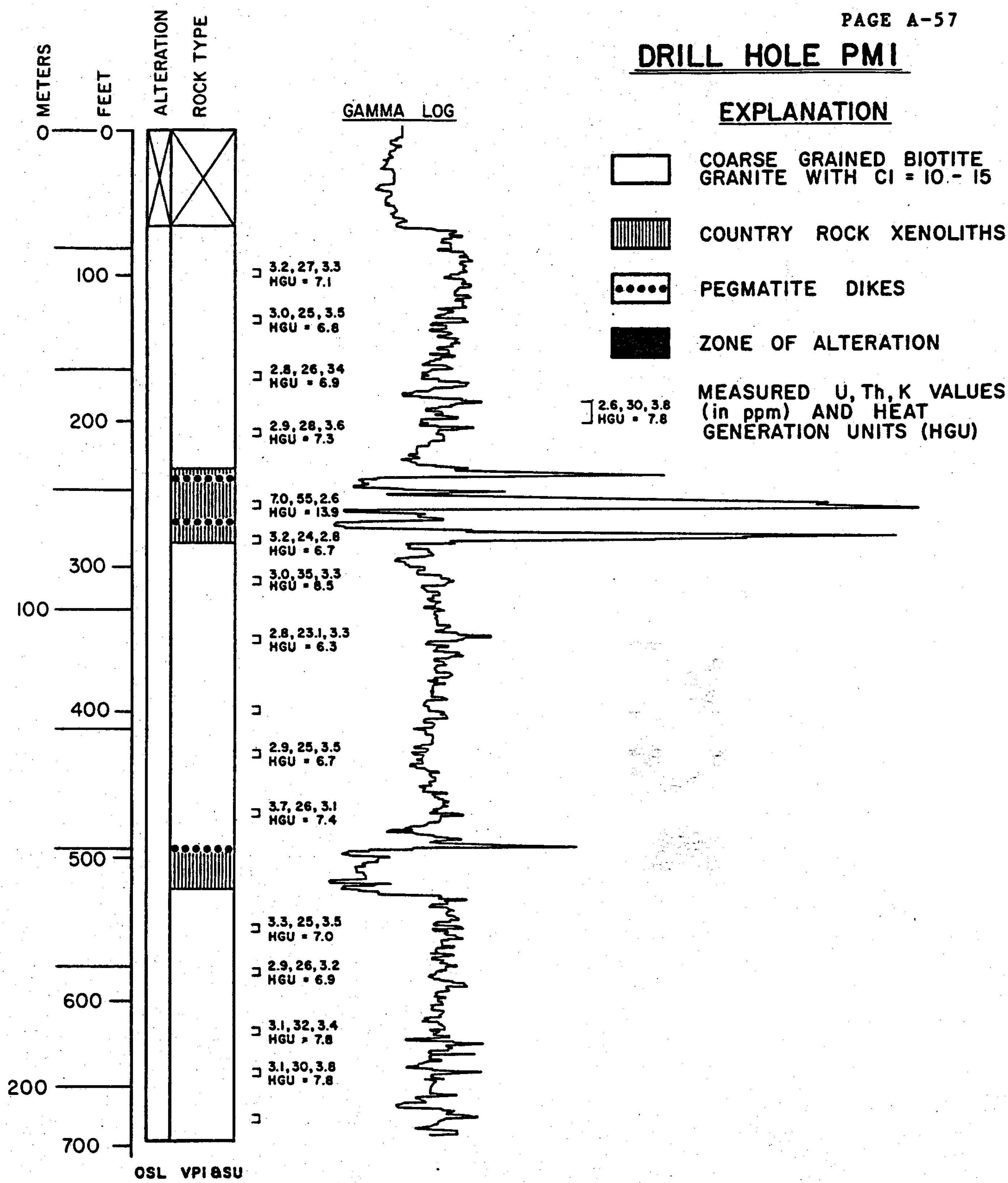

Figure A-5. Lithologic log of drill hole PM1, with corresponding alteration and gamma ray spectrometer log. Radioactivity measurements increase to the right.

produces a nearly uniform count rate throughout the hole, as would be expected from the homogeneity of the rock.

References

Crickmay, G. W., 1951, Geology of the crystalline rocks of Georgia, Georgia Geol. Survey, Bull. 58.

Cofer, H. E., 1958, Structural relations of the granites and the Associated Rocks of South Fulton Co., Ga. unpublished Ph.D. dissertation, Univ. of Illinois, 139 p.

Dallmeyer, R. D., 1978, 40Ar/39Ar incremental release ages of hornblende and biotite across the Georgia Inner Piedmont: their bearing on Late Paleozoic - Early Mesozoic tectonothermal history. Am. Jour. Sci 278, 124-149.

Higgins, M. W., 1966, The Geology of the Brevard Lineament near Atlanta, Georgia, Georgia Geol. Survey, Bull. 77, 49 p.

Higgins, M. W., 1968, Geologic map of the Brevard fault zone near Atlanta, Georgia, U.S. Geol. Survey Misc. Geol. Inv. Map 1-511.

Kulp, J. L. and F. D. Eckelmann, 1961, Potassium-argon ages of micas from the southern Appalachians: Annals of the New York Acad. Sci. 91, 408-416.

Lee, M. L. and M. J. Holdaway, 1977, Significance of Fe-Mg cordierite stability relations on temperature, pressure, and water pressure in cordierite granulites. Am. Geophys. Union Monograph 20, The Earth°s Crust, 79-94.

Richardson, S. W., 1968, Staurolite stability in a part of the system Fe-Al-Si-O-H., J. Petrol. 9, 467-488.

Smith, J. V., 1974, Feldspar Minerals, Vol. 1, Springer-Verlag, 627 p.

Smith, J. W., J. M. Wampler, and M. A. Green, 1969, Istopic dating and metamorphic isograds of the crystalline rocks of Georgia. Georgia Dept. Mines, Mining, and Geology Bull. 80, 121-139.

Streckeisen, A., 1976, To each plutonic rock its proper name. EarthScience Reviews 12, 1-33.

Tilton, G. R., 1965, Compilation of Phanerozoic geochronological data for eastern North America in Geochronology of North America, National Academy of Sciences - National Research Council Publication 1276, 217-218.

Watson, T. L., 1902, The granites and gneisses of Georgia, Georgia Geol. Survey Bull. 9- A, 637 p.

Fission Track Studies of the Liberty Hill Pluton (I) and Comments on U-Th-Pb Disequilibrium Studies of the Liberty Hill Pluton

J. Alexander Speer

Because of the importance of uranium as a radiogenic heat-producing element and its possibly mobile behavior, knowledge of its distribution and host mineralogy will provide clues and constraints on its behavior in rocks. Two fission track maps of Liberty Hill pluton thin sections have been received thus far. One is for a coarse-grained granite, K2-5 (HGVU = 5.1), containing quartz, K feldspar, plagioclase An_{23-18}, biotite, and amphibole. Accessory minerals are zircon, titanite, allanite, apatite, magnetite ilmenite, pyrite, and pyrrhotite. The secondary minerals include epidote, chlorite, calcite, and white mica. The other fission track sample is a fine-grained granite, S6-100 (HGVU = 9.2), which contains quartz, K feldspar, plagioclase An_{27-10}, biotite. Accessory minerals are allanite, zircon, apatite, fluorite, magnetite, ilmenite, and chalcopyrite. Secondary minerals are chlorite, white mica, and epidote.

Comparison of the corresponding fission track maps and thin sections for the fine-grained and coarse-grained granites show the uranium distribution to be quite heterogeneous. Qualitative estimates of the number of fission tracks is proportional to uranium content and would indicate that most of the uranium is located in the accessory minerals: titanite, allanite and zircon. Lesser amounts of uranium are observed in apatite and epidote. Variable but small numbers of tracks are associated with alteration features in the rocks: amphibole or biotite alteration to chlorite, feldspars that have undergone saussuritization or alteration to clay minerals, and Fe-bearing minerals altering to Fe oxides and hydroxides. Uranium along cracks and grain boundaries is very rare in the coarse -grained granite and is located near phases containing high amounts of uranium. Uranium along cracks and grain boundaries in the fine-grained granite is more common but still represents a small percentage of the uranium present. Figures A-6 to A-8 are photomicrographs of corresponding thin sections and fission track maps showing several types of uranium distribution in the Liberty Hill pluton.

No fission tracks were found to be associated with trains of fluid inclusions in the granites. These fluid inclusions are believed to represent early microcracks which have since healed. This suggests either that uranium was not an important component in these earlier microcracks or that it is incapable of being retained at these sites during recrystallization.

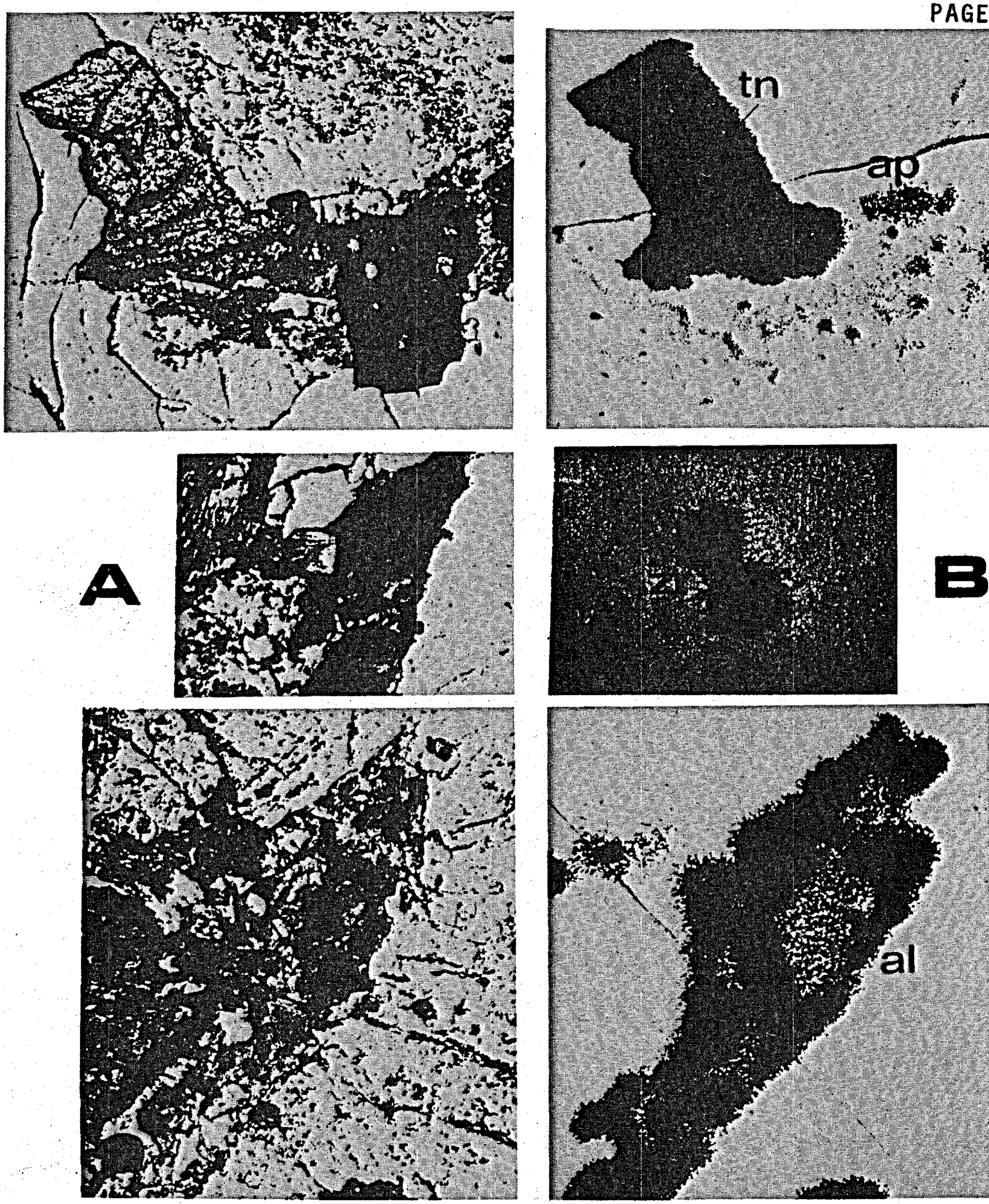

Figure A-6. Photomicrographs (a) and fission track maps (b) of mafic clots in the coarse-grained granite K2-5. High uranium minerals are allanite (al), zircon (zr), titanite (Tn) and apatite (ap). The few, dispersed fission tracks are those associated with altering Fe-bearing minerals and feldspars.

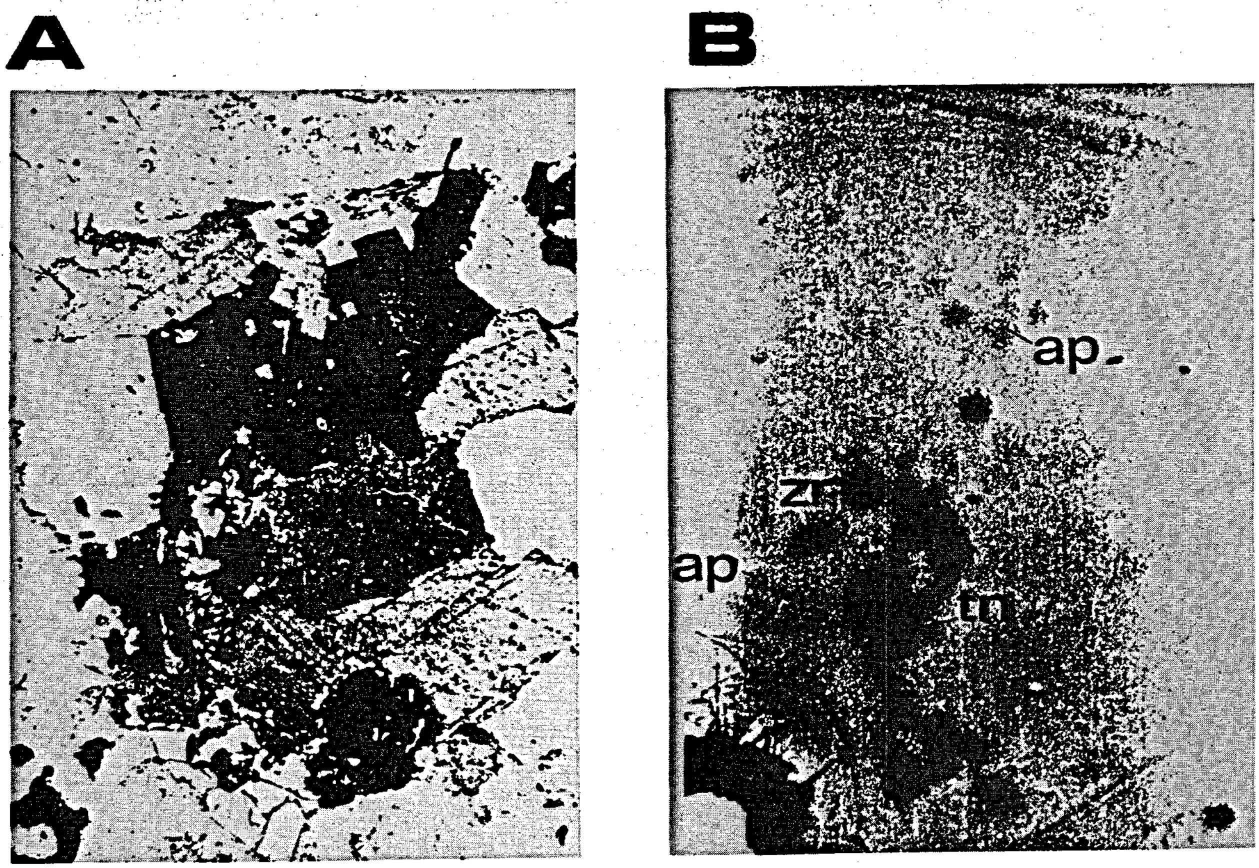

Figure A-7 . Photomicrograph (a) and fission track map (b) of a mafic silicate and oxide clot in the fine-grained granite.

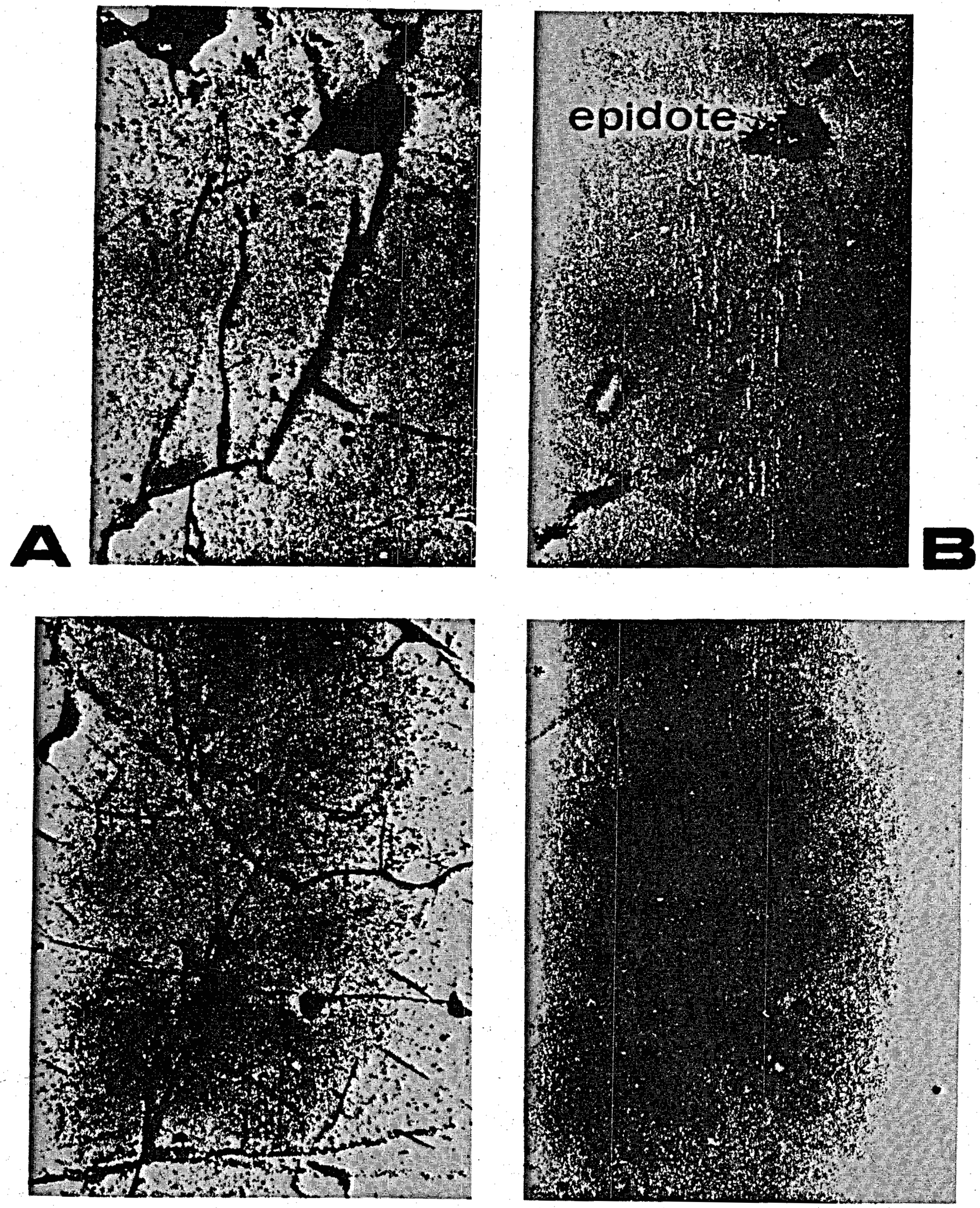

Figure A-8. Photomicrographs (a) and fission track maps (b) of uranium occurring along grain boundaries in the coarse-grained granite, K2-5, (1) and fine-grained granite, S6100, (2).

Qualitative estimates would assign at least 90% of the uranium in the Liberty Hill pluton to the accessory minerals: titanite, allanite, zircon, apatite, and epidote. Previously identified uranium sites are in uranothorianite, xenotime, and thorite. The remaining uranium occurs with altered minerals and along microcracks. The amount of uranium not associated with accessory minerals is smaller in the coarse-grained than the fine-grained granites. The essential question is whether (1) this observed uranium distribution represents all of the uranium originally present with a small amount of migration or (2) the uranium in the accessory minerals is only the immoble (unleachable) uranium and the mobile (labile) uranium has migrated away except for an amount trapped locally in chemical sinks. And if the latter is the case, how much of the labile uranium has migrated out of the system and how much of it remains trapped in the chemical sinks.

The ready mobility of uranium results from the fact that uranium may be oxidized to the very soluble uranyl ion. The U^{+4} to U^{+6} transition occurs at much greater oxygen fugacities than the magnetite to hematite transition. The occurrence of magnetite in the Liberty Hill suggests that conditions to oxidize the uranium have not been common or of long duration in the rocks. In addition, the presence of magnetite as well as ferrous silicates suggests that the rocks are capable of buffer the oxygen fugacity and prevent uranium leaching. The preservaton of easily leachable uranothorianite and presence of uranium in close proximity to iron-bearing mineral phases indicates such buffering occurred and not all labile uranium has been removed from the rocks.

Grain boundaries, halos around ferrous minerals, and altered minerals are sites which act as chemical sinks in the rocks. These sites are more dispersed and more available in the fine-grained granite than in the coarse-grained granite. The greater amount of uranium in these sites may illustrate more effective buffering of the fine-grained granite preventing uranium leaching. This more effective prevention of uranium leaching also would provide an explanation of the greater uranium content of the fine-grained granite (S6-100, 5.7 ppmU) than the coarse-grained granite (K2-5, 3.1 ppmU).

The above discussion shows that there is immoble uranium in the rock in accessory minerals and labile uranium, some of which, but not all, has migrated from its original site. These studies, however, cannot be used to determine if significant amounts of uranium have migrated out of the system. Lack of large amounts of labile uranium is not informative; positve evidence is required to demonstrate it existed and that the rocks originally had higher uranium contents. U-Th-Pb disequilibrium studies would provide the only evidence of significant uranium loss as well as its timing. Based on preliminary disequilibrium studies, Sinha and Merz (VPI&SU-5648-3) concluded that the Liberty Hill pluton suffered uranium loss nearly 230 m.y. ago and has acted as a closed system since that time. However, as pointed out by Sinha and Merz, several features of their experiment make this less than a compelling conclusion and obscure the meaning of the data.

The lead isotopic composition of K feldspars is taken to give a close approximation of the initial lead isotope ratios of the rock because of the high Pb/U ratios in the feldspar. Ludwig and Silver (1977) have shown that multicomponent lead is common in Precambrian feldspars with some feldspars having an added ^{206}Pb component resulting from the long term diffusion of ^{222}Rn from ^{238}U. This phenomenon alone would give the appearance of uranium loss if the K feldspars were used for the initial lead isotope composition. This may also account for the variation in the $^{206}Pb/^{204}Pb$ ratios of leads in microcline from a granite in the Granite Mountains of 14.3 to 19.8 reported by Stuckless and Nkomo (1978). Such a variation for the K feldspars in the Liberty Hill pluton, if used for initial lead isotopic compositions, could easily give the appearance of open system behavior of uranium even if it were immoble. In addition, considering the number of multistage subsolidus reequilibrations which occur in the K feldspars, which have an unknown effect on the lead component, using a single K feldspar for the initial lead composition is difficult to justify.

The samples from the Liberty Hill drill hole used in the disequilibrium studies represent two distinct rock types: fine-grained, biotite granite (72 and 924) and coarse-grained, amphibole-biotite granite (384, 790, and 1304). The 230 m.y. isochron is defined by values of 3 closely clustered coarse granites, a fine-grained granite and a K feldspar from a coarse-grained granite. While it is believed that the coarse-grained and fine-grained granites represent the evolution of a single batch of magma, it is not firmly established. That they both have the same initial lead isotopic ratios needs to be demonstrated rather than assumed.

References

Ludwig, K. R., and Silver, L. T., 1977, Lead isotope inhomogeneities in Precambrian igneous K-feldspar, Geochim. Cosmochim Acta., 41, 1457-1471.

Stuckless, J. S., and Nkomo, I. T., 1978, Uranium-Lead isotope systematics in uraniferous alkali-rich granites from the Granite Mountains, Wyoming: implications for uranium source rocks, Econ. Geol., 73, 427-441.

FISSION TRACK STUDY OF THE WIN-1 DRILL HOLE

S. W. Becker

Four samples from the WIN-1 drill hole (location shown in Figure A-2, VPI&SU-5103-4) have been prepared for fission track analysis at the U. S. Geological Survey in Denver. These samples were chosen to help ascertain whether the distribution of uranium in a granitic rock changes with differences in depth. Concentrations of uranium and thorium and values of heat production for these samples (reported on p. C-12, VPI&SU-5103-4) are listed in Table A-6. Uranium levels are somewhat higher in WIN 1-1865 and WIN 1-290 than in WIN 1-80 and WIN 1-1779.

All four rocks are biotite granite, with iron-titanium oxides and allanite as the common accessory phases. Chlorite, epidote, muscovite, and calcite constitute the secondary minerals.

In all samples, the highest numbers and densities of fission tracks are produced by allanite. Opaque minerals also are associated with high concentrations of fission tracks. In WIN 1-80, the sample nearest the top of the core, fission tracks were also found associated with secondary chlorite. The chlorite is commonly intergrown with iron-titanium oxides, and the oxides are associated with higher densities of fission

Table A-6. U, Th, and heat production values of samples for fission track analysis.

(depth,feet)	U(ppm)	Th(ppm)	HGVU(cal/cm3-sec)
WIN 1-80	6.4	32.8	10.4
WIN 1-290	8.1	31.4	11.3
WIN 1-1779	6.5	32.4	10.4
WIN 1-1865	9.3	49.0	15.1

tracks against a background of lower density of fission tracks produced by the chlorite. In one area of the sample, fission tracks delineate the cracks in large quartz grains. Fission tracks were also found in cracks radiating from a few allanite grains; cracks surrounding other allanite grains were devoid of tracks (Figure A-9, a, b).

In WIN 1-290, fission tracks were concentrated on allanite and opaque grains (Figure A-10, a,b); no fission tracks were found in cracks or grain boundaries.

Fission tracks in WIN 1-1779 were also produced mostly by allanite grains and opaque minerals. Tracks appear in small numbers along some grain boundaries.

In Win 1-1865, tracks are produced by allanite, opaques, and chlorite. Tracks were not found along cracks or grain boundaries.

The fission tracks show that in all samples, uranium is highly concentrated in the accessory allanite, and to a lesser extent with the iron-titanium oxides. Secondary chlorite can contain low levels of uranium. In two samples, a small amount of uranium occurs locally along cracks or grain boundaries.

It is difficult to determine from these samples whether any uranium has been lost from the rocks. In WIN 1-80 and WIN 1-1779, uranium is located locally

A

B

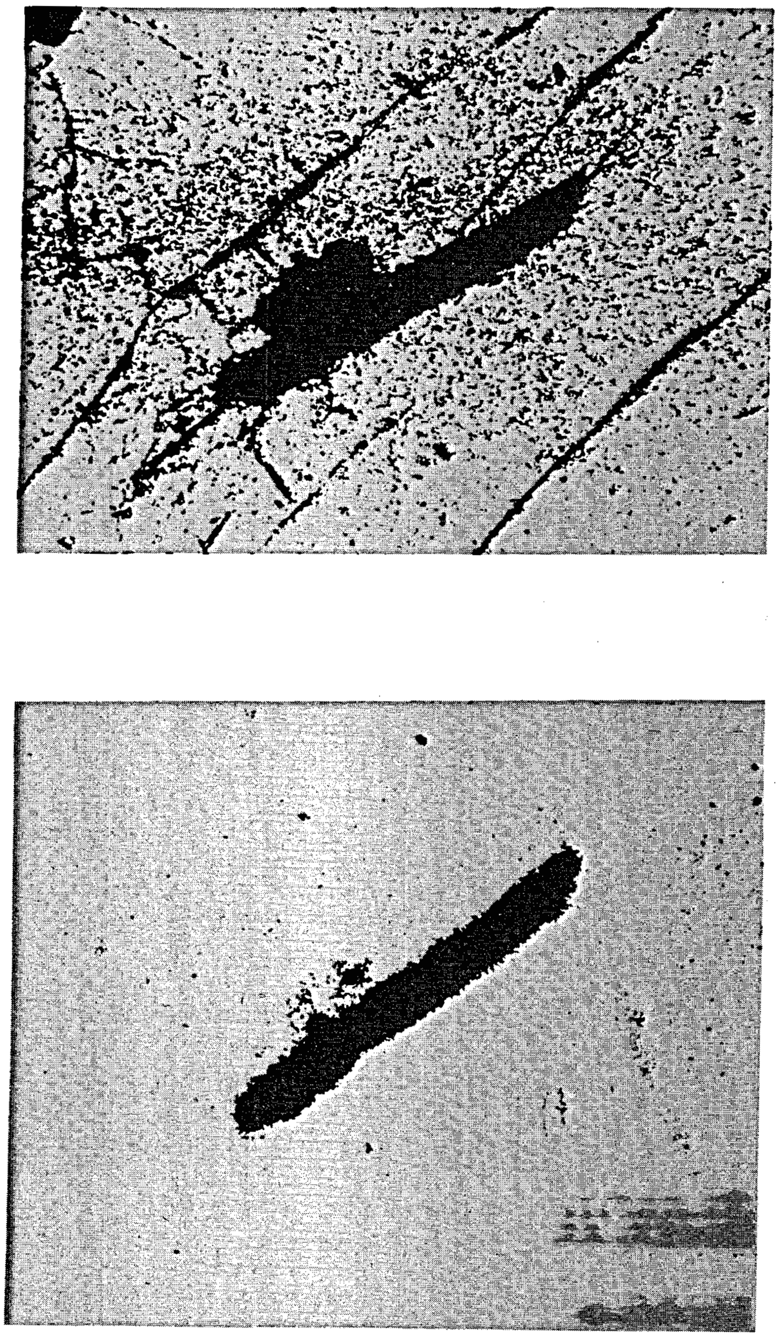

Figure A-9. (A) WN1-80. Photomicrograph of allanite grain and iron-titanium oxide; (B) corresponding fission track map.

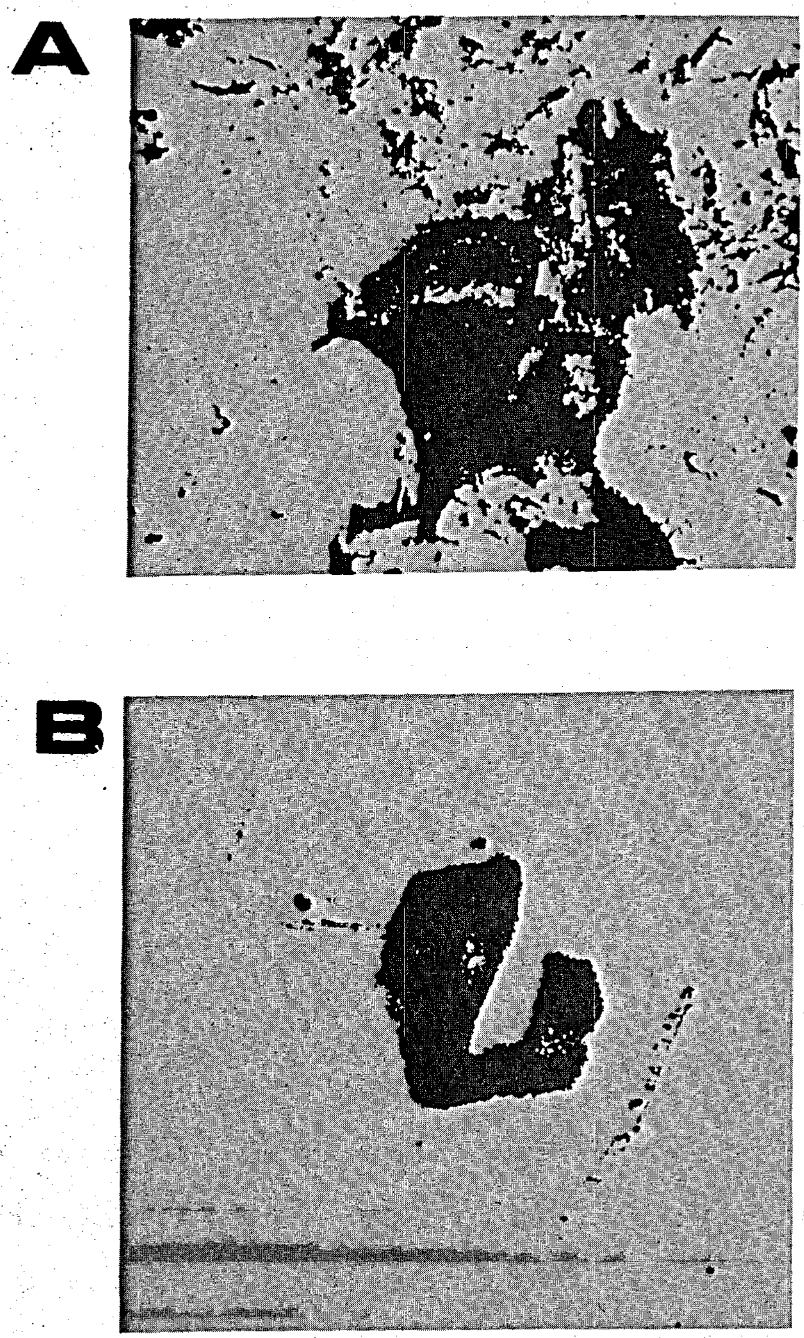

Figure A-10. WN1-290. (A) Allanite grain; (B) corresponding fission track map.

along some grain boundaries, which indicates that some uranium has migrated from its original site. These two samples also have relatively low concentrations of uranium, and may have lost uranium during alteration. Examination of the thin sections suggests, however, that the differences in uranium concentrations are primarily due to variations in the amount of allanite present. Sample WIN 1-1865 contains 5-10 times as much allanite as WIN 1-1779 (0.5% vs 0.1% or less).

The relatively high concentrations of uranium around the opaque oxides provide further evidence that, although some uranium has migrated, it has not been lost from the system in large amounts. Ferrous iron in these oxides can reduce mobile U^{6+} to immobile U^{4+} The rocks from the Winnsboro core contain large numbers of small grains of iron oxides, so that much of the migrating uranium would be trapped before it had moved far from its original site.

On the basis of the four samples studied, the distribution of uranium changes little with depth in the range 25-580 meters. The sample closest to the surface does contain more uranium along grain boundaries than any of the other samples, but uranium in WIN 1-1779 also occurs locally along grain boundaries. The location of uranium in samples in the depth range examined appears to be a function of conditions that are highly localized-nearly on a grain-to-grain scale - during alteration.

PETROLOGY OF DRILL CORE ED-1 FROM THE CUFFYTOWN CREEK PLUTON

S. W. Becker

Core has been taken from a hole 299.5 m (964 ft) deep, drilled near the center of the Cuffytown Creek pluton (VPI&SU-5648-3, Figure A1). Sixteen samples have been analyzed for major element chemistry, and measurements of heat production were made on 14 samples (Figure A-11).

In addition, numerous specimens have been chosen for petrographic examination, identification of sulfide minerals, and determination of uranium distribution by fission track methods.

Mineralogy

The granite is fairly uniform throughout the core, and closely resembles surface samples in texture and mineralogy. Minerals visible in hand speciment are quartz and alkali feldspar, ranging in width to 0.6 cm across, plagioclase to 0.4 cm, and white mica flakes 0.1-0.2 cm wide. Petrographic studies show that the alkali feldspar is microcline microperthite, and that the plagioclase is sausseritized. Grains of plagioclase may be almost entirely replaced by a single grain of white mica, or may contain many small grains

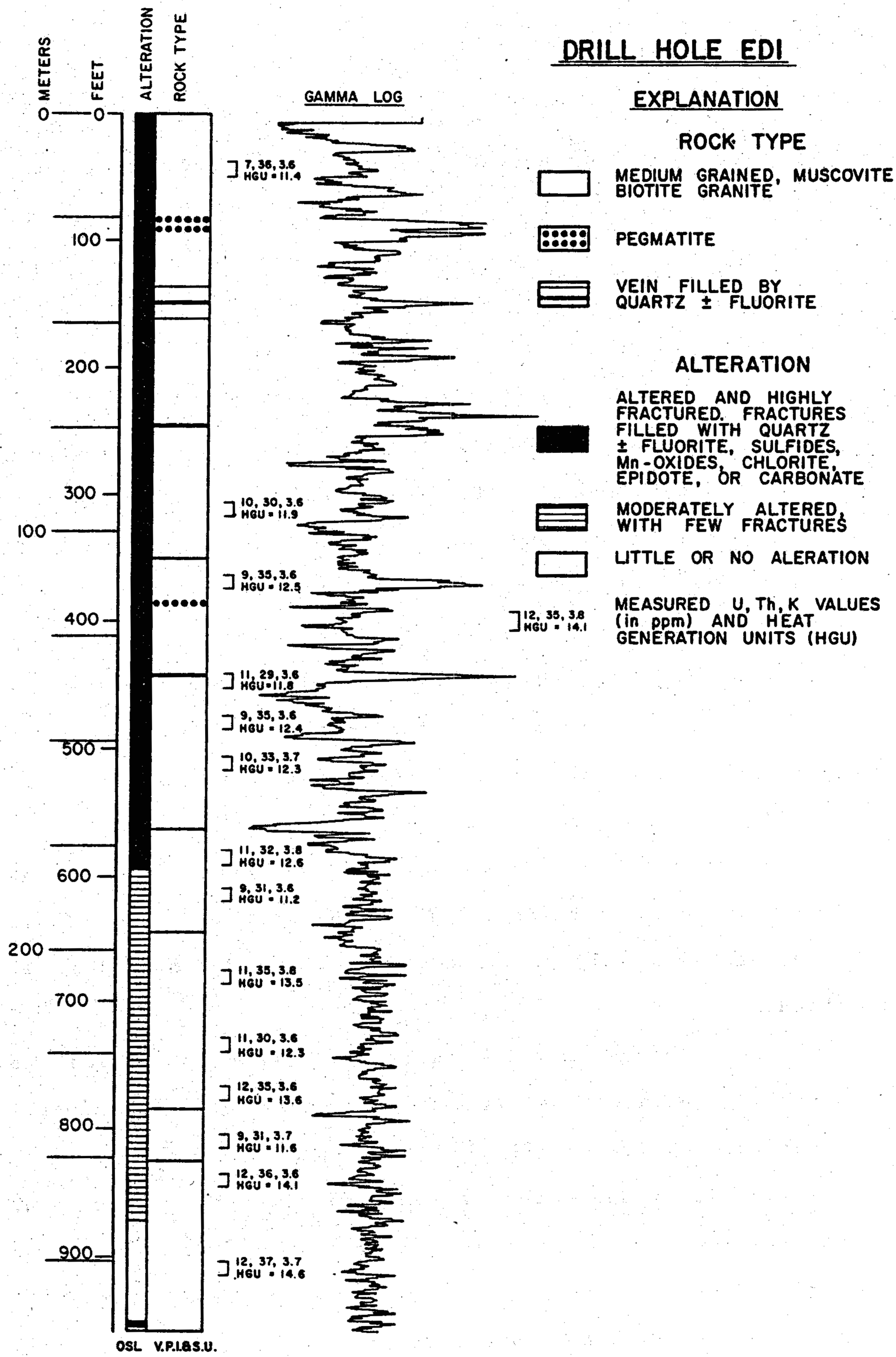

Figure A-11. Lithologic and gamma log of the ED1 drill hole.

of mica that are oriented parallel to crystallographic planes in the feldspar. Quartz plus the two feldspars constitute 95% of the rock; accessories present include fluorite, garnet, biotite, chlorite, allanite, zircon, and iron-titanium oxides.

Much of the rock is highly altered and closely fractured. The top 185 m (600 ft) of core is red in color, due to alteration of the feldspars. In thin section, samples from this zone show that the alkali feldspar is extensively kaolinized, and appears red-brown under crossed Nichols, suggesting that finely disseminated hematite is present throughout the feldspars. Plagioclase grains are also stained red brown, to a lesser extent. From 185 - 270 m (600-870 ft), the core is somewhat less altered, and usually red in color, but cut by fewer fractures. From 270-295 (872-950 ft), the rock is grey and appears to be fresh in hand specimen. In thin section, the alkali feldspars is highly kaolinized, but the red-brown stain is absent.

The fractures cutting the core, generally vertical to steeply dipping, are filled by a variety of mineral assemblages. Quartz-filled fractures are the most common, ranging in width from a few millimeters to several centimeters. Many of the fractures are filled with, or bordered by, sulfide minerals. Pyrite comprises nearly all the minerals in these zones; in one sample (305.2 m), it is accompanied by sphalerite and chalcopyrite. Bi-Pb and Bi-Te sulfides occur in one sample at 267.5 m. Some fractures are filled by fluorite ' quartz, others by epidote, chlorite, or carbonate. Associated with some fractures are black dendrites, or deposits of Mn oxides, identical in hand specimen and thin section to those seen on the surface (VPI&SU-5648-3, p. A-22).

Major Element Chemistry

Sixteen samples have been analyzed for major element content. The samples are similar in chemistry to the surface samples: $K2O = 4.59 - 5.24$, $Na2O = 4.51 - 4.89$, and $CaO = 0.13 - 0.82$. On a plot of normative Q-Ab-Or (Figure A-12), the core samples plot near the surface samples and show more variation in percent of normative quartz.

This variation may be due to the larger size of the sample population, and does not truly indicate any difference in pressure of crystallization. The Cuffytown Creek drill hole is only 300 m deep, much too shallow for any differences in depth to appear on the Q-Ab-Or diagram. The variation in normative quartz, however, is more likely due to problems encountered in calibration for silica. In any case, positions of granite composition on the Q-Ab-Or plot can be used only as a rough guide to pressure conditions when no other information is available to yield estimates of pressure.

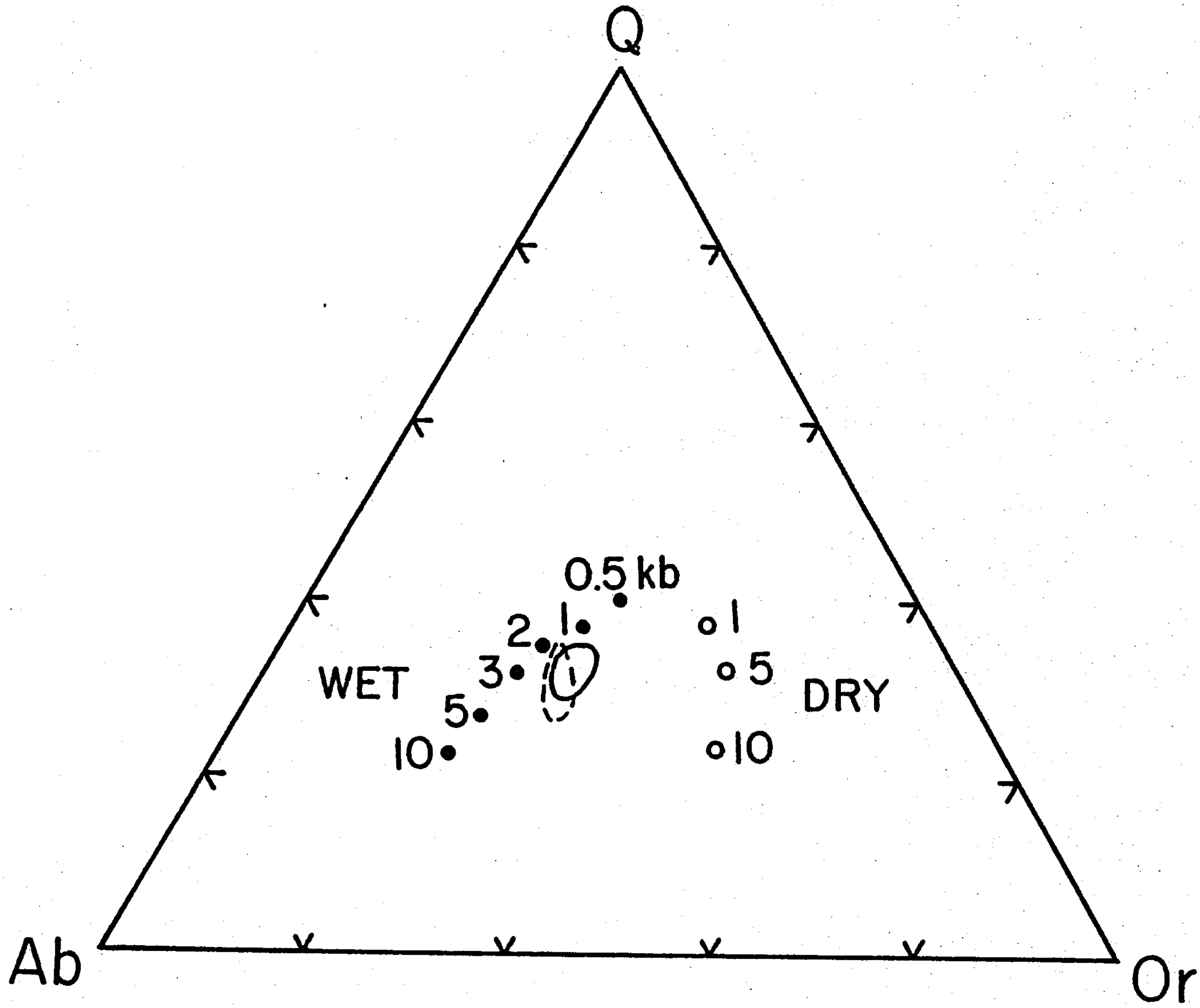

Figure A-12. Normative quartz - albite - orthoclase diagram showing compositions of Cuffytown Creek surface samples (solid line) and core samples (dashed line). Experimentally determined minima are from Tuttle and Bowen, 1958, Luth <u>et al</u>., 1964, and Luth, 1969.

U, Th, and Heat Production

Fourteen samples were analyzed by gamma ray spectrometry for U and Th content and heat production; results are shown in Table A-7. Average values are slightly higher than those found for surface samples: U = 10.2 ppm, Th = 33.3 ppm, and heat production = 12.5 HGVU, versus 8.7, 33.3, and 11.3 for surface rocks. A plot of these values (Figure A-13) shows that U, Th, and heat production increase slightly with depth.

The deepest sample, ED 1-275, has the highest concentrations of U and Th and the greatest heat production. The variations in U and Th concentrations are probably a reflection of the difference in degree of alteration of the core. Sample ED 1-275 is from the grey section of the core; samples from higher intervals represent zones that show progressively more alteration. The differences in U and Th content found in the core suggest that, in zones of extensive alteration, both U and Th have been removed from the system in small amounts. Fission track studies of samples taken throughout the core, in combination with results of fission tracks studies of other granites, may aid in determining the extent of U redistribution.

TABLE A-7

U, Th, and K contents and heat production of drill core ED1.

	U (ppm)	Th (ppm)	K (wt %)	HGVU (cal/cm^3-sec)
ED1-11	7.4	35.6	3.6	11.4
ED1-93	10.3	30.1	3.6	11.9
ED1-110	9.4	34.8	3.6	12.5
ED1-134	10.5	28.7	3.6	11.8
ED1-144	9.2	35.3	3.6	12.4
ED1-154	10.0	33.3	3.7	12.3
ED1-176	10.7	32.0	3.8	12.6
ED1-185	8.8	30.7	3.6	11.2
ED1-205	11.0	34.9	3.8	13.5
ED1-221	10.7	30.4	3.6	12.3
ED1-233	11.6	35.3	3.6	13.6
ED1-245	9.3	31.3	3.7	11.6
ED1-254	11.7	36.0	3.6	14.1
ED1-275	12.3	37.3	3.7	14.6

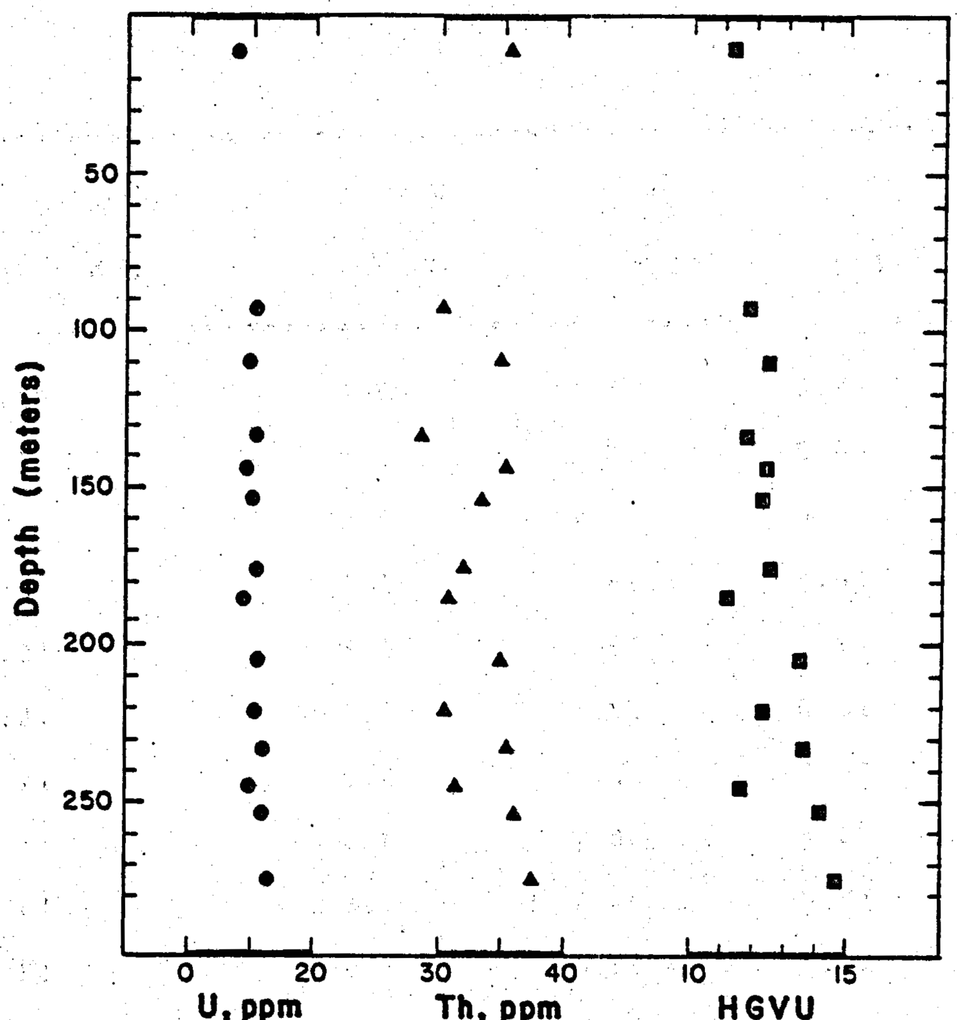

Figure A-13. Variation in U(ppm), Th (ppm), and heat production (cal/cm^3-sec) with depth in samples from ED-1.

B. GEOCHEMISTRY

A. Krishna Sinha, Principal Investigator

J. R. Sans, Research Associate

S. T. Hall, Research Associate

B. Hanan, Graduate Research Associate

S. Dickerson, Laboratory Aide

S. P. Higgins, Laboratory Aide

C. R. Miner, Laboratory Aide

C. M. Sadick, Data Entry Operator

THE BEHAVIOR OF URANIUM AND THORIUM DURING DIFFERENTIATON OF THE WOODSTOCK GRANITE

John R. Sans

The Woodstock Granite is a small oval-shaped pluton located in southwestern Baltimore County, Maryland. The Woodstock Granite intrudes the part of the Baltimore more Gneiss known as the Woodstock Dome. This report will discuss the major element and radioelement chemistry of forty-nine rock samples collected from the Woodstock Granite and the surrounding Woodstock Gneiss Dome. Sans (1978a) described the field relations and locations for these rock samples.

Of the forty-nine rock samples, twenty-seven are granite samples, twenty are gneiss samples, and two are composite samples with both a granitic and gneissic phase. The uranium, thorium and potassium content of forty-two of these samples was determined by gamma-ray spectroscopy. The preliminary interpretation of the radioelement distribution was given by Sans (1978b). The same suite of samples has now been analyzed for major element chemistry by x-ray fluorescence. A total of fifty-one chemical analyses were done on the forty-nine samples, since two of the samples contained the contact between granite and gneiss.

CIPW normative minerals were computed from the chemical analyses of the granite samples. A good indicator of the degree of differentiation of a given granite sample is provided by the Differentiation Index (DI). The DI is simply the sum of normative quartz, orthoclase and albite (DI = Q + Or + Ab). The DI for the twenty-nine granite analyses ranges from 69.2 to 91.5 percent. However, all but three of the samples fall in the much narrower range of 78.7 to 85.4 percent.

In a typical granite, one would expect a positive correlation between thorium and potassium. For example, Rogers and Adams (1969) reported that the K/Th ratio remains very nearly constant at 3×10^3 in a large variety of igneous rocks. In contrast, the Woodstock Granite shows a weak negative correlation between thorium and potassium. Furthermore, thorium shows a strong negative correlation with the Differentiation Index (DI). A least-squares fit to the data yields the following empirical relationship:

$$Th = (-0.731)(DI) + 74.8 \qquad \text{Equation 1}$$

Where Th is thorium concentration expressed in parts per million, and DI is Differentiation Index (normative Q + Or + Ab) expressed in percent. This relationship holds over the entire composition range of the Woodstock Granite.

The presence of euhedral zoned grains of allanite in the Woodstock Granite was first noted by Keyes (1895). Modal analyses for six rock samples from the Woodstock Granite were reported by Hopson (1964). He found that the modal abundance of allanite ranged from 0.1 to 0.5 percent.

Both Keyes and Hopson thought that the zoning and euhedral shape of the allanite grains suggested primary origin. It is well known that allanite typically contains high concentration of thorium. Deer and others (1962) reported a range of 0.35 to 2.23 percent ThO_2 in analyzed allanites.

We have found that rock samples from the Woodstock Granite contain 12 to 18 ppm thorium. If all of the thorium in the rock is assumed to be in the allanite, then Hopson's modal data imply a concentration of 0.24 to 2.05 percent ThO_2 in the allanite. This is the range of ThO_2 concentrations one would expect for allanite, and suggest that allanite is the dominant residence site for thorium in the Woodstock Granite. The obvious way to test this hypothesis would be to determine the ThO_2 content of the allanites from the Woodstock Granite on the electron microprobe.

As previously noted by Sans (1978b) the Woodstock Granite is concentrically zoned in thorium. The zoning obeys the following empirical relationship.

$$Th = (0.00472)(D) + 13.4 \qquad \text{Equation 2}$$

Where Th is thorium concentration expressed in parts per million, and D is the distance in meters from the nearest wall of the pluton. This relationship seems to hold for the entire Woodstock Granite from the wall contacts (zero meters) to the center of the pluton (760 meters). Obviously, since thorium concentration correlates with distance from the walls as well as Differentiaton Index (DI), the DI must correlated with the distance from the walls of the pluton. Combining equations 1 and 2, yields the following result:

$$DI = -0.00646\ D + 84.0 \qquad \text{Equation 3}$$

Where DI is Differentiation Index (normative Q + Or + Ab) expressed in percent, and D is the distance in meters from the wall of the pluton.

Equation 3 indicates that near the walls of the Woodstock Granite the DI is about 84.0 percent. In contrast, near the center (760 meters from the wall) the DI is distinctly lower at about 79.1 percent. If one considers the relationship of DI to D directly, without considering thorium, essentially the same result is obtained. This result is very curious, because one would expect a zoned pluton to be more differentiated toward the center not the margins. For example, see Bateman and Nokleberg (1978) for a recent discussion of a zoned pluton.

The uranium concentration in the Woodstock Granite ranges from 2.0 to 4.7 parts per million. Sans (1978b) noted that the uranium concentration does not correlate with the potassium concentration. He concluded that the presently observed uranium distribution is due to variable removal of uranium by weathering. We now have x-ray fluorescence analyses for the 10 major and minor elements (Na, Mg, Al, Si, P, K, Ca, Ti, Mn, Fe) in the same suite of samples from the Woodstock Granite. Uranium does not correlate with any of these 10 elements. The uranium concentrations were also checked for any correlation with the geographic location of the sample, CIPW normative minerals, Barth ' s Cations, Niggli Values, and Differentiation Index (normative Q + Or + Ab). No correlations were found. Such total lack of correlation is most unlikely, if the rock samples preserve the igneous uranium concentrations. Furthermore, all of the samples are from surface exposures and must be weathered to some degree. Hence, we draw the following two conclusions. First, the initial concentration of uranium in the Woodstock Granite was 4.7 ppm or higher. Second, the presently observed variation is due to the various degrees of weathering of the rock samples.

In summary, we draw the following conclusions about the distribution of thorium and uranium in the Woodstock Granite. (1) The thorium concentration of a rock samples from the Woodstock Granite can be predicted empirically from the Differentiation Index (normative Q + Or + Ab) of the sample. (2) The thorium concentration can also be predicted from the geographic location of the sample. In other words the pluton is concentrically zoned in thorium. (3) The thorium distribution is probably controlled by the distribution of the accessory mineral allanite. (4) The thorium concentration is related to the differentiation of the pluton, but the nature of the relationship is not clear. (5) Uranium concentrations cannot be predicted, because the uranium has been extensively removed by weathering.

References

Bateman, P.C. and Nokleberg, W. J. (1978) Solidification of the Mount Givens granodiorite, Sierra Nevada, California, J. of Geology, Vol. 86, pp. 563-579.

Deer, W. A., Howie, R. A., and Zussman, J. (1962). Rock Forming Minerals, Volume 1, Ortho-and Ring Silicates, Longmans, Green and Co. Ltd., London.

Hopson, C.A., 1964. The crystalline rocks of Howard and Montogomery Counties. in The Geology of Howard and Montgomery Counties. Maryland Geol. Survey. p. 27-215.

Keyes, C. R., 1895. Origin and relations of central Maryland granites. U. S. Geol. Suvey 15th Annual Report, p. 685-740.

Rogers, J. J.W and Adams, J. A. S. (1969) Thorium: In Handbook of geochemistry, K. H. Wedepohl, ed. VII, No. 1.

Sans, J. R. (1978a) The granitic rocks of the Maryland Piedmont, in Costain J. K., Glover, L., III, and Sinha, A. K. (1978). Evaluation and targeting of geothermal energy resources in the southeastern United states - Progress Report VPI SU - 5648-3, APRIL 1, 1978 - JUNE 30, 1978, pp B-26 - B-32. (Available from NTIS).

Sans, J. R. (1978b) Distribution of uranium, thorium and potassium in the weaklyfoliated rocks of the Maryland Piedmont, in Costain J. K., Glover, L., III, and Sinha,

A. K. (1978). Evaluation and targeting of geothermal energy resources in the southeastern United States - Progress Report VPI& SU- 5648, April 1, 1978 - June 30, 1978, pp B-33 - B-45. (Available from NTIS).

SILOAM CORES

Stephen T. Hall

One core hole each was drilled into the medium-grained Siloam granite and the porphyritic Siloam granite from the Siloam, Georgia pluton. Eighteen (18) samples from each were analyzed for major element chemistry.

In common with both the porphyritic and medium-grained Siloam surface samples, the cores from both of these phases calculated out to contain 17% normative quartz. The porphyritic core samples, like the porphyritic surface samples (geochemistry section report VPI & SU 5648-3), plot on the boundary between the syenogranite and monzogranite fields of Streckeisen s (1976) normative Or-Ab-An classification diagram. The medium-grained Siloam core samples also plot around the syenogranite-monzogranite boundary but, like the medium-grained Siloam surface samples, more samples plot within the syenogranite field.

Table B-1 shows the ranges in alkali and CaO contents of both sets of core samples. Na-K-Ca plots of the porphyritic Siloam core data yield a trend very similar to the average calc-alkaline trend given by Nockolds and Allen (1953). The Na-K-Ca plots of the medium-grained Siloam core samples do not show as good a trend but do, however, cluster around the most differentiated end of the average calcalkaline trend. A-F-M plots and Streckeisen s Or-Ab-An classification diagram plots of both cores also tend to indicate calc-alkaline affinities.

Figure B-1 shows the Siloam core normative Qz-Ab-Or data plotted on the water-saturated phase diagram. Figure B-2 shows the effect of the An component and also the fields where the surface samples plot. Ab/An ratios for both sets of core samples are about 4 to 4.5 and are therefore similar to the Siloam surface samples. Since it would be unreasonable to expect any significant change in pressure over the few hundred feet sampled in the cores, the Siloam core samples must also be considered to have equilibrated at the same pressure (between 2 and 4 Kb, VPI & SU report 5648-3) as the surface samples. That the core samples appear to indicate higher pressures must be considered an indicaction that the most differentiated granite was not encountered in the sampling.

Recent gamma-ray investigations of the Siloam surface samples by the geophysical section have shown U values to range from 3.8 to 7.7 ppm in the porphyritic phase and about 5 ppm in the medium-grained phase. Th contents range from 23.4 to 39.7 ppm in the porphyritic phase and about 33 ppm in the medium-grained phase.

PALMETTO GRANITE

Stephen T. Hall

Six (6) samples from the surface of the Palmetto, Georgia granite and fourteen (14) core samples were analyzed for major element chemistry. Of the surface samples, three analyses yielded 17% normative quartz and fell into the calc-alkaline to subalkaline syenite category in Streckeisen s (1976) normative Or-Ab-An classification diagram. The other three calculated out to 17% normative quartz and are considered monzogranites according to Streckeisen s classification. However, these three monzogranites fall within the same general area on the Or-Ab-An diagram as the three "syenite" samples and would be classified as calc-alkaline syenites if they had 17% normative quartz. With the exception of two of the shallowest samples which have 17% normative quartz and fall into Streckeisen s monzogranite category, all of the Palmetto core samples contain 17% normative quartz and are classified as subalkaline syenites. All core samples, however, fall within the same general area on the Or-Ab-An diagram and like the surface samples, the amount of normative quartz makes the difference in the classification. The monzogranitic surface samples are from the southwestern part of the body, but more sampling and analyses will be required to determine if there is any sort of chemical gradient across the pluton.

Table B-1 shows the ranges in alkali and CaO contents of the surface and core samples. Na-K-Ca and AFM diagrams of both the surface and the core show calc-alkaline affinities (Nockolds and Allen, 1953).

Figure B-1 shows the Qz-Ab-Or water-saturated phase diagram with the normative Palmetto surface and core sample data projected onto it. Figure B-2 shows the same projected normative data on the Qz-Ab-Or diagram showing the effect of An content on the $P_{H_2O} = 2$ Kb eutectic. Both the core and surface samples yield quite similar plots and are also both similar to the Liberty Hill pluton (VPI & SU 5648-3) without the most differentiated Liberty Hill samples. The Ab/An ratio of the Palmetto is also slightly less, in general, than the Liberty Hill. Both of these factors would indicate either a greater pressure of emplacement for the Palmetto (4.8 Kb) or a loss of the most differentiated or upper part of the Palmetto pluton through erosion.

PAGELAND GRANITE

Stephen R. Hall

Twelve (12) surface samples and ten (10) core samples were analyzed for major element chemistry. One of the surface samples is from the granodiorite at the center of the Pageland pluton and the rest are from the Pageland monzogranite itself (Bourland, 1978). All core samples are of the Pageland monzogranite. Norm calculation of the chemical analyses and subsequent plots on Streckeisen-s (1976) normative Or-Ab-An classification diagram show that both the core and surface monzogranite samples cluster around the boundary between the monzogranite field and the syenogranite field. They are, therefore, very similar in this respect to the Siloam (geochemisry section, report VPI & SU 5648-3) and the Rolesville (geochemistry section, report VPI & SU 5103-5) plutons. The "granodiorite" sample calculated out to be 17% normative quartz and is classified as a syenite according to Streckeisen-s classification.

Table B-1 shows the ranges in alkali and CaO contents of both the core and surface monzogranite samples and the range of U and Th values of the surface samples. The syenite surface sample has Na_2O =4.09, K_2O = 4.28, CaO = 2.64, U = 2.7, and Th = 11.5 showing that it is more mafic but with relatively high Na. AFM diagrams of both surface and core samples show alkaline to calc-alkaline affinities whereas Na-K-Ca diagrams of both surface and core samples show calc-alkaline affinities. Plots of CaO vs. SiO_2 and FeO vs SiO_2 show some linear correlations for the surface samples.

Figure B-3 shows the Qz-Ab-Or water-saturated phase diagram with the normative Pageland surface and core sample data projected onto it. Figure B-4 shows the same projected normative Pageland data on the Qz-Ab-Or diagram with the effect of An content shown. Both surface and core data plot in the same general area and Ab/ An ratios for both are in the range of 3-4 with a few samples in the range of 7-8. Considering that the most differentiated surface samples have an Ab/An ratio of between 4 and 5, a pressure of emplacement of about 3 Kb can be inferred from these two diagrams. However, this pressure value is not neccessarily accurate since other factors are not accounted for in these diagrams. In fact, since the Pageland is similar in age and chemistry to the Winnsboro and Liberty Hill plutons (Bourland, 1978) and if the contact aureole assemblages are similar to those surrounding the latter two plutons, a comparable pressure value of about 5 Kb would be implied.

TABLE B-1

Chemical Ranges (in weight percent)

	Medium-grained Siloam core	Porphyritic Siloam	Palmetto surface	Palmetto core	Pageland surface	Pageland core
Na_2O	2.80-4.31	3.60-4.00	3.30-3.84	3.23-3.72	3.17-3.81	3.53-4.08
K_2O	4.71-6.74	4.67-6.22	4.37-5.19	3.78-4.64	3.81-5.93	4.42-5.30
CaO	0.93-2.41	1.41-2.03	2.07-3.51	2.98-3.73	0.85-2.49	1.26-2.11
U (ppm)					2.8-9.6	
Th (ppm)					12.2-28.7	

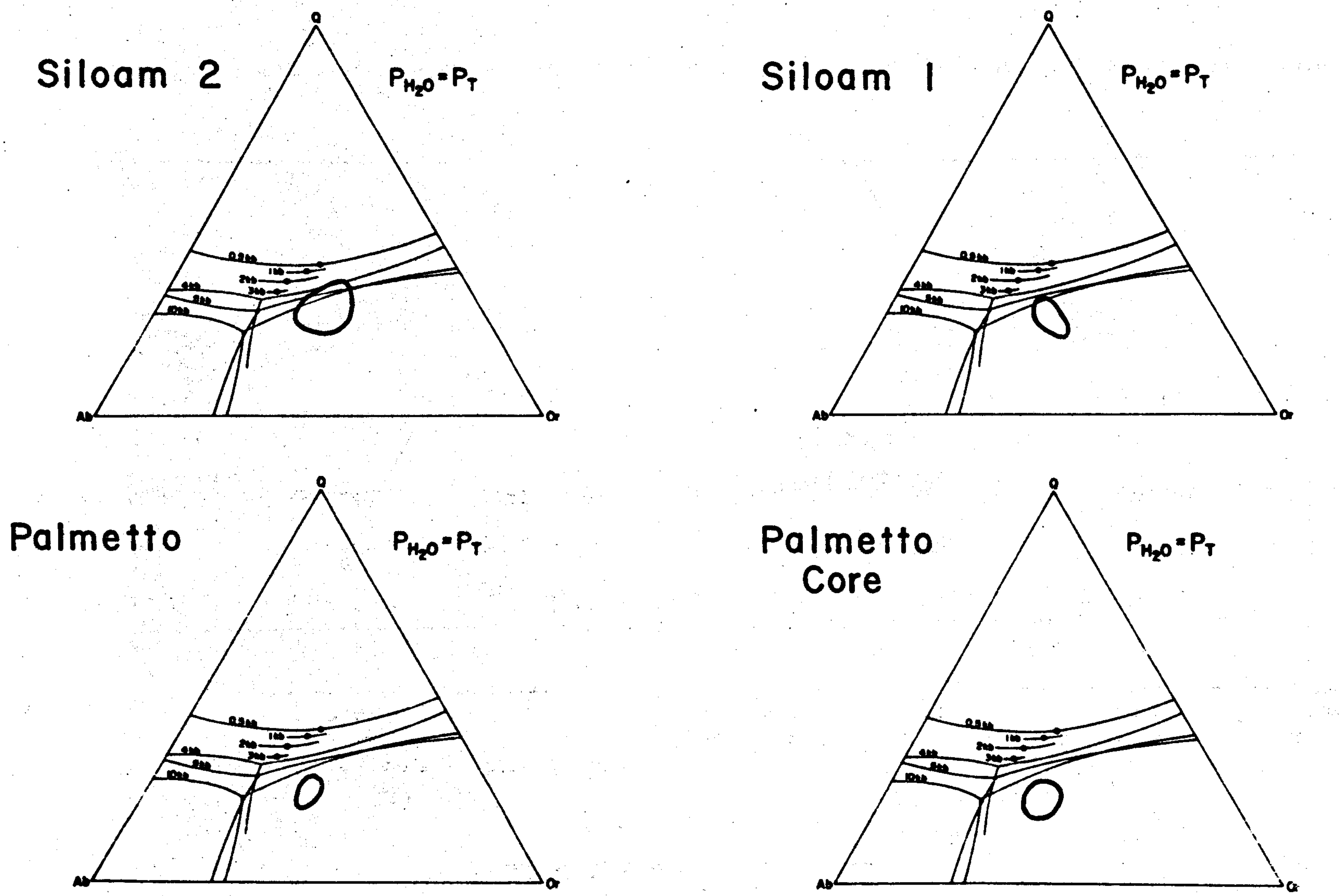

Figure B-1. Normative Qz - Ab - Or diagrams for the saturated system.

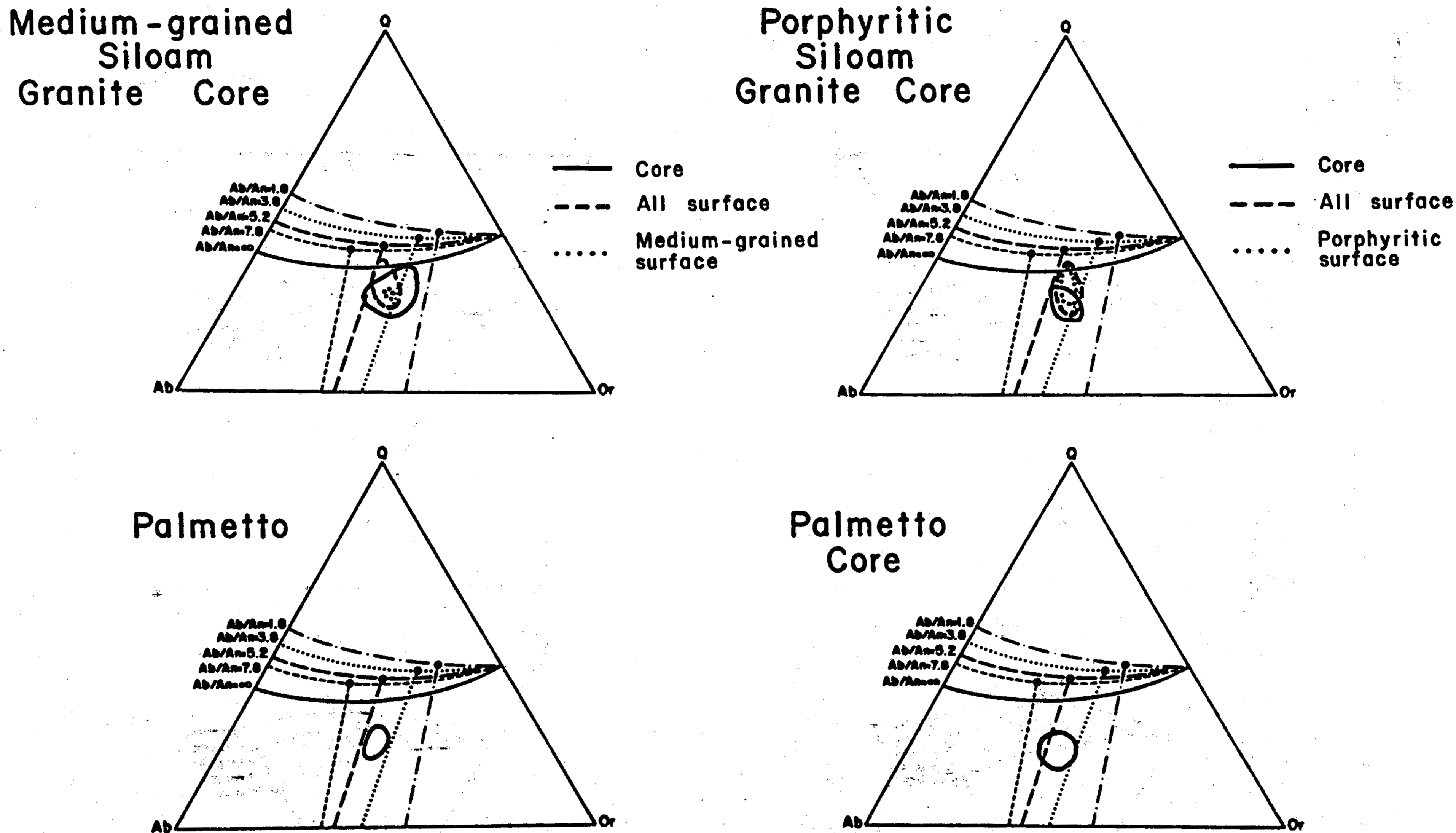

Figure B-2. Normative Qz - Ab - Or diagrams for P_{H_2O} = 2 Kb showing the effects of an An component.

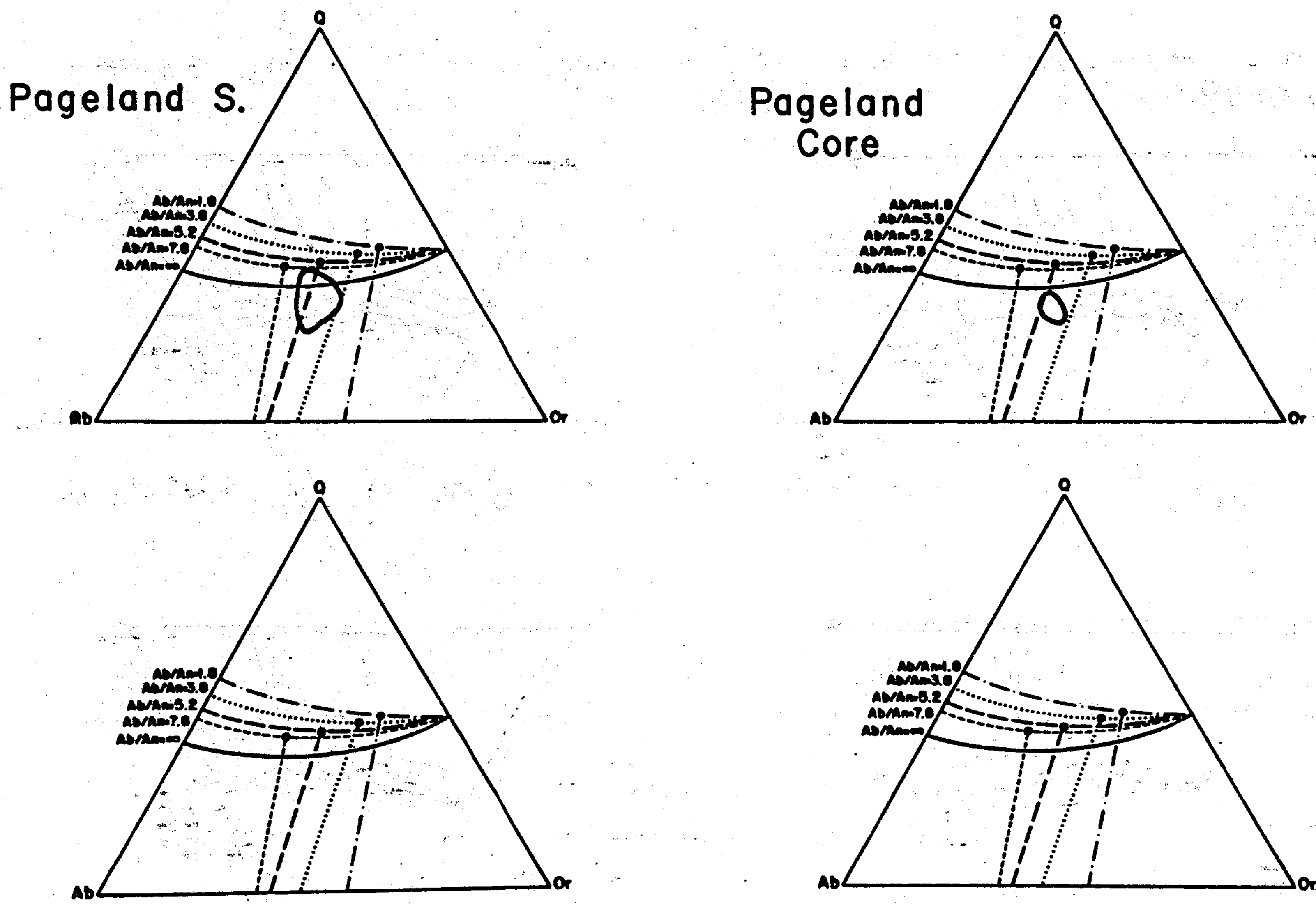

Figure B-3.

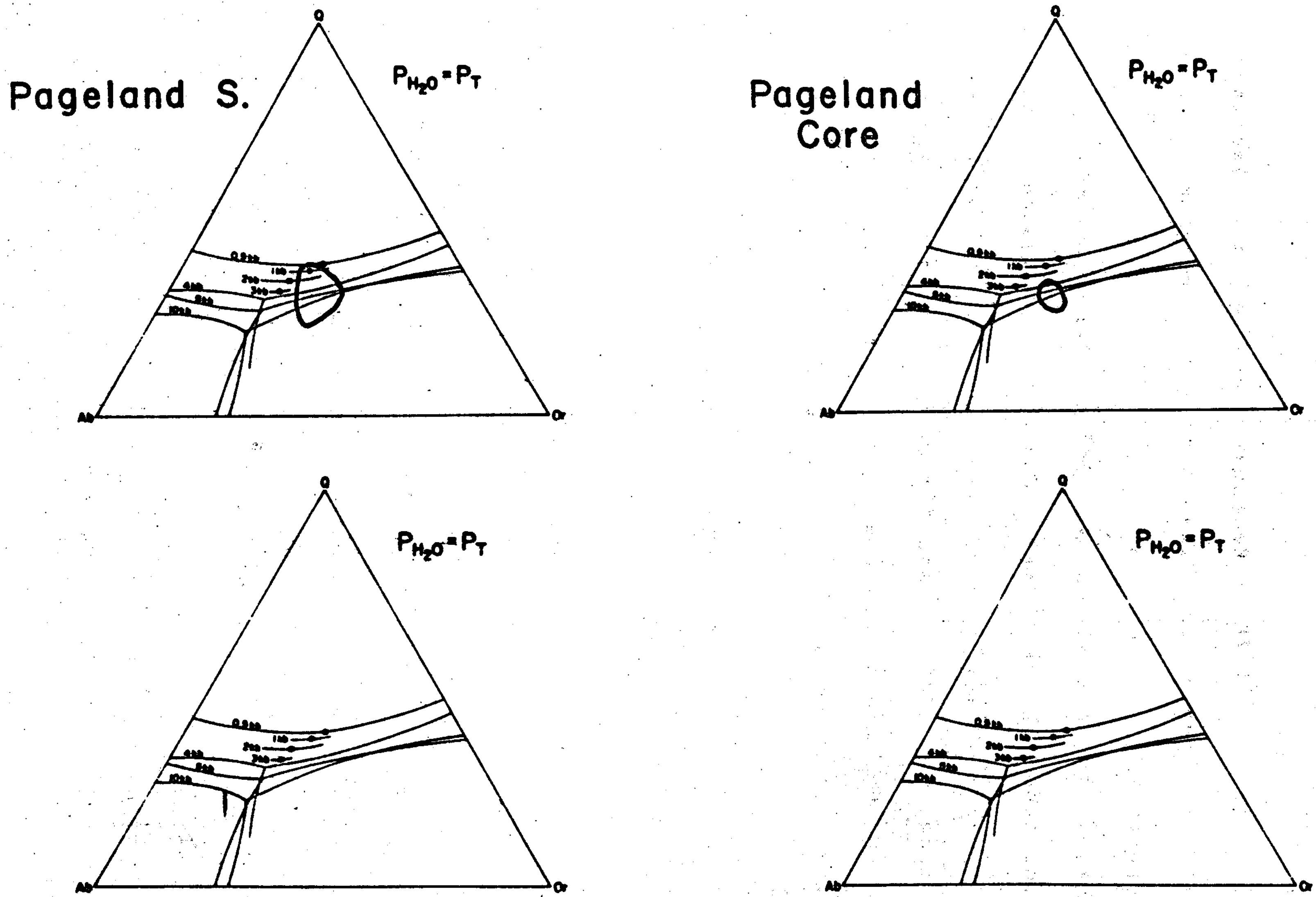

Figure B-4.

References

Bourland, W. C., 1978. Reconnaissance of the Pageland Pluton: South Carolina Geothermal Program, Final Report.

Nockolds, S. R. and Allen, R., 1953. The geochemistry of some igneous rock series: Geochem. et Cosmochem. Acta. v.4, p. 105-142.

Streckeisen, A., 1976. Classification of the common igneous rocks by means of their chemical composition. A provisional attempt: N. Jb. Miner. Mb. H. 1, p. 1-15.

C. GEOPHYSICS

John K. Costain, Principal Investigator

A. H. Cogbill, Research Associate

L. D. Perry, Research Associate

J. J. Lambiase, Research Associate

S. Dashevsky, Research Specialist

B. U. Sans, Research Specialist

M. Svetlichny, Research Specialist

T. H. Arnold, part-time Laboratory Aide

R. W. Meier, Co-op Student

Atlantic Coastal Plain Drilling Program

During the present period (July 1, 1978 - September 30, 1978), the geophysics group has been primarily occupied with the interpretation of results from the heat flow drilling program on the Atlantic Coastal Plain. To date (September 28, 1978) seventeen (17) holes have been drilled in the States of New Jersey, Delaware, Maryland, and Virginia for the purpose of determining the geothermal gradient and terrestrial heat flow. Locations of the holes are shown in Figure C-1.1. With one exception (Hole 43 at Ocean City, MD), all of the holes have been drilled to a depth of approximately 300 m, cased, and cemented to the surface. Hole 43 was cased to a depth of about 180 m.

The holes were drilled by Energy Services Co. (under contract to Gruy Federal, Inc.). The first hole was completed at Fort Monmouth, NJ on July 9, 1978. Most of the holes are being drilled with a Skytop Brewster drill which is now drilling, coring, casing, and cementing 300-m holes at the rate of one every 2.5 days. Two attempts to recover a total of 15 m of core are made in each hole. Core recovery has been variable due to difficult drilling conditions.

Most of the holes have been logged more than once in order to establish the length of time necessary to reach an equilibrium geothermal gradient. This is discussed in more detail in the following pages by S. Dashevsky.

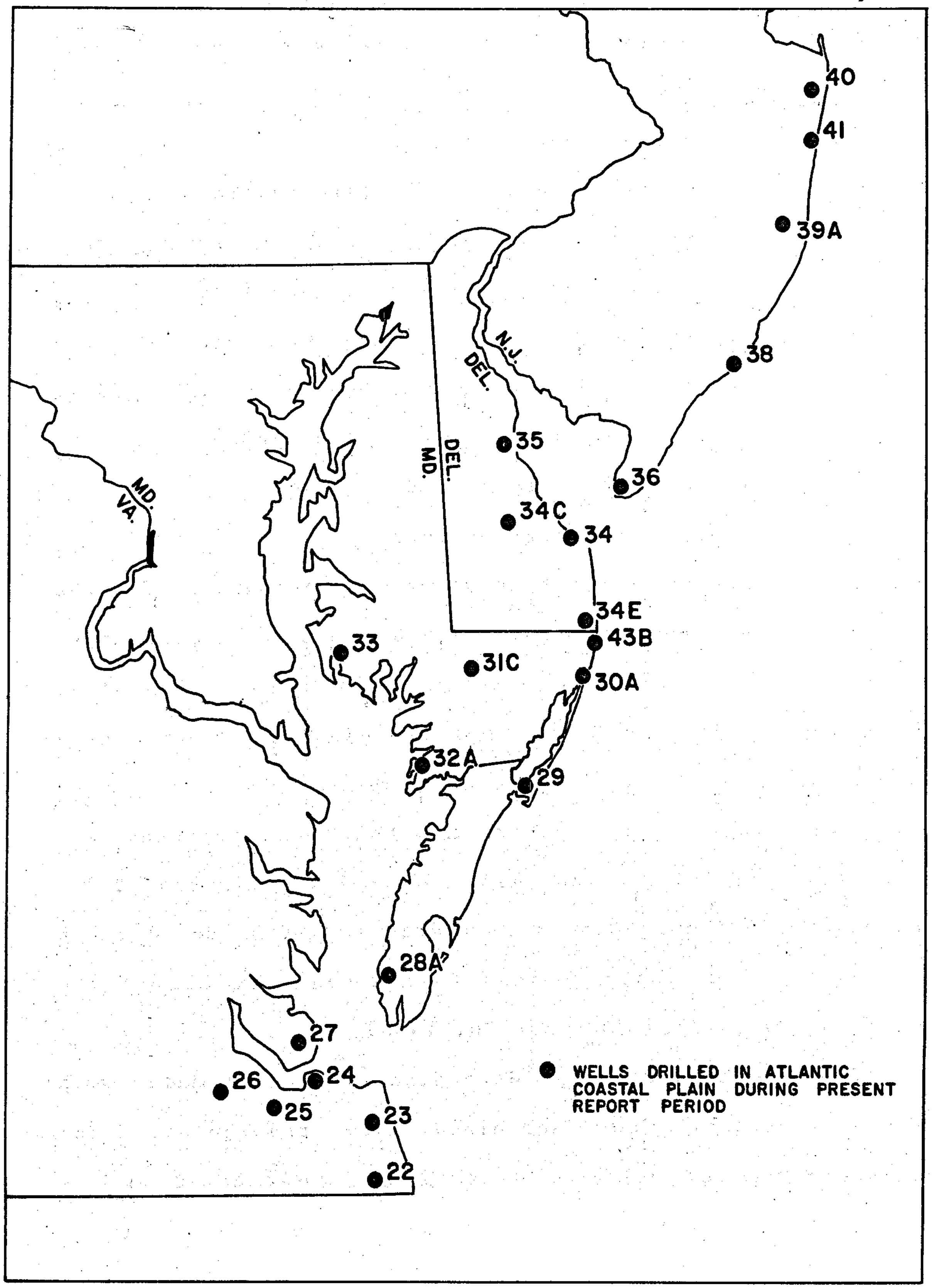
40
41
39A
38
N.J.
DEL.
DEL.
MD.
35
36
34C
34
MD.
VA.
34E
43B
33
31C
30A
32A
29
28A
27
24
26
25
23
22
WELLS DRILLED IN ATLANTIC COASTAL PLAIN DURING PRESENT REPORT PERIOD

Figure C-1.1

The drill sites were selected by VPI&SU in cooperation with State and Federal agencies, primarily on the basis of:

(1) available gravity data,

(2) available aeromagnetic data,

(3) known thickness of Coastal Plain sediments,

(4) apparent thermal anomalies based on existing data,

(5) much of the available basement core data,

(6) suitable sites for the evaluation of the radiogenic model (Progress Reports VPI&SU-5103-1, -2, -3, -4, -5, and VPI&SU-5648-1 to the Department of Energy), and

(7) proximity to energy markets.

Least-squares gradients usually can be computed for the most part over the depth interval 50 - 300 m in each hole. Average gradients range from about 25 °C/Km to a high of 45 °C/Km. (Crisfield, MD). Normal procedure for temperature logging is to sample the temperature every 0.5 m; holes which are logged soon after the hole was cemented are generally sampled at coarser intervals. Figures C-2.6 through C-2.9 show geothermal gradients over selected depth intervals and estimated depths to basement for all of the holes logged to date (October 20, 1978).

Thermal conductivity determinations are made with needle probes on core obtained from the holes. The conductivities of selected lithologies are checked with a conventional divided-bar apparatus. Table C-1.2 is a representative sampling of the thermal conductivity of core determined with needle probe techniques and shows the range of thermal conductivities to be expected in sediments of the Atlantic Coastal Plain. Final determinations of heat flow for each drill site are in progress and will be given in subsequent reports and papers when equilibrium gradients have been reached and thermal conductivity determinations are complete.

Preliminary results from the heat flow program on the Atlantic Coastal Plain suggest that areas in Maryland and Virginia warrant further exploration and study. These are, from north to south:

(1) Salisbury, Maryland

(2) Crisfield, Maryland

(3) Wallops Island, Virginia

Additional heat flow holes are planned in these areas to define the geographic extent of the thermal anomalies. Additional detailed gravity coverage is also being obtained.

Holes 25 and 26 (Figure C-1.1) drilled in Virginia offer additional confirmation of the radiogenic model. Hole 25 near Portsmouth, VA was drilled at the center of a well-defined negative gravity anomaly. Hole 26 was drilled at a location away from this anomaly, but close enough so that essentially the same stratigraphic section would be penetrated. Thermal conductivity determinations are not yet complete; however, the gradient in hole 25 (35 °C/Km is 35%

TABLE C-1.2 C-1.2-1

REPRESENTATIVE THERMAL CONDUCTIVITY VALUES
OF THE ATLANTIC COASTAL PLAIN

SAMPLE NAME	LITH CODE	DEPTH (M)	K RUN1	K RUN2	K RUN3	K RUN4	MEAN
C26-971.5		296.1	7.6	6.3			7.0
C26-972.5		296.4	7.9	6.2			7.1
C26-979.5		298.6	6.8	6.3			6.6
C26-980.5		298.9	5.9	6.2			6.1
C26-981.5		299.2	6.3	7.6			7.0
C26-982.5		299.5	7.1				7.1
C26-983.5		299.8	7.1				7.1
C26-984.5		300.1	7.4				7.4
C26-985.5		300.4	6.6				6.6
C26-986.5		300.7	6.9				6.9
C26-987.5		301.0		5.8			5.8
C26-988.5		301.3	6.1		7.5		6.8
C26-989.0		301.5	5.9	5.5	3.8		5.1
C26-990.0		301.8	3.9	5.5	4.9		4.8
C29-584.5	C	178.2	3.6	2.6	3.6		3.3
C29-585.5	C	178.5	3.8	4.0	4.2		4.0
C29-586.5	ZC	178.8	3.2	4.1	5.6		4.3
C29-587.5	C	179.1	4.8	6.1	6.9		5.9
C29-588.5		179.4	5.5		5.4		5.5
C29-589.5		179.7	5.8		6.1		6.0
C29-590.5		180.0	5.9		5.8		5.9
C29-591.5		180.3	5.3	5.3	5.5		5.4
C29-592.5		180.6	6.0	5.8	6.4		6.1
C29-593.5		180.9	7.6	6.9	6.6		7.0
C29-594.5		181.2	5.8				
C29-595.5		181.5	5.2	4.4			4.8
C29-596.5		181.8				6.0	6.0
C29-597.5		182.1					
C29-598.5		182.4		4.7		5.0	4.9
C29-599.5		182.7		3.9	4.7		4.3
C29-990.5	SZ	301.9	5.4	4.4	4.6		4.8
C29-991.5	SZ	302.2	4.9	4.7	5.4	4.2	4.8
C29-992.5	SZ	302.5	4.5	4.8	4.9		4.7
C29-993.5	WSZ	302.8	4.7	4.1	4.0		4.3
C29-994.5	SZ	303.1	4.7	5.2	4.2		4.7
C29-995.5	Z	303.4	3.7	3.1	3.7		3.5
C29-996.5	Z	303.7	3.7	3.7	3.4		3.6
C29-997.5	SZ	304.0	4.0	2.8	2.4		3.1
C29-998.5	SZ	304.3	4.1	4.2	3.7		4.0

TABLE C-1.2 C-1.2-2

REPRESENTATIVE THERMAL CONDUCTIVITY VALUES
OF THE ATLANTIC COASTAL PLAIN

SAMPLE NAME	LITH CODE	DEPTH (M)	K RUN1	K RUN2	K RUN3	K RUN4	MEAN
C29-999.5	SZ	304.6		4.2	3.9		4.1
C32-541.5		165.1		3.7			3.7
C32-542.5		165.4	3.6	3.7			3.7
C32-543.5		165.7	3.8	3.4			3.6
C32-544.5		166.0	3.6	2.8	3.1		3.2
C32-545.5		166.3	3.6	3.0			3.3
C32-546.5		166.6	3.5	3.4			3.5
C32-547.5		166.9	3.6	3.4			3.5
C32-548.5		167.2		3.1			3.1
C32-549.5		167.5	3.9	2.9	3.1		3.3
C32-550.5		167.8		3.7	3.8		3.8
C32-551.5		168.1		3.0	3.3		3.2
C32-552.5		168.4		3.6	3.8		3.7
C32-553.5		168.7		3.2	3.5		3.4
C32-554.5		169.0			3.4		3.4
C32-555.5		169.3		3.3	3.3		3.3
C32-556.5		169.6		2.9	3.5		3.2
C32-557.5		169.9		3.1	3.6		3.4
C32-558.5		170.2		3.2			3.2
C32-559.5		170.5			3.6		3.6
C32-560.5		170.8		2.8	3.1		3.0

KEY TO LITHOLOGIC CODES

S = sand
C = clay
Z = silt
M = mud
SC= sandy clay
SZ= sandy silt
SM= sandy mud
CS= clayey sand
MS= muddy sand

ZS= silty sand
Y = glauconitic
X = lignitic
W = shelly
L = limy
G = gravel
H = consolidated
V = very; greater than 50%

Example VLCS very limy clayey sand

higher than that (26 °C/Km) in hole 26. Basement was not sampled at either location, so at the present time, it is not possible to determine heat generation in basement rocks or to relate heat flow to basement heat generation. This continues to be an important objective of this program, however, and plans are underway to deepen these holes in the near future.

The lack of detailed gravity and magnetic coverage between Salisbury, MD (hole 31) and Wallops Island, VA (hole 29) has hampered the selection of heat flow drill sites in this area. Potential field anomalies in this area are much less well-defined than at Portsmouth, VA where anomalies in both the gravity and magnetic field are associated with the high geothermal gradient determined for hole 25. It is unclear at present whether the lack of definitive potential field anomalies between Wallops Island, VA and Salisbury, MD is primarily due to inadequate and/or incomplete data coverage, or whether it is due simply to lack of contrasts in density and magnetic susceptibility in basement rocks. In either case, aquisition of additional gravity data is necessary and is now in progress.

One additional factor in the geologic setting must be considered. The area between Wallops Island, VA and Salisbury, MD is not far from the projection to the east of the "38th parallel fracture zone" which is usually assumed to terminate in Highland County in northwestern Virginia. A well-defined zone of seismic activity in central Virginia may be part of an eastward extension of the 38th parallel fracture zone. We continue to prefer the interpretation that the high gradients between Salisbury, MD and Wallops Island, VA are unrelated to a possible eastward extension of the 38th parallel fracture zone in concealed basement rocks.

Sampling of basement rocks beneath the sediments of the Atlantic Coastal Plain should be given a high priority wherever possible as our program continues.

Discussions of lithologic changes in the heat flow holes in the Atlantic Coastal Plain and further interpretaton of the potential field data in the anomalous areas and in other areas will be forthcoming in subsequent reports.

GEOTHERMAL GRADIENTS, WELL LOGGING

Samuel S. Dashevsky

During the period of this report (July 1, 1978 - September 30, 1978), the VPI&SU well logging operation has closely monitored the drilling program in the Atlantic Coastal Plain. To determine and understand perturbations of the geothermal gradient imposed by drilling and cementing, the 300-meter heat-flow holes were logged repeatedly during the first several days and relogged throughout the following weeks.

Most complete coverage is available for holes 40 (Fort Monmouth, NJ) and 41 (Sea Girt, NJ). Temperature gradients over specific intervals are plotted with respect to time elapsed since cementing (Figures C-2.1 and C-2.2). An exponential cooling equation associated with the rate of decay of heat of solidification of cement in hole 41 is plotted as a solid line in Figure C-2.2. Data not presented in this report indicate that cooling might not be strictly exponential for all holes, but might have a linear component as well.

It is worthwhile to note that the standard deviation of computed least square gradients also decreased exponentially as a function of time. Figure C-2.3 shows this relationship for hole 41.

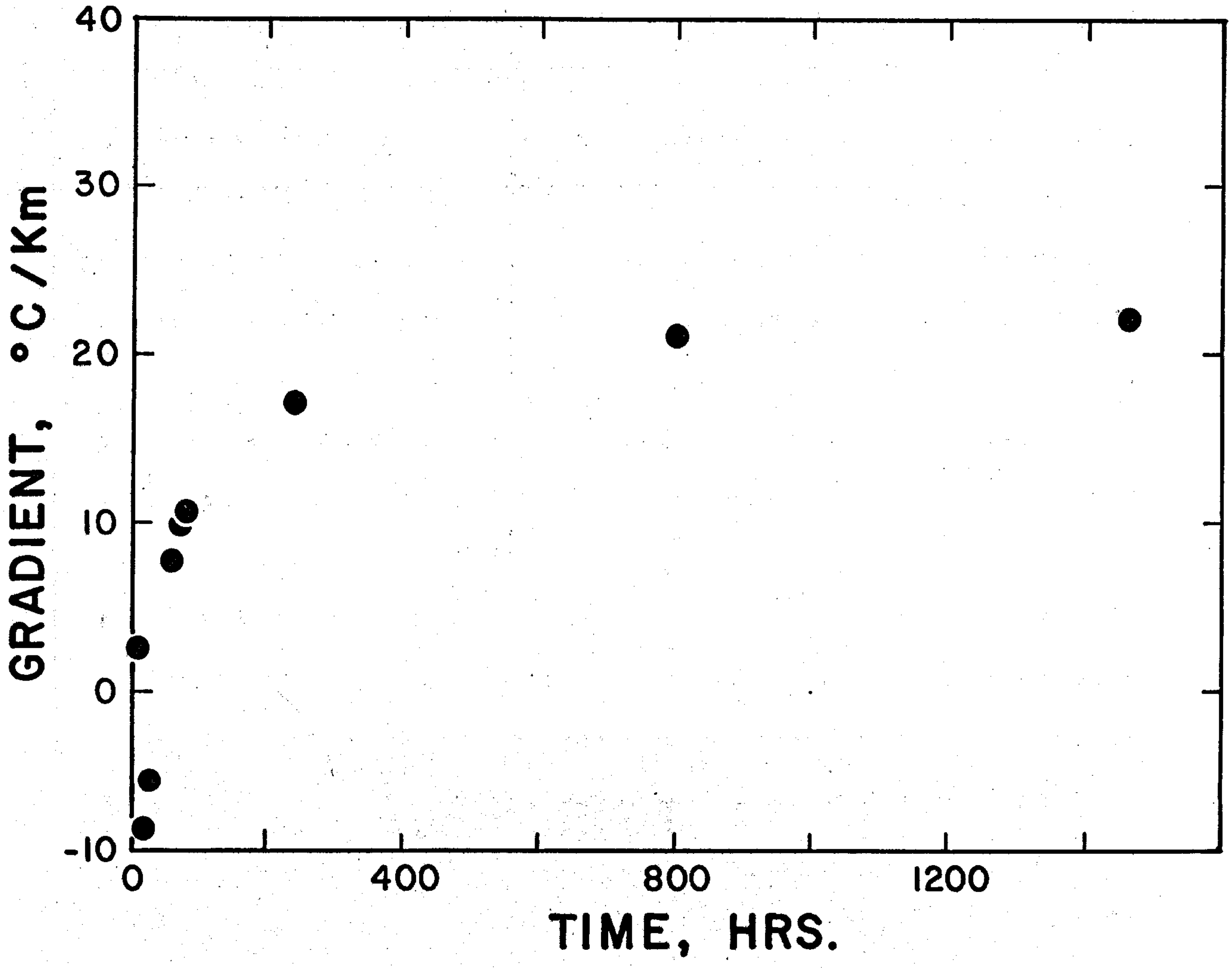

Figure C-2.1. Plot of gradients vs time since completion in hole C40, Fort Monmouth, NJ.

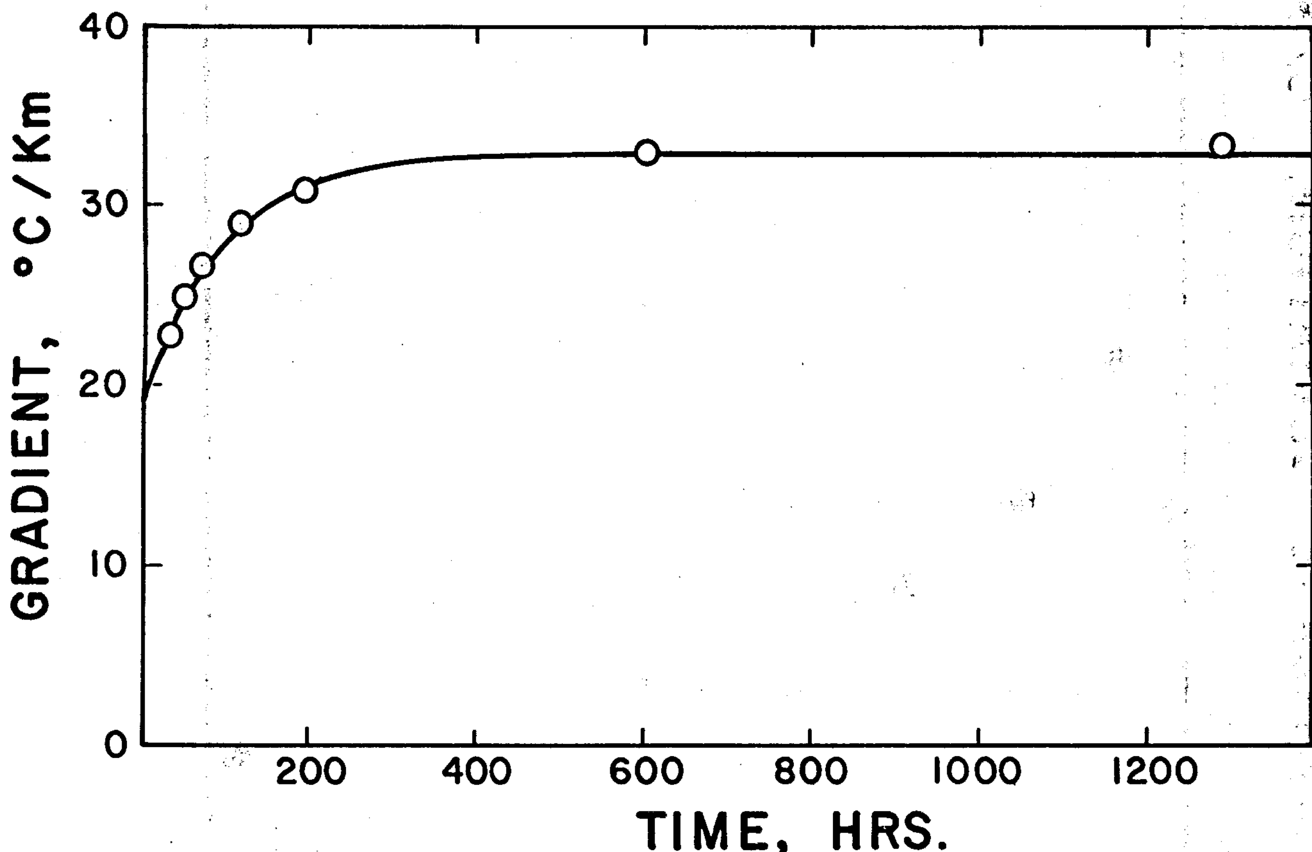

Figure C-2.2. Plot of gradient versus time since cementing in hole C41, Sea Girt, NJ. Solid line shows exponential cooling curve with the form of gradient = 32.9°c/km-13.75 Exp (0.010327 xt).

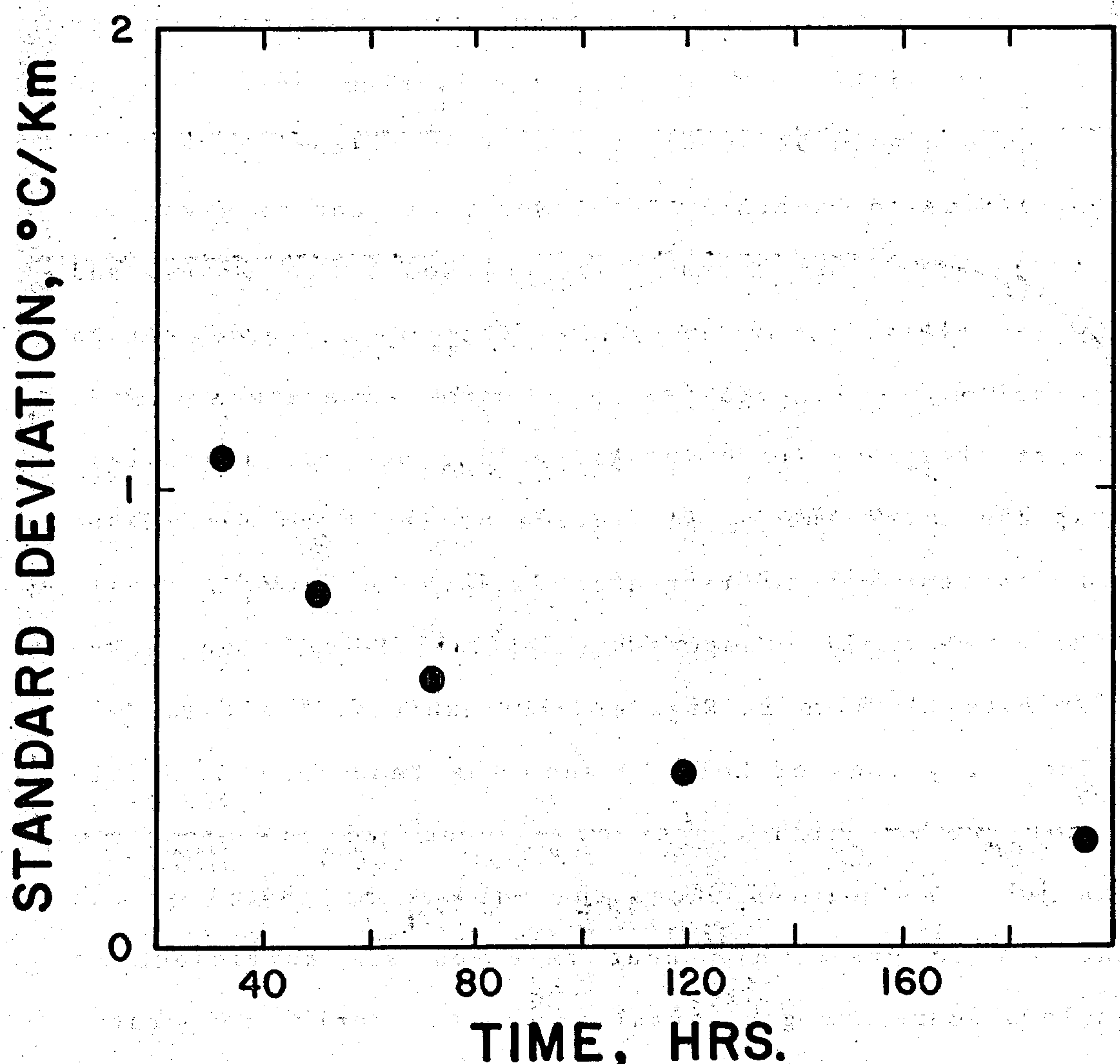

Figure C-2.3. Standard deviation of gradient versus time for hole C41, Sea Girt, NJ.

While none of the wells drilled during this report period has yet re-established an equilibrium geothermal gradient, the observed tendency is for the gradient to increase over a period of time from about four hours after cementing to within 10% of its equilibrium value at 250 hours and to within 5% at 450 hours after cementing.

In a cemented well, a large amount of heat is given off within the first six hours as cement bonds are formed and energy is released. The extreme effect of cementing is to bring the entire well to the same warm temperature with a near zero thermal gradient. As cooling begins, a gradient will appear since the upper section of the hole cools more rapidly in response to a greater difference between the in situ and the cement temperatures. Successive temperature logs of hole 40 shown in Figure C-2.4 exhibit this trend.

The early logs of hole 40 show the temperature profile of a hole with a high degree of washout and an incomplete cement job. In hole 40 where the void space filled by the cement was so great, the heat released was sufficient to entirely obscure the geothermal gradient. Early temperature logs show this hole as a monotemperature plug beginning at a depth of 150 m where the top of the cement is indicated by a +5°C step in temperature.

In hole 41, the combination of a higher ambient thermal gradient with a lesser degree of washout allowed the geothermal gradient to show beneath the masking effect of

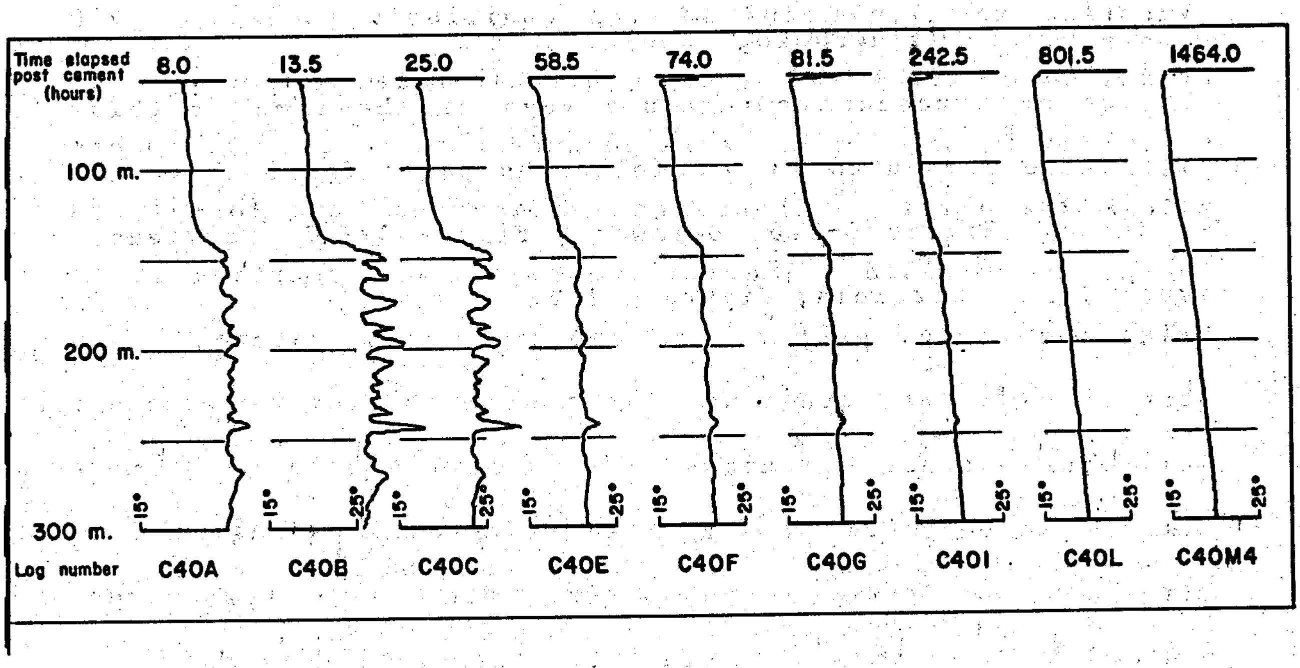

Figure C-2.4. Successive temperature logs of Hole C-40 eight hours post cementing through 1464 hours.

the cement (Figure C-2.5). Washout in this hole was confined to more discrete depth intervals than in C40. The large positive temperature spikes are at depths where sections have been washed out and subsequently contain large pockets of heat generating cement.

The most recent temperature logs at the time of this writing are presented in the following pages for each well: New Jersey, Figure C-2.6, Delaware, Figure C-2.7, Maryland, Figure C-2.8, Virginia, Figure C-2.9.

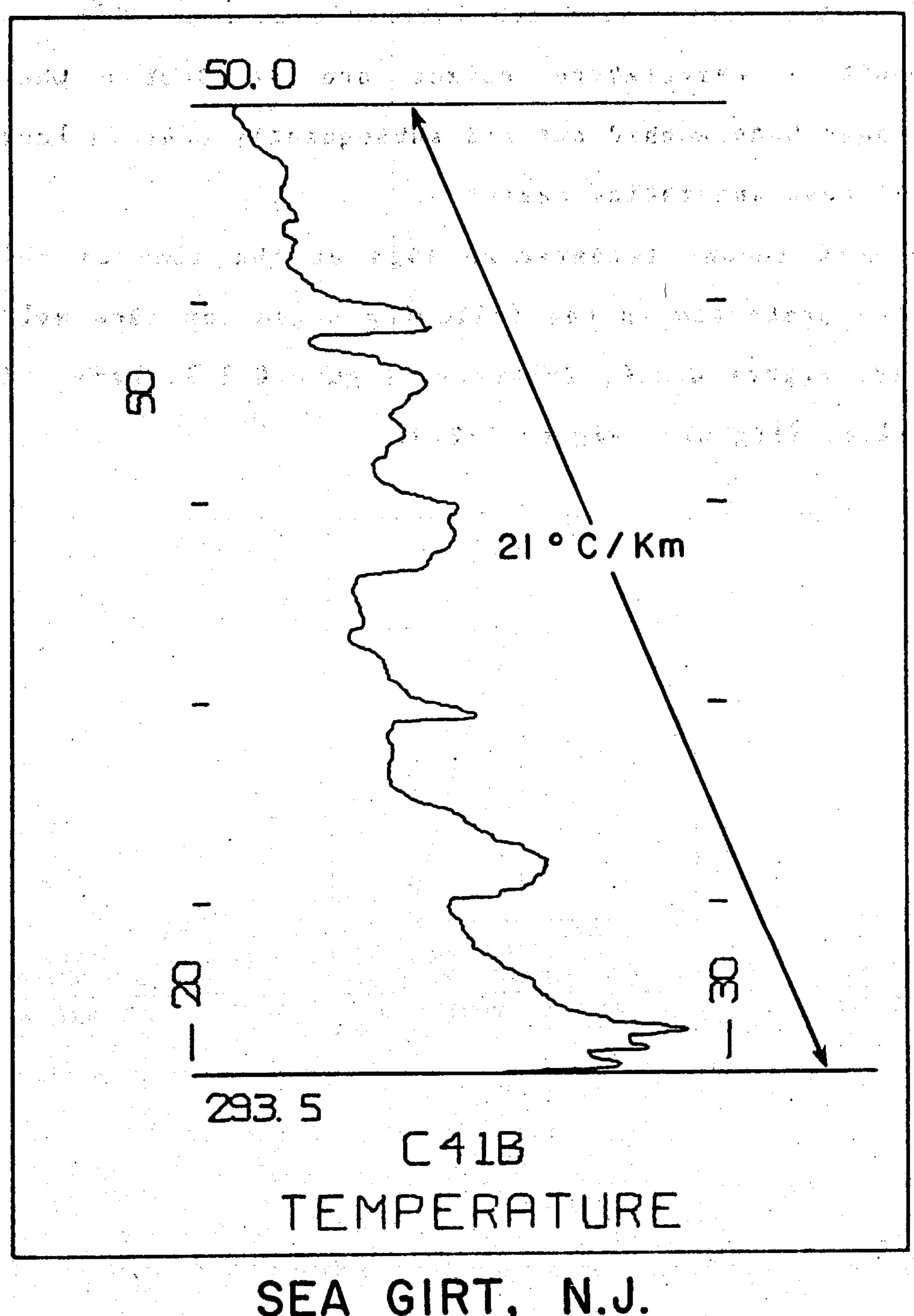

Figure C-2.5. Early log of Hole 41 showing temperature gradient of 21°C/km at 32 hours post cementing.

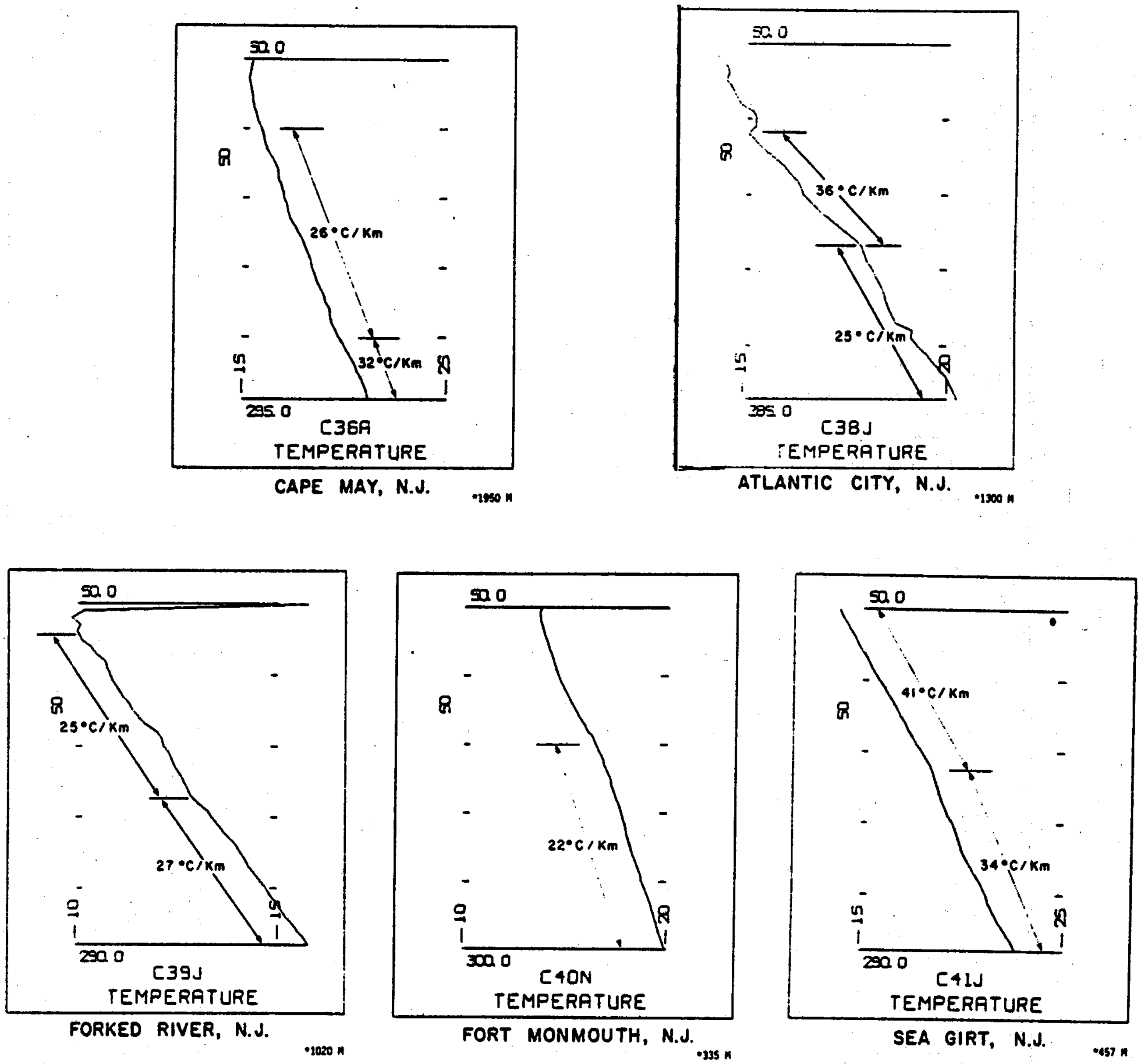

Figure C-2.6. Most recent temperature logs to date in New Jersey

*Estimated depths to basement

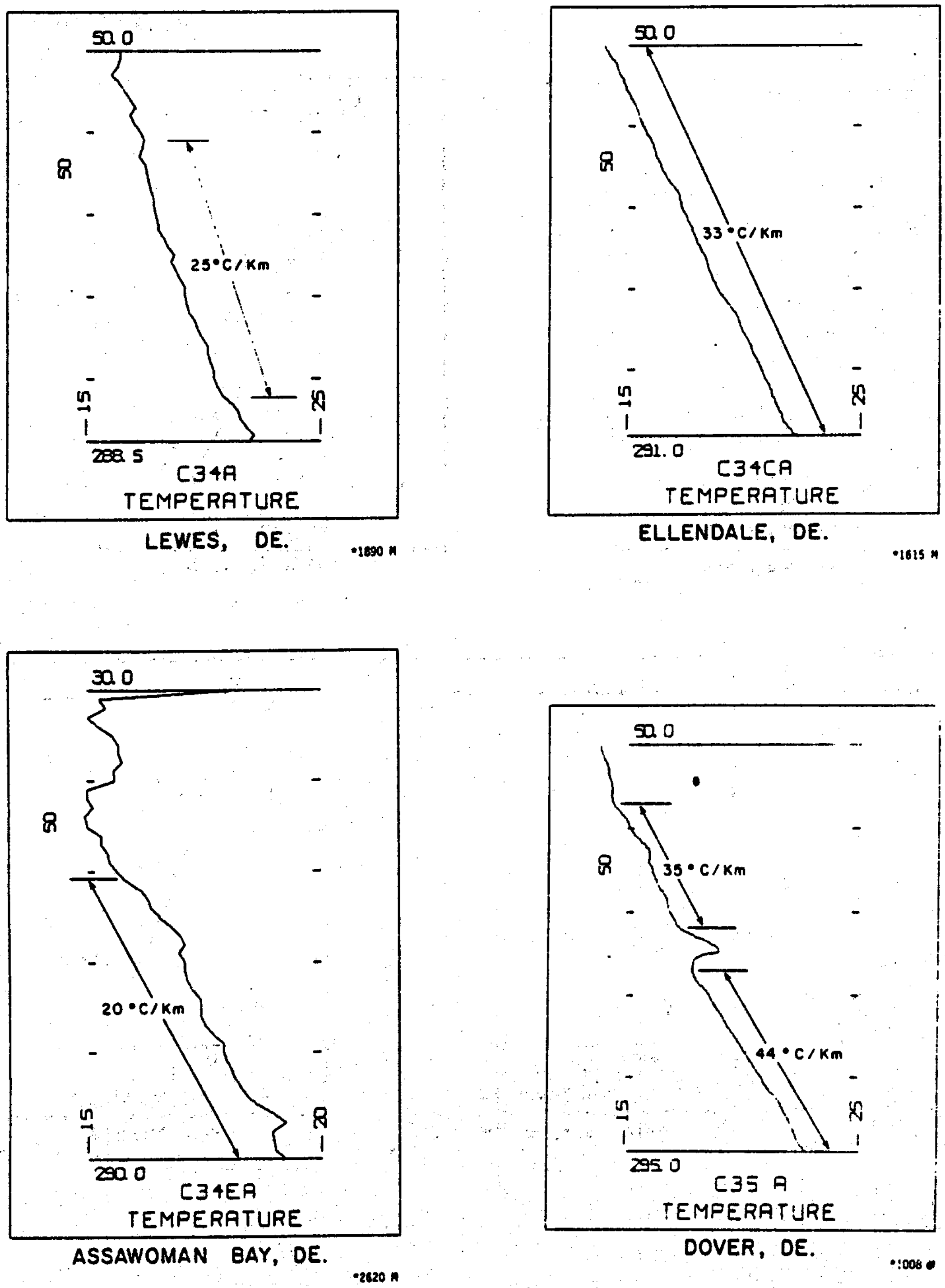

Figure C-2.7. Most recent temperature logs to date in Delaware

*Estimated depths to basement

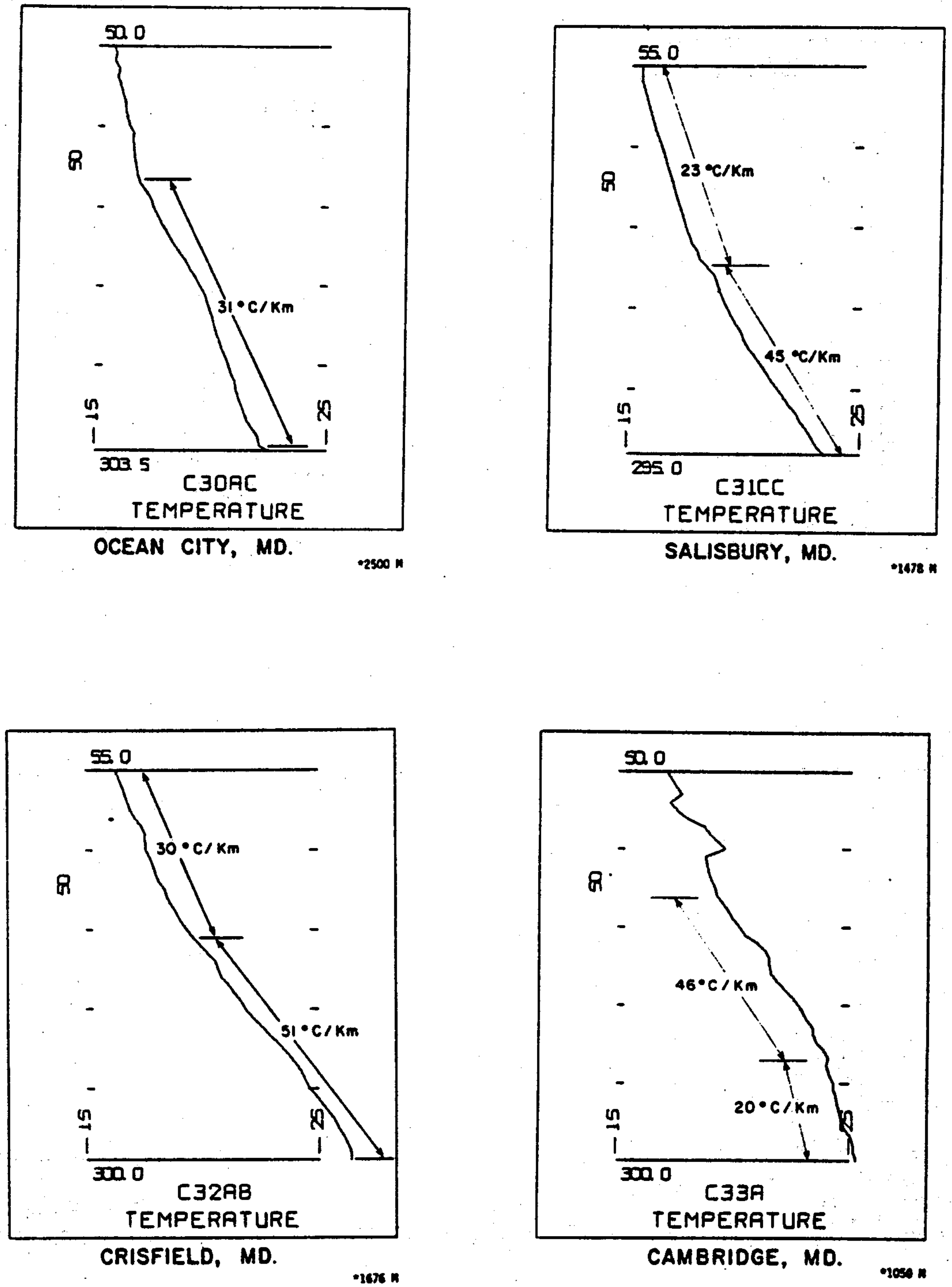

Figure C-2.8. Most recent temperature logs to date in Maryland

*Estimated depths to basement

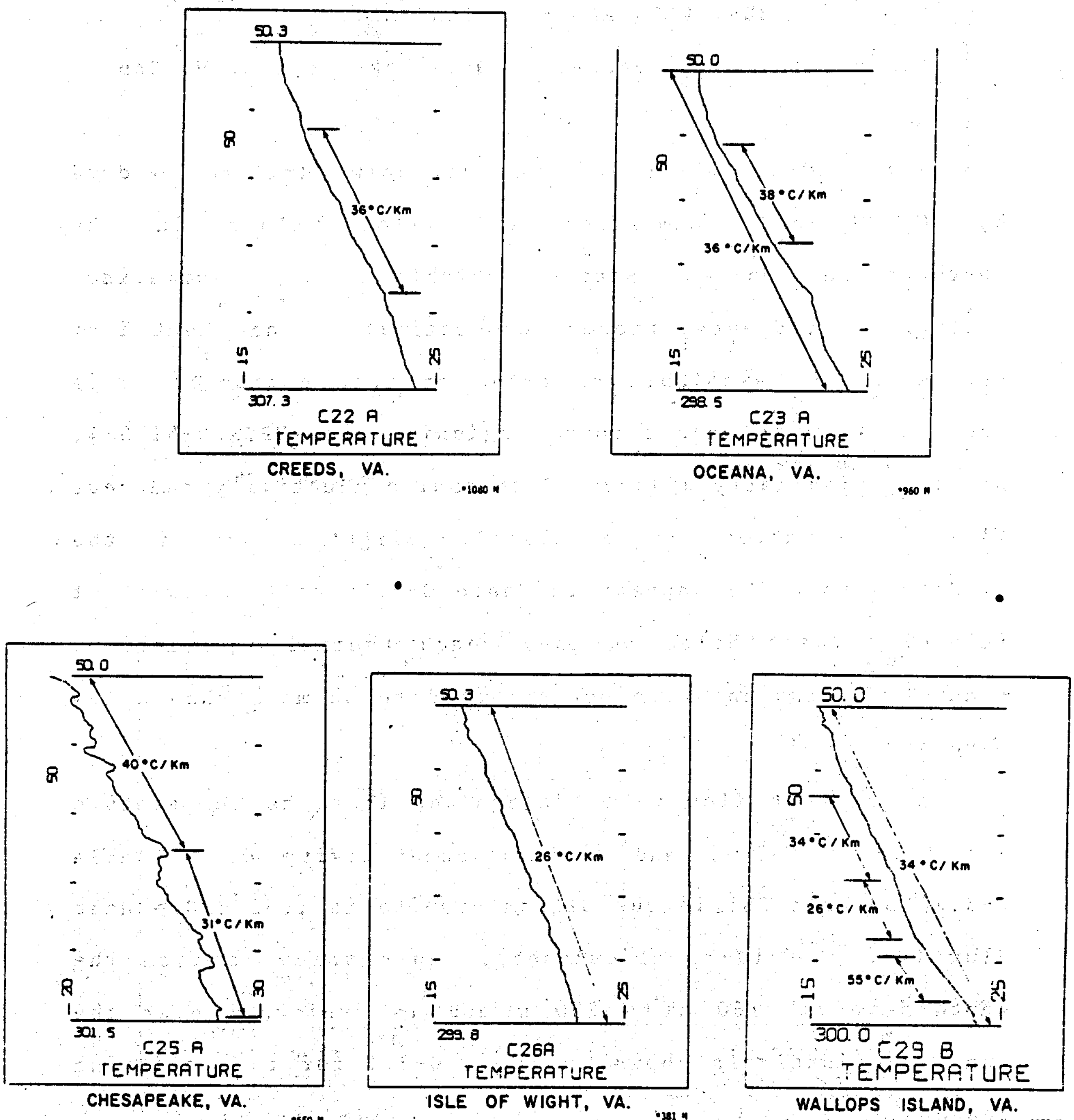

Figure C-2.9. Most recent temperature logs to date in Virginia

*Estimated depths to basement

HEAT FLOW AND HEAT GENERATION

J. K. Costain, L. D. Perry, S. Dashevsky, and B. U. Sans

Figure C-3.1 shows locations of holes drilled to date by VPI&SU and summarizes heat flow values in the southeastern United States. Table C-3.1 summarizes geothermal gradients, thermal conductivities, and heat flow determinations available to date for this contract. This table appears in each report, beginning with VPI&SU-5103-4, and is periodically updated as thermal conductivity and heat flow determinations are completed. Slight changes in the gradients that will appear in Table C-3.1 are the result of relogging these holes as they reach thermal equilibrium. Changes in gradients are not expected to be more than a few percent.

A new heat flow value determined from the temperature log (Figure C-3.2) and thermal conductivity data (Table C-3.2) of hole SM1 in the Siloam granite is 1.53 HFU = Heat Flow Unit - = 10-6 cal/cm2-sec). This value is from the depth interval 160 m to 250 m and is preferred over the shallower intervals shown in Table C-3.1 for the following reasons.

Water is continuously flowing from the hole at the surface and could be entering the hole along zones of alteration. The radical change in the gradient (7.83 °C/Km to 18.88 °C/Km) at a depth of approximately 155 m (See

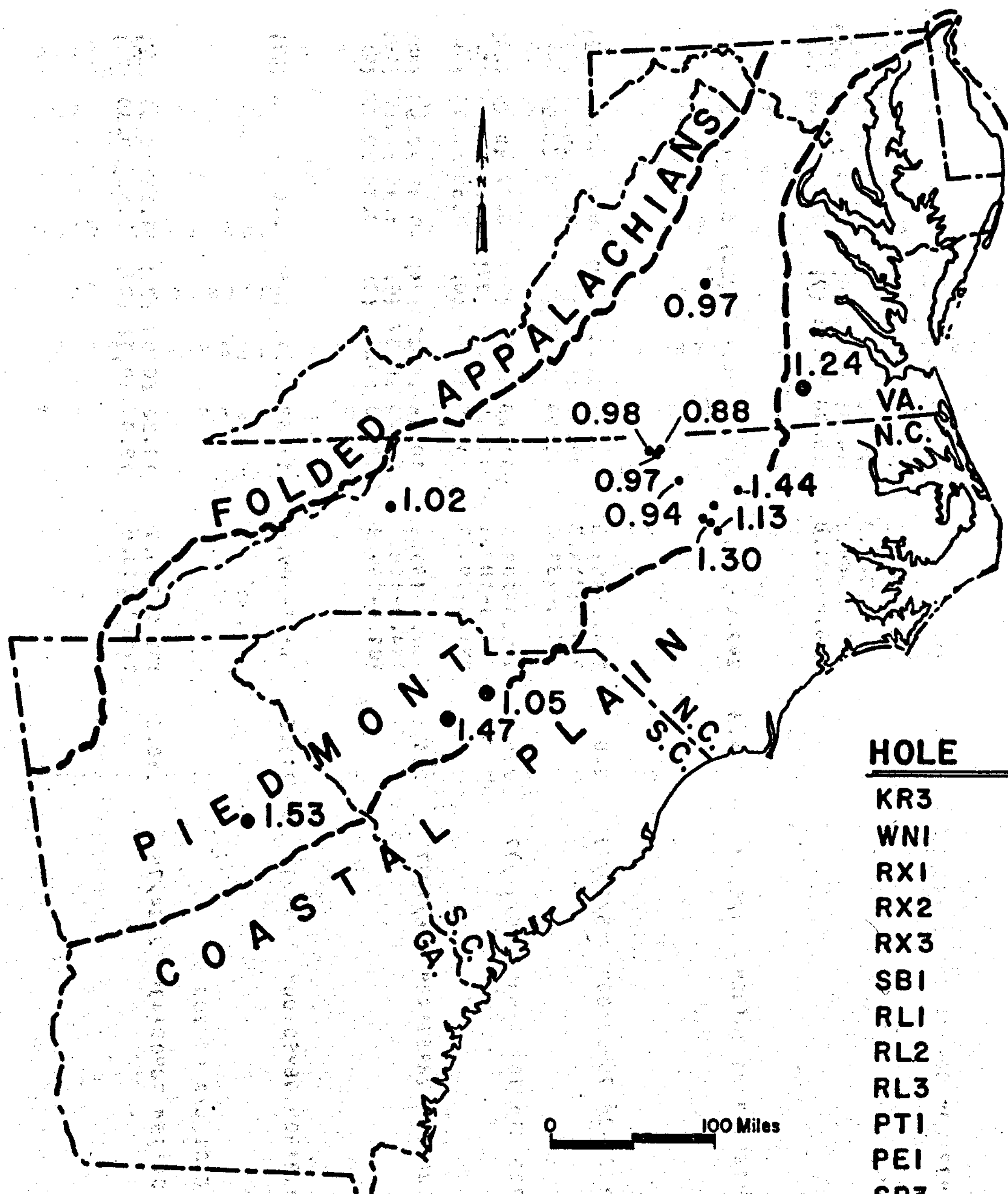

HOLE	Q
KR3	1.05
WN1	1.47
RX1	0.98
RX2	0.97
RX3	0.88
SB1	0.94
RL1	1.44
RL2	1.30
RL3	1.13
PT1	1.24
PE1	0.97
SP3	1.02
SM1	1.53

Figure C-3.1. Locations of holes drilled to date by VPI&SU and summarizes heat flow values.

LOCATION	LATITUDE	LONGITUDE	DATE LOGGED	HOLE DEPTH (METERS)	DEPTH INTERVAL (METERS)	GRADIENT[3] (°C/KM)	CONDUCTIVITY[3] (MCAL/CM-SEC-°C)	HEAT FLOW (CAL/CM^2-SEC)
LIBERTY HILL - KERSHAW PLUTON, LANCASTER CO., S.C.								
KR3	34°32'20"	80°44'51"	11/18/76	277	316.8-404.3	14.91 ±0.02 (36)	7.14 ±0.57 (24)*	1.06 ±0.09[1]
					334.3-341.8	14.68 ±0.07 (4)	6.94 ±0.47 (3)*	1.02 ±0.07
					344.3-356.8	15.06 ±0.07 (6)	7.09 ±0.54 (5)*	1.07 ±0.0
					359.3-369.3	14.88 ±0.07 (5)	7.33 ±0.20 (4)*	1.09 ±0.04
					371.8-384.3	14.85 ±0.06 (6)	7.07 ±0.28 (5)*	1.05 ±0.05
					386.8-401.8	15.00 ±0.13 (7)	6.94 ±0.69 (6)*	1.04 ±0.11
RION PLUTON, FAIRFIELD CO., S.C.								
WN1	34°18'48"	81°08'42"	7/5/77	574.3	242.4-571.74	18.18 ±0.04 (220)	8.06 ±0.24 (26)	1.47 ±0.05[1]
ROXBORO METAGRANITE, PERSON CO., N.C.								
RX1	36°23'12"	78°58'00"	5/19/77	240	146.8-249.3	10.83 ±0.03 (42)	8.97 ±0.41 (32)	0.97 ±0.05[1]
					146.8-184.3	11.03 ±0.06 (16)	9.08 ±0.11 (15)	1.00 ±0.02[1]
					219.3-231.8	10.94 ±0.12 (16)	8.76 ±0.59 (5)	0.96 ±0.08[1]
RX2	36°25'31"	79°01'53"	5/19/77	214	149.3-209.3	11.20 ±0.04 (25)	8.77 ±0.45 (23)	0.98 ±0.05[1]
					149.3-189.3	11.30 ±0.07 (17)	8.87 ±0.21 (16)	1.00 ±0.03[1]
					191.8-209.3	11.05 ±0.04 (8)	8.54 ±0.73 (7)	0.94 ±0.08[1]
RX3	36°25'39"	78°53'42"	8/7/77	211.5	134.9-199.9	10.36 ±0.22 (14)	8.33 ±0.58 (14)	0.86 ±0.08[1]
					144.3-169.9	10.43 ±0.37 (6)	8.40 ±0.67 (10)	0.88 ±0.10[1]
					181.9-194.9	9.00 ±0.46 (3)	8.14 ±0.25 (4)	0.73 ±0.06[1]
SLATE BELT PERSON CO., N.C.								
SB1	36°19'40"	78°50'00"	6/5/77	211.5	41.7-209.2	11.63 ±0.11 (66)	8.06 ±0.66 (47)	0.94 ±0.09[1]
ROLESVILLE BATHOLITH AND CASTALIA PLUTON FRANKLIN CO., N.C.								
CS1	36°04'15"	78°07'43"	2/24/78	210.6	142.2-209.7	19.26 ±0.03 (28)	7.52 ±0.39 (26)	1.45 ±0.08[11]
					145.0-210.0	19.06 ±0.12 (27)	7.52 ±0.39 (26)	1.43 ±0.08[1]

RL2	36°47'17"	78°25'04"	2/24/78	212.8	29.7-209.7	18.92 ±0.07 (73)	7.23 ±0.34 (14)	1.37 ±0.07[1][1]
					104.7-124.7	17.40 ±0.18 (9)	7.30 ±0.38 (7)	1.27 ±0.08[1]
					192.2-209.7	18.71 ±0.18 (9)	7.16 ±0.31 (6)	1.34 ±0.07[1]
RL3	35°57'05"	78°20'00"	2/23/78	121.9	42.4-129.9	14.06 ±0.08 (36)	8.03 ±0.93 (27)	1.13 ±0.14[1]
					42.4- 94.9	13.57 ±0.15 (22)	8.22 ±0.70 (12)	1.12 ±0.11[1]
					97.4-129.9	13.79 ±0.10 (14)	7.88 ±1.08 (15)	1.09 ±0.16[1]
RL4	35°43'36"	78°19'45"	2/24/78	196.3	54.7-194.7	13.26 ±0.27 (57)		
					54.7- 89.7	5.23 ±0.23 (15)		
					92.2-194.7	15.44 ±0.08 (42)		
RL5	35°51'17"	78°28'54"	2/23/78	211.5	22.3-209.8	16.31 ±0.03 (76)		
					22.3- 69.8	15.57 ±0.22 (20)		
					72.3-129.8	16.02 ±0.06 (24)		
					132.3-209.8	16.87 ±0.03 (32)		
PETERSBURG GRANITE, SUSSEX CO., VA.								
PT1	36°49'45"	77°19'15"	10/21/77	253.0	94.7-159.7	18.18 ±0.08 (27)	6.67 ±0.54 (25)	1.21 ±0.10[1]
					197.2-249.7	19.20 ±0.12 (26)	6.57 ±0.57 (25)	1.26 ±0.12[1]
PAGELAND PLUTON, LANCASTER CO., S.C.								
PG1	34°42'02"	80°27'51"	2/17/78	213.4	32.5-205.0	11.71 ±0.08 (70)		
					32.5- 75.0	15.31 ±0.23 (18)		
					77.5-165.0	10.73 ±0.06 (36)		
					167.5-205.0	12.83 ±0.03 (10)		
LAKESIDE CUMBERLAND CO., VA.								
LK1	37°41'25"	78°08'52"	9/16/77	205.0	59.3-204.3	13.46 ±0.07 (58)		
					59.3- 81.8	11.49 ±0.07 (10)		
					121.3-144.3	14.30 ±0.17 (10)		
					164.3-204.3	13.31 ±0.05 (17)		
PEGMATITE BELT,								

GOOCHLAND CO., VA.								
PE1	37°45'56"	78°05'37"	9/21/77	200.0	41.8-201.8	13.27 ±0.15 (65)	6.37 ±0.99 (40)	0.85 ±0.14[1]
					41.8- 59.3	8.39 ±0.27 (9)	7.22 ±0.34 (3)	0.61 ±0.05[1]
					116.8-194.3	15.40 ±0.09 (34)	6.30 ±0.98 (37)	0.97 ±0.16[1]
CUFFYTOWN EDGEFIELD, S.C.								
ED1	33°55'11"	82°07'10"	6/10/78	294.0	62.5-290.0	16.55 ±0.10 (92)		
					62.5-175.0	14.29 ±0.16 (46)		
					177.5-290.0	17.59 ±0.04 (46)		
PALMETTO COWETA CO., GA								
PM1	33°29'55"	84°41'58"	6/11/78	208.3	30.0-208.3	14.64 ±0.08 (73)		
					30.0- 82.5	16.74 ±0.38 (22)		
					85.0-160.0	14.41 ±0.74 (31)		
					162.5-208.3	16.94 ±0.05 (20)		
SILOAM GREENE CO., GA.								
SM1	32°27'17"	83°08'53"	6/10/78	210.0	27.5-207.0	14.52 ±0.12 (73)	8.19 ±0.54 (28)	1.19 ±0.09
					27.5- 55.0	12.15 ±1.20 (12)	8.22 ±0.51 (6)	1.00 ±0.17
					57.5-110.0	13.62 ±0.03 (22)	8.20 ±0.72 (11)	1.12 ±0.11
					112.5-120.0	26.40 ±1.38 (4)	8.00 ±0.24 (2)	2.11 ±0.18
					122.5-157.5	7.83 ±0.21 (15)	8.31 ±0.23 (4)	0.65 ±0.04
					160.0-205.0	18.88 ±0.08 (19)	8.11 ±0.46 (5)	1.53 ±0.09
SM2	33°28'41"	83°11'35"	6/10/78	210.0	27.5-210.0	18.27 ±0.08 (74)		
SPRUCE PINE MITCHELL CO., N.C.								
SP3	35°54'50"	82°07'18"	5/19/76	1220.0	209.1-1059.1	14.45 ±0.13 (89)	6.62 ±1.19 (88)	0.96±0.18[1]
					209.1- 519.1	16.39 ±0.03 (32)	6.72 ±1.51 (35)	1.10 ±0.25[1]
					534.1- 849.1	14.72 ±0.04 (35)	6.38 ±0.97 (36)	0.94 ±0.15[1]
					849.1-1059.1	9.36 ±0.07 (19)	6.74 ±0.94 (32)	0.63 ±0.09[1]

STATE FARM						
GOOCHLAND CO., VA.						
SF1	37°40'01"	77°48'06"	5/22/78	207.5	27.5-107.5	15.03 ±0.10 (72)
					32.5-100.0	15.50 ±0.11 (28)
					102.5-207.5	15.10 ±0.30 (42)
PHELPS DODGE						
DAVIDSON CO., N.C.						
PD1	35°42'24"	80°02'19"	3/20/78	630.0	50.0-630.0	13.58 ±0.05(117)
					250.0-550.0	14.11 ±0.07 (61)

1 - INDICATES HEAT FLOW VALUE IS THE PRODUCT OF A MEAN GRADIENT AND A MEAN THERMAL CONDUCTIVITY
3 - VALUE IN PARENTHESES IS THE NUMBER OF TEMPERATURE POINTS OR THE NUMBER OF THERMAL CONDUCTIVITY VALUES
4 - THERMAL CONDUCTIVITY VALUES FROM 1.270 CM THICK SAMPLES
5 - GRADIENT FROM THE SEDIMENTARY COVER OF THE PLUTON
6 - GRADIENT FROM WITHIN THE PLUTON

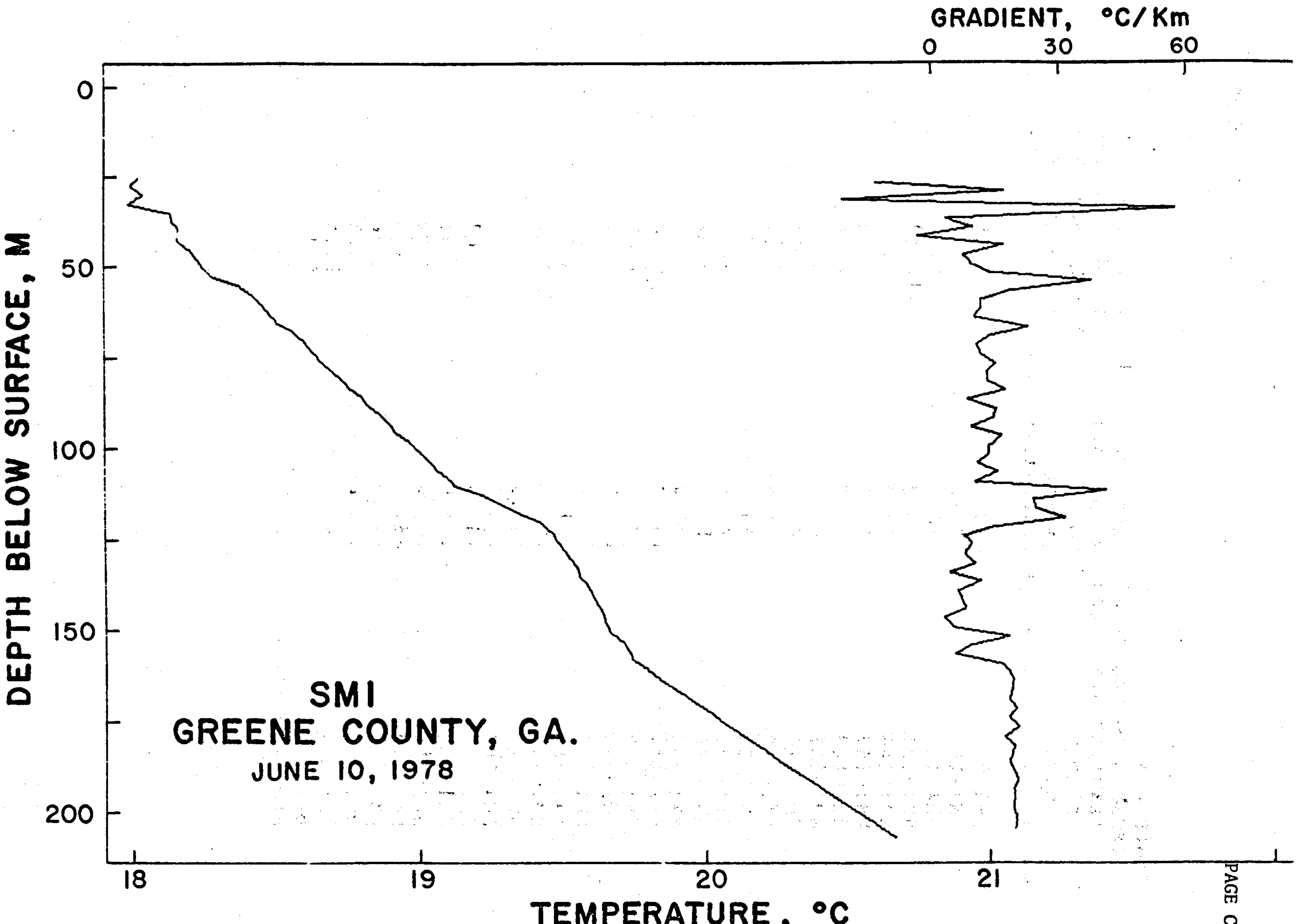

Figure C-3.2. New heat flow value of Hole SM1 in the Siloam granite.

TABLE C-3.2 C-3.2-1

THERMAL CONDUCTIVITY VALUES FROM CORE OF DRILL HOLE SM1
(SAMPLES ARE 2.680 CM IN DIAMETER BY 1.270 CM THICK)

SAMPLE NAME	DEPTH (METERS)	THERMAL CONDUCTIVITY MCAL/CM-SEC-°C
SM1-97	29.6	8.24
SM1-105	32.0	8.64
SM1-113	34.6	8.00
SM1-121	36.8	10.29
SM1-144	43.9	8.77
SM1-167	51.0	8.29
SM1-183	55.7	7.34
SM1-207	63.0	8.48
SM1-214	65.2	8.34
SM1-222	67.6	8.04
SM1-230	69.9	7.30
SM1-243	74.2	8.77
SM1-284	86.6	8.46
SM1-309	94.0	8.53
SM1-331	100.7	6.68
SM1-339	103.2	8.40
SM1-362	110.3	9.36
SM1-370	112.6	7.83
SM1-385	117.4	8.17
SM1-440	134.0	8.35
SM1-463	141.1	7.97
SM1-502	153.0	8.44
SM1-510	155.4	8.47
SM1-564	172.0	5.47
SM1-588	179.1	8.37
SM1-618	188.5	8.06
SM1-627	191.0	8.66
SM1-635	193.4	7.42
SM1-642	195.7	8.05
Mean		8.12
Standard Deviation		0.73

Figure C-3.2) is associated with one of these zones. The change in gradient is not related to a change in thermal conductivity. Also, there is a second altered zone at a depth of 122.5 - 125.9 m corresponding to another radical change in the gradient (26.40 °C/Km to 7.83 °C/Km). If water enters the hole from the altered zone at 155 m, flows up the hole, and exits by the altered zone at 122 m, then the gradient would be low between 122 m and 155 m as observed. Bringing warm water up the hole would also raise the gradient in the interval immediately above 122 m as observed. The change in the gradient from 13.62 °C/Km to 26.40 °C/Km is not accounted for in this model but could be related to a similar effect. The fact that water is flowing at the surface precludes the determinations of a reliable gradient from intervals above the altered zones. The interval below 155 meters is considered to be unaffected because of the lack of noise in the gradient.

Heat generation data for the same hole is given in Table C-3.3.

The heat flow at the Siloam, GA site is the highest value we have encountered to date in the Piedmont in the southeastern United States. Assuming rocks of similar heat generation are concealed beneath sediments of the Atlantic Coastal Plain, and assuming the linear relationship between heat flow and heat generation determined to date in the southeastern United States, geothermal gradients of 45 °C/Km

TABLE C-3.3 HEAT GENERATION DATA FROM CORE OF DRILL HOLE SM1

LOCATION	SAMPLE NO. DEPTH(M)	DENSITY, GM/CM³	URANIUM (U),PPM	THORIUM (TH),PPM	POTASSIUM (K),%	RATIO, TH/U	HEAT GENERATION, A X 10⁻¹³ CAL/CM³-SEC
SILOAM-1	GA SM1-032	2.63	9.4	42.7	3.7	4.5	13.3
SILOAM-1	GA SM1-047	2.65	8.2	40.4	4.1	4.9	12.4
SILOAM-1	GA SM1-065	2.63	8.7	38.3	3.6	4.4	12.2
SILOAM-1	GA SM1-077	2.63	7.2	36.2	4.3	5.0	11.1
SILOAM-1	GA SM1-093	2.66	8.7	42.8	4.5	4.9	13.2
SILOAM-1	GA SM1-099	2.64	7.4	39.2	4.1	5.3	11.6
SILOAM-1	GA SM1-105	2.63	6.1	25.9	4.4	4.3	8.8
SILOAM-1	GA SM1-114	2.65	5.4	36.2	4.1	6.6	10.1
SILOAM-1	GA SM1-120	2.64	7.5	45.2	4.4	6.0	12.8
SILOAM-1	GA SM1-129	2.66	5.1	33.8	3.9	6.7	9.4
SILOAM-1	GA SM1-135	2.67	4.6	34.2	3.9	7.5	9.2
SILOAM-1	GA SM1-141	2.66	4.4	29.8	4.2	6.8	8.4
SILOAM-1	GA SM1-151	2.65	6.9	41.7	4.0	6.0	11.8
SILOAM-1	GA SM1-160	2.66	5.6	39.8	3.8	7.1	10.7
SILOAM-1	GA SM1-166	2.66	9.4	31.3	5.0	3.3	11.9
SILOAM-1	GA SM1-171	2.68	22.2*	80.2*	3.4	3.6	27.4*
SILOAM-1	GA SM1-181	2.64	6.0	36.9	3.8	6.2	10.4
SILOAM-1	GA SM1-190	2.67	4.8	38.9	3.7	8.1	10.1
SILOAM-1	GA SM1-199	2.66	7.4	43.5	3.6	5.8	12.4
Mean values		2.65	6.8	37.6	4.0	5.6	11.1
Standard deviations		0.02	1.7	5.1	0.4	1.3	1.5

*....value omitted from mean

should be found in sediments of the Atlantic Coastal Plain if a thermal conductivity of 4 x 10-3 cal/cm-°C-sec is assumed for the sediments and if a heat generation of 15 HGU is assumed in basement rocks. Gradients of 45 °C/Km are also consistent with a sediment thermal conductivity of 3.5 x 10-3 cal/cm-°C-sec and a basement heat generation of 12 HGU. These theoretical predictions are consistent with values of the geothermal gradient now being determined in Coastal Plain sediments and described elsewhere in this progress report.

LINEAR RELATIONSHIP BETWEEN HEAT FLOW AND HEAT GENERATION

J. K. Costain and L. D. Perry

Figure C-4.1 shows the relationship between heat flow and heat generation for all holes available to date in the southeastern United States. Table C-4.1 summarizes heat flow and heat generation values used in the linear relationship. With the exception of values derived from plutonic rocks with a large geographic outcrop (Castalia/Rolesville batholith and Petersburg batholith) all of the values define a linear relationship of the form:

$$Q = 0.65 + 7.9A$$

(regression coefficient = 0.996)

The addition of values (Q = 1.53, A = 11.1) from hole SM1 in the Siloam granite provides much needed confirmation of the linear relation in the region above q = 1.13 and A = 6.0. Heretofore, only the value for hole WN1 was available in this region.

Preliminary heat generation values of 11 HGU (HGU = heat generation unit = 10-13 cal/cm3-sec) and 12 HGU for the second Siloam hole and the Cuffytown Creek hole, respectively will provide additional values in this region when thermal conductivity studies are completed.

It is noteworthy that an excellent linear relationship between heat flow and heat generation has now been

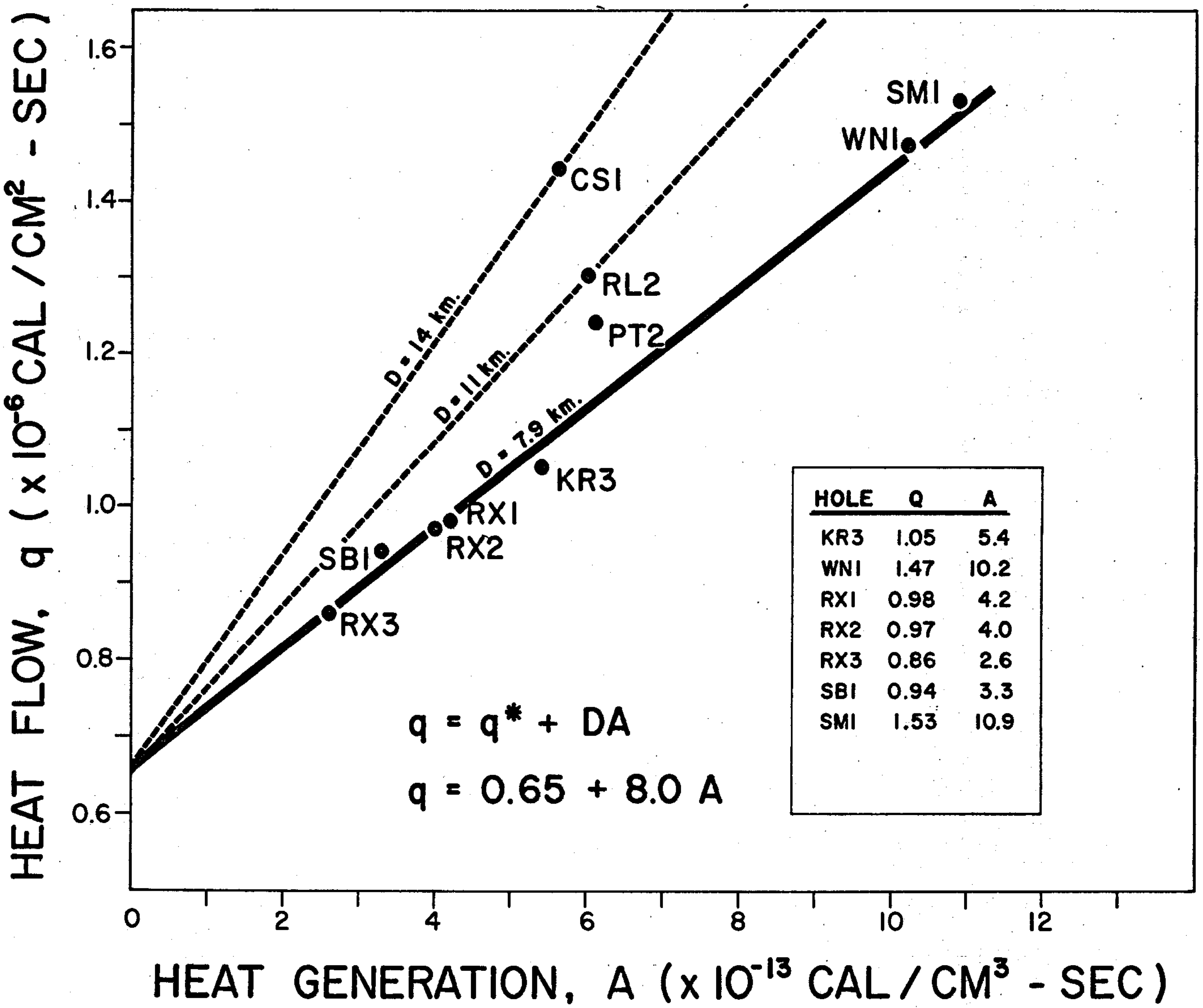

Figure C-4.1. Relationship between heat flow and heat generation for all holes available to date in the southeastern United States.

TABLE C-4.1

HEAT FLOW (q) AND HEAT PRODUCTION (Å) VALUES FROM PLUTONS OF THE SOUTHEASTERN UNITED STATES

LOCATION	LATITUDE	LONGITUDE	Q, CAL/CM^2-SECx10^{-6}	A, CAL/CM^3-SECx10^{-13}
LIBERTY HILL-KERSHAW PLUTON, LANCASTER CO., S.C.				
KR3	34°32'20"	80°44'51"	1.05	5.4
RION PLUTON, FAIRFIELD CO., S.C.				
WN1	34°18'48"	81°08'42"	1.47	10.2
ROXBORO METAGRANITE, PERSON CO., N.C.				
RX1	36°23'12"	78°58'00"	0.98	4.2
RX2	32°25'31"	79°01'53"	0.97	4.0
RX3	32°25'39"	78°53'42"	0.86	2.6
SLATE BELT, PERSON CO., N.C.				
SB1	36°19'40"	78°50'00"	0.94	3.3
ROLESVILLE BATHOLITH AND CASTALIA PLUTON (CS1), FRANKLIN CO., N.C.				
CS1	36°04'15"	78°07'43"	1.44	5.6
FL2	36°47'28"	78°25'04"	1.30	6.0
PETERSBURG GRANITE, SUSSEX CO., VA.				
PT1	36°49'45"	77°19'15"	1.24	6.1
SILOAM GRANITE, GREENE CO., GA.				
SM1	32°27'17	83°08'53	1.53	11.1

established for the smaller, post- and pre-metamorphic plutons in the southeastern United States. To date, the only values we have that do not fall on the linear relationship

$$Q = 0.65 + 7.9A$$

are near or in the larger syntectonic plutonic complexes such as the Rolesville batholith (RL2), Castalia pluton (CS1), and Petersburg batholith (PT1). We continue to prefer the interpretation that D is related to the thickness of a layer of heat-producing elements rather than to a logarithmic decrement.

☆U.S. GOVERNMENT PRINTING OFFICE: 1979-640-014 4515 REGION NO. 4